

mgr Tomasz Kulesza

**ROLA TRANSPORTERÓW FOSFORANOWYCH W ROZWOJU
KŁĘBUSZKOWEJ KALCYFIKACJI ORAZ W INDUKCJI
INSULINOOPORNOŚCI PODOCYTÓW**

**The role of phosphate transporters in the development of glomerular calcification
and in the induction of insulin resistance in podocytes**

Rozprawa na stopień naukowy doktora
w dziedzinie nauk medycznych i nauk o zdrowiu w dyscyplinie nauki medyczne

Promotor dr hab. inż. Agnieszka Piwkowska, prof. IMDiK PAN



Obrona rozprawy doktorskiej przed Radą Naukową
Instytutu Medycyny Doświadczalnej i Klinicznej
im. M. Mossakowskiego Polskiej Akademii Nauk

Warszawa, 2023

Składam serdeczne podziękowania...

*Promotor **dr hab. inż. Agnieszce Piwkowskiej, prof. IMDiK PAN**
za sprawowanie opieki merytorycznej, poświęcony czas oraz przyjazną atmosferę pracy.*

*Wszystkim współautorom
dr hab. Dorocie Rogackiej, prof. IMDiK PAN,
dr Irenie Audzeyenka,
dr Marlenie Typiak,
dr Patrycji Rachubik
za owocną współpracę, dzięki której możliwe było powstanie niniejszego cyklu publikacji.*

***Śp. prof. Stefanowi Angielskiemu**
za chęć dzielenia się wiedzą, uśmiechem i życzliwością.*

*Wszystkim **Koleżankom i Kolegom**
z Pracowni Molekularnej i Komórkowej Nefrologii IMDiK PAN
za wspólne pokonywanie trudności napotkanych na naukowej ścieżce.*

***Rodzicom i Babci** za nieustające wsparcie.*

Spis treści

Lista publikacji będących podstawą rozprawy doktorskiej.....	4
Wykaz skrótów	5
1. Streszczenie polskojęzyczne i anglojęzyczne	7
2. Innowacyjność rozprawy	11
3. Wstęp.....	12
4. Cel pracy	17
5. Metodologia	18
6. Omówienie i podsumowanie najważniejszych wyników	24
7. Wnioski	33
8. Bibliografia	35
9. Kopie publikacji będących podstawą rozprawy.....	41
10. Pisemne oświadczenia autorów prac tworzących zbiór	82

Lista publikacji będących podstawą rozprawy doktorskiej

Wyniki zaprezentowane w rozprawie doktorskiej zostały zamieszczone w niniejszych publikacjach:

1. Kulesza T, Typiak M, Rachubik P, Audzeyenka I, Rogacka D, Angielski S, Saleem MA, Piwkowska A. **Hyperglycemic environment disrupts phosphate transporter function and promotes calcification processes in podocytes and isolated glomeruli.** *J Cell Physiol.* 2022; 237(5): 2478-2491; IF₅ = 6,398
2. Kulesza T, Typiak M, Rachubik P, Rogacka D, Audzeyenka I, Saleem MA, Piwkowska A. **Pit 1 transporter (SLC20A1) as a key factor in the NPP1-mediated inhibition of insulin signaling in human podocytes.** *J Cell Physiol.* 2023; doi: 10.1002/jcp.31051; IF₅ = 6,398
3. Kulesza T, Piwkowska A. **The impact of type III sodium-dependent phosphate transporters (Pit 1 and Pit 2) on podocyte and kidney function.** *J Cell Physiol.* 2021; 236(10): 7176-7185; IF₅ =6,398

Badania, których wyniki przedstawiono w cyklu publikacji stanowiących podstawę rozprawy doktorskiej finansowane były z grantu Narodowego Centrum Nauki OPUS 15 (2018/29/B/NZ4/02074).

Wykaz skrótów

- ANKH** (*ang. progressive ankylosis protein homolog*) – homolog białka postępującej ankylozy;
- Akt** (*ang. protein kinase B*) – kinaza białkowa B;
- ATP** – adenozyno-5'-trifosforan;
- AUC** (*ang. area under the curve*) – pole powierzchni pod krzywą;
- BSA** (*ang. bovine serum albumin*) – albumina surowicy bydłowej;
- CTRL** – kontrolne szczury rasy Wistar;
- DKD** (*ang. diabetic kidney disease*) – cukrzycowa choroba nerek;
- FBS** (*ang. fetal bovine serum*) – płodowa surowica bydłowa;
- GFB** (*ang. glomerular filtration barrier*) – kłębuszkowa bariera filtracyjna;
- GLUT 4** (*ang. facilitated glucose transporter member 4*) – transporter glukozy typu 4;
- Glv-1** (*ang. Gibbon ape leukemia virus receptor*) – receptor wirusa białaczki gibbonowatych;
- HG** (*ang. high glucose medium*) – medium hodowlane z wysokim stężeniem (30 mM) glukozy;
- HI** (*ang. high insulin medium*) – medium hodowlane z wysokim stężeniem (100 nM) insuliny;
- INS** – insulina;
- IR** (*ang. insulin receptor*) – receptor insulinowy;
- mRNA** (*ang. messenger RNA*) – matrycowy RNA;
- NaPi 2c** (*ang. sodium-dependent phosphate transport protein 2C*) – zależny od sodu transporter fosforanowy typu 2c;
- NPP1** (*ang. nucleotide pyrophosphatase/phosphodiesterase 1*) – nukleotydowa pirofosfataza/fosfodiesteraza 1;
- PBS** (*ang. phosphate buffered saline*) – buforowana fosforanami sól fizjologiczna;
- Real-time PCR** (*ang. real-time polymerase chain reaction*) – reakcja łańcuchowa polimerazy w czasie rzeczywistym;
- Pi** – nieorganiczny fosforan;
- PPi** – pirofosforan;
- Pit 1** (*ang. sodium-dependent phosphate transporter 1*) – zależny od sodu transporter fosforanowy 1;
- Pit 2** (*ang. sodium-dependent phosphate transporter 2*) – zależny od sodu transporter fosforanowy 2;
- PWK** – przestrzeń wewnątrzkomórkowa;

PZK – przestrzeń zewnątrzkomórkowa;

Rab5a (*ang. Ras-related protein Rab-5A*) – białko Rab5a związane z białkami Ras;

RONS (*ang. reactive oxygen/nitrogen species*) – reaktywne formy tlenu i azotu;

SD (*ang. slit diaphragm*) – szczelina filtracyjna;

SDS (*ang. sodium dodecyl sulfate*) – laurylosiarczan sodu;

SG (*ang. standard glucose medium*) – medium hodowlane ze standardowym stężeniem (11 mM) glukozy;

shControl – ludzkie komórki podocytarne będące kontrolą do komórek z wyciszoną ekspresją genu *SLC20A1*;

shPit 1 – ludzkie komórki podocytarne z wyciszoną ekspresją genu *SLC20A1*;

shRNA (*ang. short harpin RNA*) – interferujący RNA o strukturze „spinki do włosów”;

siRNA (*ang. small interfering RNA*) – krótki interferujący RNA;

SLC (*ang. solute carrier family*) – rodzina błonowych białek transportujących;

STZ – szczury rasy Wistar z cukrzycą wyindukowaną podaniem streptozotocyny;

TNAP (*ang. tissue nonspecific alkaline phosphatase*) – tkankowa niespecyficzna fosfataza zasadowa;

T2D (*ang. type 2 diabetes*) – cukrzyca typu 2;

VC (*ang. vascular calcification*) – naczyniowa kalcyfikacja;

VSMC (*ang. vascular smooth muscle cell*) – komórka mięśni gładkich naczyń krwionośnych;

XPR1 (*ang. xenotropic and polytropic retrovirus receptor 1*) – ksenotropowy i politropowy receptor retrowirusowy 1.

1. Streszczenie polskojęzyczne i anglojęzyczne

Rola transporterów fosforanowych w rozwoju kłębuszkowej kalcyfikacji oraz w indukcji insulinooporności podocytów

Podocyty to wyspecjalizowane komórki nabłonka trzewnego, które wraz z śródbłonkiem naczyń włosowatych kłębuszka nerkowego oraz błoną podstawną tworzą unikalną strukturę jaką jest kłębuszkowa bariera filtracyjna (GFB). W morfologii podocyta wyróżnić można wypustki stopowate, które zazębiając się ze sobą tworzą szczeliny filtracyjne (SD) – wysoce dynamiczne, a co za tym idzie najbardziej wrażliwe na uszkodzenia elementy GFB. To właśnie SD zapobiegają przedostawaniu się makromolekuł (m. in. białek) z osocza krwi do ultrafiltratu w torebce Bowmana. Podocyty wykazują również wrażliwość na działanie insuliny, przy czym zmiany w homeostazie tego hormonu wpływają na fizjologię omawianych komórek. Cukrzyca i jej powikłanie, jakim jest cukrzycowa choroba nerek (DKD), to przykłady najczęstszych zaburzeń prowadzących do uszkodzenia podocytów. Przewlekła hiperinsulinemia i hiperglikemia, obecne w przebiegu DKD powodują insulinooporność podocytów, a w rezultacie postępującą dezintegrację GFB, i albuminurię. Uszkodzenie GFB jest często niezauważane w początkowych stadiach choroby ze względu na skąpoobjawową manifestację.

Kolejnym szkodliwym powikłaniem choroby cukrzycowej jest kalcyfikacja tkanek miękkich. Z powodu rozregulowanej gospodarki hormonalnej oraz nieprawidłowej funkcji nerek dochodzi do retencji w organizmie jonów fosforanowych (Pi). Długotrwała hiperfosfatemia sprzyja deponowaniu złogów fosforanu wapnia w organach, w których w warunkach fizjologicznych ten proces nie zachodzi. Do tej pory naukowcy najlepiej opisali patomechanizm kalcyfikacji naczyń krwionośnych (VC). Badacze ustalili istotny udział w tym zjawisku sodozależnych transporterów fosforanowych (NaPi 2c, Pit 1, Pit 2), których funkcją jest dokomórkowy transport Pi, oraz transportera XPR1 odpowiedzialnego za transport Pi do przestrzeni pozakomórkowej. W homeostazie fosforanowej bierze również udział nukleotydowa pirofosfataza/fosfodiesteraza 1 (NPP1), która poprzez hydrolizę nukleotydów generuje pirofosforan – najsilniejszy inhibitor kalcyfikacji. Zarówno NPP1, jak i Pit 1 są także czynnikami regulującymi wewnątrzkomórkową sygnalizację insulinową.

Celem badań prowadzonych w ramach niniejszej rozprawy doktorskiej było określenie wpływu środowiska cukrzycowego na homeostazę fosforanową w podocytach.

W szczególności skupiono się na określeniu udziału białek transportujących fosforan w rozwoju kłębuszkowej kalcyfikacji, a także w rozwoju insulinooporności podocytów.

W pierwszej części badań ustalono, iż warunki wysokiego stężenia glukozy (HG) prowadzą do zmian w ilości i komórkowej lokalizacji analizowanych transporterów fosforanowych. W błonie komórkowej podocytów zmniejszyła się ilość sodozależnych transporterów Pi, natomiast zwiększyła się translokacja XPR1 do błony plazmatycznej. Dodatkowo, stwierdzono mniejszą błonową ekspozycję NPP1, co skutkowało mniej wydajną produkcją PPI w przestrzeni zewnątrzkomórkowej (PZK). Powyższe obserwacje sugerują, iż w warunkach HG może dochodzić do nasilenia procesów kalcyfikacyjnych z powodu retencji jonów Pi w PZK oraz osłabienia działania naturalnych inhibitorów mineralizacji.

Następnie zbadano rolę białek Pit 1 i NPP1 w sygnalizacji insulinowej w podocycie. Po raz pierwszy wykazano, iż w podocytach z wyindukowaną insulinoopornością dochodzi do formowania się kompleksów enzymu NPP1 zarówno z transporterem Pit 1 oraz z receptorem insulinowym (IR). Ponadto stwierdzono, że wyciszenie genu *SLC20A1* kodującego białko Pit 1 prowadzi do utraty wrażliwości komórek podocytarnych na insulinę. Objawiało się to zahamowaniem dokomórkowego transportu glukozy oraz internalizacją IR i insulinozależnego transportera glukozy typu 4 (GLUT 4). Wskazuje to na fakt, iż białko Pit 1, oprócz roli transportera Pi, jest kluczowym czynnikiem warunkującym wrażliwość podocytów na insulinę.

Powyższe ustalenia pozwalają na lepsze zrozumienie mechanizmu uszkodzenia komórek podocytarnych w przebiegu choroby cukrzycowej i mogą przyczynić się do rozwoju wydajniejszych narzędzi diagnostycznych i terapeutycznych. Nowo poznane mechanizmy nie tylko wzbogacają wiedzę dotyczącą fizjologii komórki podocytarnej, lecz w dalszej perspektywie mogą istotnie poprawić komfort życia osób cierpiących z powodu cukrzycy i jej powikłań.

The role of phosphate transporters in the development of glomerular calcification and in the induction of insulin resistance in podocytes

Podocytes are specialized cells of the visceral epithelium, which, together with the glomerular capillary endothelium and the basement membrane, form a unique structure – the glomerular filtration barrier (GFB). In the morphology of the podocyte, foot processes can be distinguished, which, by interlocking with each other, form slit diaphragms (SD) – highly dynamic, and thus the most sensitive to damage, elements of the GFB. It is SD that prevents macromolecules (including proteins) from entering the ultrafiltrate in the Bowman's capsule. Podocytes are also insulin sensitive cells, and alterations in the homeostasis of this hormone affect their physiology. Diabetes and its complication, diabetic kidney disease (DKD), are examples of the most common disorders leading to podocyte injury. Chronic hyperinsulinemia and hyperglycemia present in the course of DKD cause insulin resistance of podocytes and, as a result, progressive disintegration of GFB, which leads to albuminuria. GFB damage is often overlooked in the initial stages of the disease due to its oligosymptomatic manifestation.

Soft tissues calcification is another deleterious complication of diabetes. Due to dysregulated hormonal balance and abnormal kidney function, phosphate ions (Pi) are retained in the body. Long-lasting hyperphosphatemia favors the deposition of calcium phosphate salts in organs where this process does not occur under physiological conditions. So far, scientists have most accurately described the pathomechanism of vascular calcification (VC). From these studies it is known that mechanism of VC involves the significant participation of sodium-dependent phosphate transporters (NaPi 2c, Pit 1, Pit 2), whose function is the transport of Pi into the cell, and the XPR1 is transporter responsible for the export of Pi from the cell. Nucleotide pyrophosphatase/phosphodiesterase 1 (NPP1) also participates in maintaining phosphate homeostasis, mainly by generation of pyrophosphate (PPi) – the strongest inhibitor of calcification – as a result of hydrolysis of nucleotides. Both NPP1 and Pit 1 are also regulators of intracellular insulin signaling.

The aim of the research within this doctoral dissertation was to determine the influence of the diabetic environment on phosphate homeostasis in podocytes. In particular, the role of Pi transport system in the development of glomerular calcification and the formation of insulin resistance of podocytes was investigated.

In the first part of the study, it was established that high glucose (HG) concentration leads to changes in the amount and cellular location of the analyzed phosphate transporters. In the cell membrane of the podocyte, the amount of sodium-dependent Pi transporters decreased, while the translocation of XPR1 to the plasma membrane elevated. In addition, membrane exposure of NPP1 was also reduced, resulting in attenuated production of PPi in the extracellular space (ES). The above-mentioned observations suggest that under HG conditions, the calcification processes are intensified due to the retention of Pi ions in ES and the reduction of the efficiency of natural mineralization inhibitors.

Next, the role of Pit 1 and NPP1 proteins in insulin signaling in the podocyte was determined. It was discovered for the first time that complexes of the NPP1 enzyme with both the Pit 1 transporter and the insulin receptor (IR) are formed in insulin resistant podocytes. In addition, silencing of the *SLC20A1* gene encoding the Pit 1 protein led to the insensitivity of podocytes to insulin, which was manifested by inhibition of glucose uptake and internalization of IR and insulin-dependent glucose transporter type 4 (GLUT 4). This indicates that Pit 1 protein, besides its role as the Pi transporter, is a key factor determining the sensitivity of podocytes to insulin.

The above-mentioned findings allow for a better understanding of the mechanism of podocyte damage in the course of diabetes and may contribute to the development of more efficient diagnostic and therapeutic tools. The newly discovered mechanisms not only enrich the knowledge on the physiology of the podocyte, but in the long run may significantly improve the quality of life of people suffering from diabetes and its complications.

2. Innowacyjność rozprawy

Badania przedstawione w niniejszej rozprawie doktorskiej po raz pierwszy udowodniły, że:

- podocyty posiadają w swojej błonie plazmatycznej białka transbłonowe (NaPi 2c, Pit 1, Pit 2, XPR1), których główną funkcją jest transport jonów fosforanowych;
- wysokie stężenie glukozy prowadzi do zmniejszenia całkowitej ilości oraz ilości frakcji błonowej transportera Pit 1 w podocycie, co promuje procesy kalcyfikacji kłębuszka nerkowego;
- długotrwała inkubacja podocytów z insuliną powoduje tworzenie kompleksów białka NPP1 z transporterem Pit 1, co skutkuje zahamowaniem sygnałowania insulinowego w tych komórkach;
- wyciszenie genu *SLC20A1* kodującego transporter Pit 1 powoduje zniesienie wrażliwości komórek podocytarnych na działanie insuliny.

3. Wstęp

Cukrzyca typu 2 (T2D) jest definiowana jako grupa zaburzeń metabolicznych objawiających się przewlekłą hiperglikemią. Patogeneza T2D opiera się na insulinooporności, czyli braku wrażliwości na insulinę tkanek, które w warunkach fizjologicznych odpowiadają na działanie tego hormonu¹. Jedną z konsekwencji upośledzenia gospodarki węglowodanowej w przebiegu T2D są groźne dla zdrowia zaburzenia w mikrokrążeniu krwi. Do najpoważniejszych powikłań choroby cukrzycowej, które są bezpośrednio powiązane z wyżej wymienionymi nieprawidłowościami można zaliczyć naczyniową kalcyfikację (VC) i cukrzycową chorobę nerek (DKD)^{2,3}. Dodatkowo warto zaznaczyć, iż DKD jest najczęstszą przyczyną końcowego stadium niewydolności nerek w krajach rozwiniętych⁴.

Jedną ze struktur, w której mikrokrążenie odgrywa kluczową rolę i która ulega bezpośredniemu uszkodzeniu w DKD jest kłębuszek nerkowy. To sieć naczyń włosowatych otoczonych z zewnątrz torebką Bowmana, a ograniczona przez dwa naczynia oporowe – tętniczkę doprowadzającą i odprowadzającą. Naczynia włosowate kłębuszka nerkowego nie są wspierane przez tkankę śródmiąższową, jak ma to miejsce w innych rejonach ludzkiego ciała. Za stabilizację tej unikatowej struktury odpowiedzialne jest mezangium oraz podocyty – wyspecjalizowane komórki nabłonka trzewnego⁵. To właśnie podocyty, obok śródbłonka naczyń włosowatych i błony podstawnej, są najbardziej dynamicznym elementem kłębuszkowej bariery filtracyjnej (GFB) odpowiedzialnej za filtrację osocza i produkcję moczu pierwotnego^{6,7}.

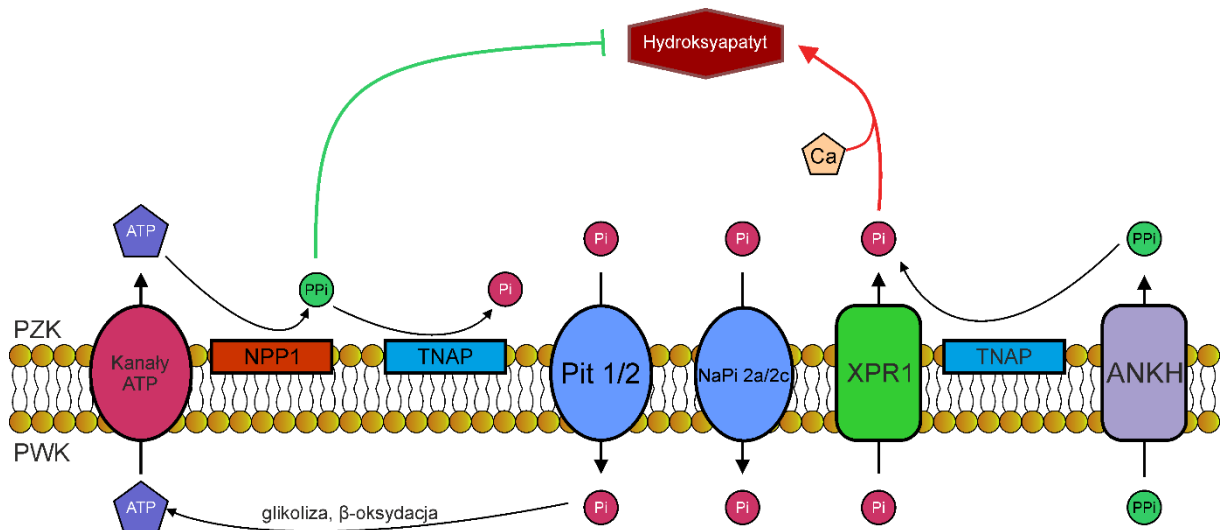
W morfologii podocyta można wyróżnić trzy elementy: ciało komórki, wypustki główne oraz odchodzące od nich wypustki stopowate, które oplatają naczynia włosowate kłębuszka. Zazębiające się wypustki stopowate sąsiednich podocytów tworzą wyjątkową strukturę – szczelinę filtracyjną (SD). Jest ona najbardziej wrażliwą częścią GFB, która jako pierwsza ulega uszkodzeniu w przebiegu wielu glomerulopatii, m. in. DKD. Objawia się to mikroalbuminurią, przeradzającą się w jawny białkomocz wraz z postępem choroby⁸. Co więcej, SD to nie tylko element aktywnie uczestniczący w filtracji krwi. Poprzez obecność charakterystycznych dla podocyta białek (nefryny, podocyny, Neph1) pozwala na wzajemną sygnalizację między przyległymi komórkami⁹. Dlatego też zmiany morfologiczne, takie jak spłaszczenie, poszerzanie się i zlewanie szczelin filtracyjnych obserwowane w przebiegu DKD, oprócz hamowania procesu powstawania ultrafiltratu, wpływają również na metabolizm

i prawidłowe funkcjonowanie podocytów. Ma to ogromne znaczenie, ponieważ są one komórkami terminalnie zróżnicowanymi, nie wykazującymi zdolności do proliferacji i odnowy¹⁰.

Podocyty są komórkami wrażliwymi na insulinę, a ich prawidłowe funkcjonowanie jest ściśle powiązane z fizjologiczną odpowiedzią na ten hormon. W badaniach *in vivo* na myszach ze specyficzną delecją receptora insulinowego (IR) w podocytach zaobserwowano objawy charakterystyczne dla DKD, na czele z albuminurią¹¹. Warto zaznaczyć, iż zmiany te rozwinęły się u zwierząt z prawidłową glikemią. Powyższe dane wskazują na znaczenie insulinooporności podocytów w dezintegracji kłębuszkowej bariery filtracyjnej, czego najpoważniejszą konsekwencją jest utrata białka z moczem. Insulina stymuluje także dokomórkowy transport glukozy w komórkach podocytarnych¹². Po przyłączeniu się insuliny do podjednostki α IR dochodzi do autofosforylacji podjednostki β tego białka, co aktywuje dokomórkowy szlak sygnalizacyjny. Następująca w dalszej kolejności fosforylacja kinazy białkowej B (PKB, znanej również jako Akt) stymuluje translokację pęcherzyków egzosomalnych zawierających transporter glukozy typu 4 (GLUT 4) do błony komórkowej podocyta, co w konsekwencji pozwala na napływ glukozy¹³. Inkubacja podocytów w środowisku hiperglikemicznym imitującym warunki panujące w przebiegu cukrzycy, prowadzi do insulinooporności tych komórek, manifestującej się jako spadek dokomórkowego transportu glukozy z udziałem białka GLUT 4^{14,15} oraz do ich uszkodzenia i apoptozy^{16,17}.

Kalcyfikacja tkanek miękkich to patologiczne zjawisko polegające na odkładaniu się złogów fosforanu wapnia w postaci hydroksyapatytu, przede wszystkim w ścianach naczyń krwionośnych lub zastawkach serca. Strukturą, która jako pierwsza ulega uszkodzeniu w procesie wapnienia są komórki mięśni gładkich naczyń krwionośnych (VSMC). Szacuje się, że u około 40% pacjentów cierpiących z powodu przewlekłej niewydolności nerek rozwija się naczyniowa kalcyfikacja¹⁸. Dodatkowo, istnieje ścisła korelacja pomiędzy VC a progresją uszkodzenia nerek, przy czym związek ten jest znacznie ściślej zaznaczony u chorych z DKD¹⁹. Ponadto, upośledzona funkcja nerek u diabetyków skutkuje rozregulowaniem równowagi mineralnej organizmu. Wraz ze współwystępującymi zaburzeniami metabolicznymi obserwuje się wzrost poziomu nieorganicznego fosforanu (Pi) w surowicy oraz spadek stężenia pirofosforanu (PPi), najsilniejszego endogennego inhibitora wapnienia^{20,21}. Z kolei przewlekła hiperfosfatemia prowadzi do nasilonej ekspresji genów promujących formowanie hydroksyapatytu czego wypadkową jest obraz charakterystyczny dla VC^{22,23}. Ze względu

na fakt, iż jony Pi są swobodnie filtrowane w kłębuszku nerkowym, a ich nadmiar inicjuje procesy wapnienia, dokładne zrozumienie mechanizmu kalcyfikacji jest kluczowe w zapobieganiu uszkodzenia tej podstawowej jednostki funkcjonalnej nerki. Ponieważ ciało komórki podocytarnej jest swobodnie zawieszona w przestrzeni moczowej kłębuszka, w której – ze względu na swoją wielkość – nieobecne są białkowe inhibitory kalcyfikacji (albumina, osteopontyna, fetuina A)²⁴, to właśnie podocyt wydaje się być elementem najbardziej narażonym na kłębuszkową kalcyfikację. Co więcej, z danych literaturowych wynika, że podocyt, zarówno pod kątem funkcjonowania, jak i procesów molekularnych, wykazuje duże podobieństwo do komórek mięśni gładkich²⁵. Dlatego też zmiany zachodzące w podocytach w przebiegu DKD mogą być tożsame z mechanizmami obserwowanymi w VSMC podczas wapnienia naczyń krwionośnych.



Ryc. 1. Schematyczna prezentacja systemu enzymów i transporterów uczestniczących w homeostazie fosforanowej

W zachowaniu homeostazy fosforanowej – obok czynników hormonalnych, takich jak parathormon czy witamina D – uczestniczą wyspecjalizowane białka transportowe i enzymatyczne (Ryc. 1). W nerkowej reabsorpcji jonów Pi biorą udział sodozależne transportery fosforanowe typu II (NaPi 2a i NaPi 2c) zlokalizowane głównie w kanalikach proksymalnych. Natomiast sodozależne transportery typu III (Pit 1 i Pit 2) są odpowiedzialne za dokomórkowy napływ Pi i występują w większości tkanek organizmu^{26,27}. Co ważne, transporter Pit 1 jest kluczowym czynnikiem indukującym mineralizację macierzy kostnej przez osteoblasty²⁸. Kolejnym białkiem uczestniczącym w dokomórkowym transporcie Pi jest ksenotropowy i politropowy receptor renowirusowy 1 (XPR1). W badaniach na myszach

Ansermet i in. wykazali, iż inaktywacja XPR1 w kanalikach proksymalnych nerki upośledza reabsorpcję Pi, co prowadziło do wystąpienia objawów charakterystycznych dla zespołu Fanconiego – glikurii, aminoacydurii, oraz albuminurii²⁹. Istnieje także system ściśle kontrolujący ilość najsilniejszego drobnocząsteczkowego inhibitora mineralizacji jakim jest PPI. Należy do niego izoforma 1 nukleotydowej pirofosfatazy/fosfodiesterazy (NPP1). Enzym ten jest odpowiedzialny za kontrolę tkankowej kalcyfikacji poprzez hydrolizę zewnątrzkomórkowych nukleotydów (głównie ATP), której jednym z produktów jest PPI³⁰⁻³². Do przestrzeni zewnątrzkomórkowej PPI może być także przetransportowany dzięki transbłonowemu homologowi białka postępującej ankylozy (ANKH)³³. Tamże, PPI może funkcjonować jako inhibitor kalcyfikacji, dopóki nie ulegnie hydrolizie do dwóch cząsteczek Pi przez tkankową niespecyficzną fosfatazę zasadową (TNAP).

Białko Pit 1 (znane także jako SLC20A1 lub Glvr-1), obok funkcji transportera jonów Pi oraz uczestniczenia w fizjologicznej mineralizacji tkanki kostnej, bierze aktywny udział w procesie kalcyfikacji tkanek miękkich. Istnieje szereg doniesień na temat jego roli w rozwoju VC. Za pomocą siRNA Li i in. stworzyli VSMC, które cechowała obniżona ekspresja Pit 1³⁴. Inkubowanie tych komórek w medium hodowlanym z podwyższonym stężeniem jonów Pi nie zainicjowało procesów kalcyfikacji, co miało miejsce w przypadku komórek kontrolnych. Ustalenia te zostały potwierdzone przez Masumoto i in., którzy hodując skrawki szczurzych aort w pożywce ze zwiększonym stężeniem fosforanu i wapnia zaobserwowali nasiloną mineralizację badanych preparatów tkankowych, a we wspomnianej kalcyfikacji uczestniczyło białko Pit 1³⁵. Warto zaznaczyć, iż w aortach szczurów uremicznych wzrasta ilość mRNA Pit 1³⁶, co również dowodzi udziału tego białka w mechanizmie VC, będącej konsekwencją niewydolności nerek. Istnieją także doniesienia o roli białka Pit 1 w fizjologii samych podocytów. Kiedy w szczurzych komórkach podocytarnych wyindukowano nadekspresję transportera SLC20A1, u zwierząt zaobserwowano białkomocz i hipoalbuminemię³⁷. Większość kłębuszków nerkowych badanych szczurów wykazywała zmiany sklerotyczne, takie jak dezintegracja GFB, hiperplazja mezangium i adhezja kapilar do ściany torebki Bowmana. Podocyty utraciły swoje wypustki stopowate, a nadprodukcja białek przez uszkodzone komórki doprowadziła do poszerzenia i usztywnienia błony podstawnej, co pogłębiało defekt GFB. Dalsze badania wykazały, że zastosowanie kwasu ryzedronowego (bisfosfonianu wykorzystywanego w leczeniu osteoporozy) zapobiega powstaniu opisanych wyżej zmian³⁸. Co interesujące, w dokomórkowym sygnałowaniu insulinowym, które jest

kluczowe dla prawidłowego funkcjonowania podocytów, pośrednio uczestniczy białko Pit 1. Wyciszenie ekspresji tego transportera w hepatocytach uwrażliwiło komórki wątroby na działanie insuliny oraz usprawniło metabolizm glukozy³⁹.

Drugim białkiem, które istotnie wpływa na szlak sygnałowy zależny od insuliny jest NPP1. Przyłączenie się NPP1 do podjednostki α IR prowadzi do zmian konformacyjnych receptora insulinowego, wskutek czego niemożliwa staje się jego autofosforylacja, co na tak wczesnym etapie hamuje dalszą transdukcję sygnału^{40,41}. Aby NPP1 mógł pełnić rolę inhibitora IR konieczna jest jego aktywność katalityczna⁴². Najnowsze badania wykazują, iż wysokie stężenia kwasu moczowego – często obserwowane w cukrzycy i DKD – powodują zwiększenie powinowactwa NPP1 do IR, co przyczynia się do rozwoju insulinooporności⁴³. Jednakże, główną funkcją NPP1 jest enzymatyczny rozkład zewnątrzkomórkowych nukleotydów, co czyni go ważnym elementem w recyklingu tych związków i mediatorem w sygnałowaniu purynergicznym. Badania naszego zespołu wykazały, że zewnątrzkomórkowe nukleotydy powodują wzrost przepuszczalności GFB dla albuminy poprzez nadprodukcję tlenu azotu i rearanżację cytoszkieletu w podocytach⁴⁴. Natomiast sygnałowanie purynergiczne jest niezbędne w regulacji wewnątrzkomórkowego stężenia jonów wapnia w komórkach kłębuszka nerkowego⁴⁵. Choć powszechnie przyjmuje się, że zewnątrzkomórkowe nukleotydy odgrywają istotną rolę w fizjologii podocytów, brak jest informacji odnośnie udziału enzymu NPP1 w rozwoju kłębuszkowej kalcyfikacji bądź insulinooporności podocytów.

Do tej pory wiedza na temat równowagi fosforanowej w komórkach podocytarnych była znacznie ograniczona. Ze względu na fakt, iż u pacjentów cierpiących na niewydolność nerek istnieje związek między rozregulowaniem homeostazy fosforanowej a insulinoopornością⁴⁶, wydaje się zasadne, aby określić rolę systemu enzymów i transporterów fosforanowych w rozwoju kłębuszkowej kalcyfikacji i insulinooporności podocytów. Zważywszy na powyższe informacje, szczególna uwaga powinna być poświęcona dwóm białkom – transporterowi Pit 1 oraz enzymowi NPP1.

4. Cel pracy

4.1. Cel główny

Celem pracy było wyjaśnienie wpływu środowiska cukrzycowego na homeostazę fosforanową w podocytach, z uwzględnieniem roli białek transportujących fosforan w regulacji sygnałowania zależnego od insuliny oraz rozwoju kłębuszkowej kalcyfikacji.

4.2. Cele szczegółowe

- Ilościowe ustalenie zewnątrzkomórkowego poziomu P_{Pi} i ATP oraz ocena stopnia kalcyfikacji zarówno w podocytach jak i kłębuszkach nerkowych w warunkach hiperglikemicznych.
- Ustalenie poziomu ekspresji białek biorących udział w reabsorpcji Pi (NaPi 2a/2c, Pit 1/2) i eksporcie Pi (XPR1), a także ich komórkowej lokalizacji i roli w procesie kalcyfikacji.
- Analiza ekspresji genów, a także aktywności oraz komórkowej lokalizacji białek zaangażowanych w regulację zewnątrzkomórkowego stężenia P_{Pi} (TNAP, NPP1) w warunkach normo- i hiperglikemii.
- Określenie roli białek biorących udział w homeostazie Pi (Pit 1, NPP1) w regulacji sygnałowania zależnego od insuliny oraz insulinozależnego dokomórkowego transportu glukozy.

4.3. Uzasadnienie połączenia wskazanych publikacji w niniejszy zbiór

Kłębuszkowa kalcyfikacja jest skomplikowanym procesem, w którym uczestniczy wiele białek i enzymów. W pierwszym etapie prowadzonych badań skupiono się na scharakteryzowaniu systemu białek transportujących Pi w komórkach podocytarnych. Oceniono ich rolę i wpływ na gromadzenie się złogów hydroksyapatytu w kłębuszku nerkowym. W kolejnej części badań położono nacisk na ustalenie mechanizmu uszkodzenia podocytów, w szczególności na sposób w jaki białka uczestniczące w homeostazie Pi przyczyniają się do rozwoju insulinooporności tych komórek.

5. Metodologia

5.1. Hodowla podocytów ludzkich

Ludzkie immortalizowane komórki podocytarne otrzymano dzięki uprzejmości prof. Moin A. Saleema z Uniwersytetu w Bristolu. W wyniku transfekcji wrażliwego na temperaturę genu *SV40-T* namnażanie podocytów było możliwe poprzez hodowanie ich w temperaturze 33°C. Po osiągnięciu pożądanej konfluencji komórki inkubowano w temperaturze 37°C przez 10-14 dni, w trakcie których dochodziło do różnicowania podocytów i produkcji specyficznych dla nich białek (nefryny, podocyny, synaptopodyny, CD2AP)⁴⁷.

Podocyty hodowano w pożywce RPMI-1640 (Thermo Fisher Scientific) z dodatkiem 10% FBS oraz 100 U/ml penicyliny i 100 mg/ml streptomycyny (Thermo Fisher Scientific) w następujących układach badawczych:

- Standardowe stężenie glukozy (**SG**, 11 mM) oraz wysokie stężenie glukozy (**HG**, 30 mM, 5 dni) – dane literaturowe wskazują, iż pięciodniowa inkubacja podocytów w warunkach HG prowadzi do ich insulinooporności co objawia się zahamowaniem insulinozależnego dokomórkowego transportu glukozy^{14,15,48};
- **SG** oraz wysokie stężenie insuliny (**HI**, 100 nM, 5 min/1h/24h).

5.2. Doświadczenia z wykorzystaniem szczurów rasy Wistar

Eksperymenty przeprowadzono na samcach szczurów rasy Wistar, które utrzymywano w cyklu 12h światła/12h ciemności, ze swobodnym dostępem do paszy i wody pitnej. Eksperymenty przeprowadzono zgodnie z dyrektywą 2010/63/UE, a protokół został zatwierdzony przez Lokalną Komisję Etyczną w Bydgoszczy (nr 51/2018 i 47/2018 BIS). Cukrzycę wyindukowano poprzez dootrzewnowe podanie streptozotocyny (STZ, 80 mg/kg). Grupę kontrolną (CTRL) stanowiły szczury o wieku tożsamym ze szczurami z grupy badawczej. Eksperymenty przeprowadzono po 14 dniach od wyindukowania cukrzycy. Szczury umieszczono w oddzielnych klatkach metabolicznych na 48h, ze swobodnym dostępem do paszy i wody pitnej. Zwierzętom pozwolono na adaptację do warunków przez pierwsze 24h. W ciągu następnych 24h zbierano mocz, w którym oznaczono dobowe wydalenie kreatyniny i albuminy. Następnie dokonano eutanazji zwierząt i natychmiast pobrano krew, w celu oceny

poziomu albuminy, fosforanów, kreatyniny oraz aktywności fosfatazy zasadowej. Pomiaru parametrów biochemicznych dokonano w zewnętrznym laboratorium.

5.3. Western blot

Aby ocenić obecność analizowanych białek w podocytach lizaty komórkowe nakładano na 10% żel poliakrylamidowy (20 – 30 µg białka na ścieżkę żelu) i rozdzielano pod względem masy cząsteczkowej za pomocą elektroforezy SDS-PAGE. Następnie białka poprzez elektrotransfer przenoszono na membrany z polifluorku winylidenu. Kolejnym krokiem była całonocna inkubacja membran ze specyficznymi przeciwciałami pierwszorzędowymi skierowanymi przeciwko badanym białkom (Tabela 1). Detekcja białek odbywała się przez zastosowanie przeciwciał drugorzędowych sprzężonych z peroksydazą chrzanową (Sigma Aldrich). Otrzymane prążki analizowano densytometrycznie w programie Quantity One (Bio-Rad).

Tabela 1. Spis przeciwciał pierwszorzędowych użytych w badaniach.

Białko	Rozcieńczenie	Producent
Pit 1	1:4000 (WB), 1:25 (IF), 1:25 (IHC)	Biorbyt
Pit 2	1:1000 (WB), 1:25 (IF), 1:100 (IHC)	Biorbyt (WB, IF), Novus Biological (IHC)
NaPi 2c	1:500 (WB), 1:30 (IF), 1:100 (IHC)	Novus Biological (WB), MyBioSource (IF), Biorbyt (IHC)
XPR1	1:450 (WB), 1:25 (IF), 1:50 (IHC)	Sigma Aldrich (WB, IF), Novus Biological (IHC)
NPP1	1:100 (WB), 1:15 (IF)	Santa Cruz Biotechnology
β-aktyna	1:5000 (WB)	Sigma Aldrich
Nefryna	1:50 (IF)	Santa Cruz Biotechnology
IRβ	1:250 (WB), 1:20 (IF)	Santa Cruz Biotechnology
p-IRβ (Tyr 1150/1151)	1:250 (WB)	Santa Cruz Biotechnology
IRα	1:1500 (WB), 1:30 (IF)	Thermo Fisher Scientific
Akt	1:350 (WB)	Santa Cruz Biotechnology
p-Akt (Ser 473)	1:350 (WB)	Santa Cruz Biotechnology
Rab5a	1:50 (IF)	ABclonal
GLUT 4	1:300 (WB)	Santa Cruz Biotechnology

WB – Western blot, IF – immunofluorescencja, IHC – immunohistochemia.

5.4. Biotynylacja

Aby ocenić obecność analizowanych białek w błonie komórkowej, podocyty inkubowano z 1 mg/ml roztworem biotyny (Thermo Fisher Scientific) w temperaturze 4°C przez 30 min. Niezwiązaną biotynę usunięto przez pięciokrotne przemywanie komórek PBS z 100 mM glicyną,

a następnie wykonano lizaty komórkowe. Część lizatu zamrożono w celu oceny całkowitej ilości badanych białek. Drugą część próbki inkubowano ze złożem Neutr/Avidin (Thermo Fisher Scientific) na kołyszce obrotowej w temperaturze 4°C przez noc. Białka obecne w błonie komórkowej pokryte biotyną wiązały się ze złożem awidynowym. Tak przygotowane próbki były poddane dalszej analizie Western blot.

5.5. Immunoprecypitacja

W celu identyfikacji kompleksów białkowych lizaty komórkowe oczyszczono przy użyciu Protein G PLUS-Agarose (Santa Cruz Biotechnology) na rotorze w temperaturze 4°C przez 30 min. Tak przygotowane próbki inkubowano z odczynnikiem IP/WB Optima B lub IP/WB Optima C (Santa Cruz Biotechnology) wzbogaconym o przeciwciało anty-NPP1 na kołyszce obrotowej w temperaturze 4°C przez noc. Aby eluować kompleksy białkowe, lizaty ogrzewano w buforze obciążającym zawierającym SDS w temperaturze 96°C przez 10 min. Następnie eluat poddano analizie Western blot.

5.6. Immunofluorescencja i obrazowanie pęcherzyków endosomalnych

Podocyty utrwalono w 4% formaldehydzie w temperaturze pokojowej przez 20 min, permabilizowano w 0,1% Triton X-100, a następnie inkubowano w roztworze blokującym (2% FBS, 2% BSA, 0,2% żelatyna rybia) w temperaturze pokojowej przez 1h. Komórki następnie inkubowano z przeciwciałami pierwszorzędowymi (Tabela 1) w temperaturze 4°C przez noc. Następnego dnia szkiełka zanurzono w roztworze przeciwciał drugorzędowych (Thermo Fisher Scientific) w temperaturze 4°C na 2h. Do wykrywania pęcherzyków endosomalnych użyto zestawów komercyjnych pHrodo™ Green Dextran i pHrodo™ Red Dextran (Thermo Fisher Scientific) zgodnie z protokołem producenta. Obrazowania fluorescencyjnego dokonano przy użyciu mikroskopu konfokalnego (Eclipse Ti, Nikon Instruments).

5.7. Immunohistochemia

Utrwalone w formalinie i zatopione w parafinie skrawki nerek szczurów CTRL i STZ odparafinowano przy użyciu odczynnika Histochoice (Sigma Aldrich) i ponownie uwodniono w szeregu malejących stężeń roztworu etanolu (100%, 95%, 90%, 70%, i 50%). Indukowane ciepłem odkrywanie epitopów przeprowadzono przez ogrzewanie szkiełek w 10 mM buforze

cytrynianowym w temperaturze 100°C przez 20 min. Po blokowaniu szkiełek w 5% BSA w PBS, preparaty inkubowano z przeciwciałami pierwszorzędowymi (Tabela 1) w temperaturze 4°C przez noc. Następnego dnia skrawki nerek inkubowano z przeciwciałami drugorzędowymi (Cell Signaling Technology) w temperaturze pokojowej przez 30 min i barwiono używając substratu SignalStain DAB (Cell Signaling Technology) Na koniec preparaty podbarwiono hematoksyliną i odwodniono. Skrawki tkanek obrazowano za pomocą mikroskopu świetlnego (Eclipse Ti, Nikon Instruments).

5.8. *Transdukcja lentiwirusowa*

Aby wyciszyć gen *SLC20A1* kodujący transporter Pit 1, podocyty transdukowano specjalnie zaprojektowanymi cząstkami lentiwirusowymi: GIPZ *SLC20A1* shRNA Viral Particles oraz GIPZ Non-silencing shRNA Viral Particles (Dharmacon) jako kontrola negatywna. Selekcję podocytów wykazujących ekspresję shRNA przeprowadzono przy użyciu puromycyny. Następnie podocyty hodowano w temperaturze 37°C w celu różnicowania. Wyciszanie genu oceniono za pomocą real-time PCR i immunofluorescencji.

5.9. *Izolacja mRNA i real-time PCR*

Całkowite RNA izolowano przy użyciu zestawu RNeasy Plus Mini Kit (Qiagen), a jego czystość i stężenie oceniono za pomocą urządzenia NanoDrop (Thermo Fisher Scientific). Następnie wyizolowany RNA poddano analizie PCR z odwrotną transkrypcją. Otrzymane komplementarne DNA analizowano metodą real-time PCR z wykorzystaniem aparatu LightCycler 480 (Roche) przy użyciu specyficznych starterów oraz fluorescencyjnych sond. Dzięki metodzie $\Delta\Delta C_t$ z genem β -aktyny jako genem referencyjnym określono względną ilość specyficznych transkryptów mRNA.

5.10. *Aktywność TNAP i eNPP*

Aktywność TNAP oznaczono za pomocą zestawu SteamTAG Alkaline Phosphatase Activity Assay Kit (BioCat) zgodnie z zaleceniami producenta

Pomiaru aktywności ektonukleotydowej pirofosfatazy/fosfodiesterazy (eNPP) dokonano przy użyciu 5'-monofosforanu p-nitrofenylotymidyny (pNTMP) jako substratu. Podocyty poddano lizie w 200 mM buforze Tris-HCl z dodatkiem 1% Triton X-100 i 1,6 mM MgCl₂.

Po 20 minutowej inkubacji lizatu z 1 mg/ml roztworem substratu, zmierzono absorbancję powstającego żółto zabarwionego produktu przy $\lambda = 405$ nm.

5.11. Ocena intensywności kalcyfikacji kłębuszków nerkowych i podocytów

Preparaty szczurzych nerek były odparafinowane i uwodnione w taki sam sposób jak w przypadku analizy immunohistochemicznej. Skrawki inkubowano w 2% roztworze barwnika Alizarin Red S (Sigma Aldrich) w temperaturze pokojowej przez 1h. Po odpłukaniu barwnika preparaty podbarwiono hematoksyliną i odwodniono.

Ludzkie podocyty były utrwalone i permabilizowane identycznie jak w przypadku barwienia immunofluorescencyjnego. Komórki następnie barwiono w 2% roztworze Alizarin Red S w temperaturze pokojowej przez 1h. Po tym czasie nadmiar barwnika odpłukano wodą destylowaną. Skrawki szczurzych nerek oraz zabarwione podocyty obrazowano za pomocą mikroskopu świetlnego (Eclipse Ti, Nikon Instruments). Do ilościowej oceny intensywności kalcyfikacji użyto programu ImageJ (National Institutes of Health).

5.12. Poziom ATP

Pomiar wykonano za pomocą komercyjnego zestawu ATP Determination Kit (Invitrogen) zgodnie z zaleceniami producenta. Otrzymaną luminescencję mierzono za pomocą luminometru Sirius 2 (Berthold Technologies).

5.13. Dookomórkowy transport glukozy

24h przed rozpoczęciem doświadczenia podocyty inkubowano w pożywce bez FBS i antybiotyków. Ocenę prowadzono przez dodanie 1 μCi /studzienkę (1,2- ^3H)-dezoksy-D-glukozy rozcieńczonej w „zimnej” glukozie o końcowym stężeniu wynoszącym 50 μM . Radioaktywność zewnątrzkomórkową mierzono w pożywce zebranej z nad komórek. Aby ocenić radioaktywność wewnątrzkomórkową podocyty poddano lizie w 0,5 M NaOH. Pomiarów dokonano aparatem MicroBeta2 Microplate Counter (Perkin Elmer).

5.14. Aktywność oksydazy NADPH i poziom RONS

W celu ustalenia aktywności oksydazy NADPH zastosowano pomiar chemiluminescencji indukowanej lucygeniną za pomocą luminometru Sirius 2 (Berthold Technologies). Metoda

polegała na ocenie AUC w celu wyznaczenia ilości anionu ponadtlenkowego i odniesienia jej do scharakteryzowanej wcześniej krzywej wzorcowej⁴⁹.

Dioctan 2',7'-dichlorodihydrofluoresceiny (H₂DCFDA) zastosowano jako fluorosondę do oceny wytwarzania RONS. H₂DCFDA była wewnątrzkomórkowo transformowana do 2',7'-dichlorodihydrofluoresceiny (DCF). Pomiar fluorescencji DCF przeprowadzono za pomocą czytnika EnSpire (Perkin Elmer) przy E_{ex}/E_{em} = 485/525 nm.

5.15. Analiza statystyczna

Wyniki zaprezentowano jako średnia ± standardowy błąd średniej (SEM). Do analizy rozkładu otrzymanych danych wykorzystano test Shapiro-Wilka. Jeśli rozkład danych podlegał rozkładowi normalnemu grupy porównywano wykorzystując testy parametryczne (test t-Studenta bądź ANOVA). W przeciwnym wypadku stosowano testy nieparametryczne. Poziom istotności ustalono na poziomie $p < 0,05$. Wszystkie analizy wykonano w programie Prism 8.4.3 (GraphPad).

6. Omówienie i podsumowanie najważniejszych wyników

6.1. Rola transporterów fosforanowych w kłębuszkowej kalcyfikacji indukowanej wysokim stężeniem glukozy

Publikacja 1⁵⁰

W ludzkim organizmie formowanie się hydroksyapatytu jest stanem pożądanym tylko w przypadku mineralizacji kości i zębów. Jeśli wytrącanie się soli fosforanu wapnia ma miejsce w innych tkankach, prowadzi to do groźnych dla zdrowia konsekwencji, m. in. do usztywnienia ścian naczyń krwionośnych w przebiegu VC, upośledzenia funkcji zastawek serca czy rozwoju niewydolności nerek wraz z postępującym białkomoczem^{51,52}. Wymienione zaburzenia są najczęściej obserwowane jako powikłania choroby cukrzycowej. Do tej pory badacze najdokładniej poznali mechanizm rozwoju VC, kładąc nacisk na udział transporterów fosforanowych i białek enzymatycznych kontrolujących poziom samego Pi. Jednakże, w przebiegu T2D jedną z pierwszych struktur doznających uszkodzenia jest kłębuszek nerkowy. Moment ten wydaje się być często niezauważalny ze względu na swój skąpoobjawowy przebieg. Dlatego też kluczowe jest ustalenie patomechanizmu deregulacji GFB przez hiperfosfatemię i następującą kalcyfikację.

W pierwszym etapie badań oceniono stopień zaburzenia homeostazy fosforanowej oraz jej wpływ na nerkową kalcyfikację. W tym celu posłużono się szczurzym modelem z cukrzycą wyindukowaną streptozotocyną (szczury STZ). Dzięki analizie parametrów biochemicznych krwi i moczu tychże zwierząt zaobserwowano nieprawidłowości dotyczące funkcji nerek, które są charakterystyczne dla pacjentów cierpiących z powodu DKD⁵³. W porównaniu do szczurów kontrolnych (CTRL), u szczurów STZ stwierdzono prawie siedemnastokrotny wzrost wydalania albuminy z moczem, któremu towarzyszyła hipalbuminemia oraz podwyższone stężenie kreatyniny w surowicy (Tabela 5). U szczurów STZ w porównaniu do szczurów CTRL doszło także do deregulacji gospodarki fosforanowej, o czym świadczy 44% wzrost surowiczego stężenia jonów Pi, a także dwukrotny wzrost aktywności fosfatazy zasadowej. Oprócz powyższych nieprawidłowości, dzięki wybarwieniu złogów fosforanu wapnia w preparatach nerek badanych zwierząt, u szczurów STZ stwierdzono wzmożone procesy kalcyfikacyjne (Fig. 1). Co warte zauważenia, analogiczne obserwacje odnotowano

w przypadku ludzkich komórek podocytnych hodowanych w warunkach wysokiego stężenia glukozy (Fig. 8).

Chcąc ustalić czy w rozwoju kłębuszkowej kalcyfikacji uczestniczą białka transportujące nieorganiczny Pi, preparaty szczurzych nerek poddano analizie immunohistochemicznej (Fig. 2A-B). W badaniu tym ustalono istotny spadek ilości sodozależnych transporterów fosforanowych typu II (NaPi 2c) oraz typu III (Pit 1 i Pit 2) w kłębuszkach nerkowych szczurów STZ (Fig. 2C-E). Nie zmieniła się natomiast ilość białka XPR1 odpowiedzialnego za eksport jonów Pi (Fig. 2F).

W celu potwierdzenia prawidłowości ustalonych w modelu *in vivo*, postanowiono scharakteryzować stopień ekspresji genów kodujących analizowane transportery fosforanowe oraz ilość i lokalizację tych białek *in vitro* w ludzkich immortalizowanych podocytach. Wykorzystując metodę real-time PCR ustalono obecność transkryptów genów *SLC20A1*, *SLC20A2*, *SLC34A3* i *XPR1*, które kodują odpowiednio białka Pit 1, Pit 2, NaPi 2c oraz XPR1 (Fig. 3A). W barwieniu immunofluorescencyjnym badane transportery zlokalizowane były głównie w błonie komórkowej podocyta oraz w wypustkach stopowatych sąsiadujących komórek, o czym świadczy wysoka intensywność fluorescencji (Fig. 3B). W podocytach hodowanych w warunkach HG doszło do spadku produkcji białka Pit 1, zarówno na poziomie transkrypcji jak i translacji. Odnotowano 19% zmniejszenie ilości mRNA (Fig 4A) oraz 48% redukcję w ilości samego białka (Fig. 4E). Podobną zależność ustalono w przypadku białka Pit 2, gdzie jego ilość w warunkach HG zmniejszyła się o 34% (Fig. 4F), przy czym ekspresja genu *SLC20A2* pozostawała na niezmiennym poziomie. Nie stwierdzono natomiast zmian w ilości transporterów NaPi 2c i XPR1 w podocytach inkubowanych w środowisku HG w porównaniu do warunków kontrolnych.

Wszystkie dotychczas analizowane białka pełnią swoją funkcję w błonie komórkowej. Dlatego kolejnym etapem niniejszych badań było ustalenie w jaki sposób warunki hiperglikemiczne wpływają na komórkową lokalizację transporterów Pi w podocycie. Dzięki metodzie biotynylacji białek błony komórkowej odkryto, iż w warunkach HG dochodzi do zmniejszenia ilości wszystkich sodozależnych transporterów fosforanowych w błonie plazmatycznej podocyta. Największy, bo aż 60% spadek w błonowej lokalizacji odnotowano dla transportera Pit 1 (Fig 5A). W podobnym stopniu zmniejszyła się ilość białek Pit 2 i NaPi 2c w błonie komórkowej podocyta, odpowiednio o 36% i 41% (Fig. 5B-C). Natomiast w środowisku HG odnotowano prawie czterokrotny wzrost ilości transportera XPR1 w błonie

plazmatycznej, którego główną rolą jest eksport jonów Pi (Fig. 5D). Powyższe dane sugerują, iż w środowisku hiperglikemicznym może dochodzić do retencji jonów Pi w PZK z powodu zmniejszenia sodozależnego dokomórkowego transportu fosforanów z udziałem białek Pit 1, Pit 2 oraz NaPi 2c i nasilonego eksportu Pi poprzez białko XPR1.

Oprócz transporterów Pi w homeostazie fosforanowej uczestniczą także białka enzymatyczne, które ściśle kontrolują poziom fosfatemii. Dlatego też w dalszych etapach badań w ludzkich komórkach podocytnych ustalono stopień ekspresji i aktywności dwóch kluczowych enzymów – NPP1 oraz TNAP. Środowisko HG spowodowało 14% spadek ekspresji genu *ENPP1*, kodującego białko NPP1 (Fig. 6A), natomiast nie zauważono różnic w ekspresji genu *ALPL*, który koduje enzym TNAP (Fig. 6B). Jednak pomimo stałej ilości mRNA, aktywność TNAP zwiększyła się o 24% w warunkach HG w porównaniu do SG (Fig. 6D). Można więc domniemywać, iż w podocytach narażonych na przewlekłą hiperglikemię wzrasta produkcja jonów Pi. Warto zwrócić uwagę na fakt, iż warunki hiperglikemiczne nie wpłynęły na ogólną aktywność eNPP (Fig. 6C). Jednakże enzym NPP1 jest również białkiem transbłonowym i z tego powodu postanowiono sprawdzić jego ilość w błonie komórkowej podocyta. Okazało się, iż w środowisku HG dochodzi do ponad 60% spadku w ilości NPP1 w błonie plazmatycznej (Fig. 6E). Konsekwencją tegoż zjawiska, jest 22% spadek w zewnątrzkomórkowym stężeniu PPi (Fig. 7C), który jest jednym z produktów hydrolizy nukleotydów katalizowanej przez NPP1. Dodatkowo, redukcja zewnątrzkomórkowej ilości PPi jest także potwierdzeniem zwiększonej aktywności TNAP, ponieważ enzym ten bierze udział w hydrolizie PPi do dwóch cząsteczek Pi.

Podsumowując, niniejsze badania po raz pierwszy wykazały obecność w ludzkich podocytach sodozależnych transporterów fosforanowych oraz dowiodły, iż warunki hiperglikemiczne wpływają na ich ilość i rozmieszczenie w komórce. Obserwacje uzyskane w ramach badań *in vitro* potwierdziły wyniki uzyskane w badaniach *in vivo* na szczurzym modelu z cukrzycą wyindukowaną podaniem streptozotocyny. U szczurów STZ zaobserwowano spadek ilości sodozależnych transporterów Pi w kłębuszkach nerkowych. Stwierdzono także zwiększenie aktywności TNAP w ludzkich podocytach oraz zmniejszenie ilości białka NPP1 w błonie komórkowej, co w rezultacie przyczyniło się do spadku zewnątrzkomórkowego stężenia PPi, będącego jednym z najsilniejszych inhibitorów mineralizacji. Powyższe zmiany mogą przyczynić się do nasilenia procesów zwapnienia

zarówno w ludzkich podocytach w warunkach HG, jak i w nerkach szczurów z wyindukowaną cukrzycą.

6.2. *Transporter Pit 1 jako kluczowy czynnik w zależnej od NPP1 inhibicji sygnalizacji insulinowej w ludzkich podocytach*

Publikacja 2⁵⁴

Insulina jest hormonem odgrywającym znaczącą rolę w fizjologii komórki podocytarnej. Oprócz stymulacji dokomórkowego transportu glukozy przez transporter GLUT 4⁵⁵, insulina – przyłączając się do swojego receptora^{56,57} – inicjuje szereg różnorodnych procesów wewnątrzkomórkowych umożliwiających prawidłowe funkcjonowanie podocytów, a w konsekwencji kłębuszkowej bariery filtracyjnej. Badania prowadzone w naszym zespole udowodniły, że główną wypadkową zaburzenia w sygnałowaniu insulinowym jest rearanżacja podocytarnego cytoszkieletu. Zjawisko to prowadzi do zmian w morfologii podocyta, indukcji stresu oksydacyjnego, a także do utraty spójności SD tworzonej przez wypustki stopowate, co w konsekwencji powoduje dezintegrację GFB i zwiększenie przepuszczalności tej struktury dla albuminy⁵⁸⁻⁶³. Mając na uwadze wcześniejsze ustalenia roli białek Pit 1 i NPP1 w procesach kalcyfikacyjnych zachodzących w podocytach, a także fakt, iż omawiane cząsteczki biorą udział w sygnalizacji insulinowej^{39,64}, postanowiono sprawdzić w jaki sposób przyczyniają się one do rozwoju insulinooporności podocytów w przebiegu DKD.

W pierwszym etapie prowadzonych badań sprawdzono czy hodowla ludzkich podocytów w warunkach hiperinsulinemicznych (HI, 100 nM) przez 5 min, 1h i 24h wpływa na ekspresję genów kodujących analizowane białka oraz na ilość tychże białek. Ustalono 22% zwiększenie ilości transkryptu genu *ENPP1* po 1h inkubacji podocytów z insuliną, przy czym po dobie wzrost ten osiągnął 30% (Fig. 1A). Natomiast ilość mRNA Pit 1 zwiększyła się o 30% już po pięciominutowej inkubacji z insuliną, a przyrost ten utrzymywał się przez cały analizowany okres (Fig. 1B). Odwrotną tendencję zaobserwowano na poziomie białka. Pięciominutowa inkubacja podocytów z insuliną spowodowała prawie 50% spadek ilość enzymu NPP1 w porównaniu do komórek kontrolnych, natomiast ilość transportera Pit 1 spadła o 30% (Fig. 1C). Zaobserwowany wzrost ilości mRNA może być mechanizmem kompensującym redukcję ilości dwóch badanych białek. Następnie ustalono wzrost aktywności eNPP już po 5 minutowej hodowli podocytów warunkach HI, który utrzymywał się do 1h (Fig. 1D). Powyższe obserwacje potwierdza spadek zewnątrzkomórkowego stężenia ATP (Fig. 1D). Dodatkowo warto zauważyć, że już krótkotrwała inkubacja podocytów w warunkach HI

doprowadziła do rozwoju stresu oksydacyjnego, o czym świadczy zwiększona aktywność oksydazy NADPH oraz wzrost ilości RONS (Fig. 1E).

Ważnym elementem prowadzonych badań było ustalenie momentu, w którym podocyty tracą wrażliwość na działanie insuliny. W tym celu dokonano pomiaru poziomu dokomórkowego transportu glukozy. Warunki hiperinsulinemiczne spowodowały wzrost poboru glukozy przez podocyty tylko w dwóch analizowanych punktach czasowych – po 5 min oraz po 1h. Natomiast po 24h inkubacji w środowisku HI dokomórkowy transport glukozy był porównywalny do transportu glukozy do komórek kontrolnych (Fig. 2A), co może świadczyć o rozwoju insulinooporności podocytów. Aby potwierdzić powyższe ustalenia, zbadano stopień fosforylacji receptora insulinowego (IR) oraz kinazy białkowej B (Akt). Są to jedne z głównych elementów szlaku sygnalizacyjnego zależnego od insuliny, a fosforylacja tych molekuł umożliwia translokację pęcherzyków egzosomalnych zawierających transporter GLUT 4 do błony komórkowej i następowy napływ glukozy. Największy wzrost poziomu fosforylacji IR i Akt uzyskano dla podocytów inkubowanych w warunkach HI przez 5 min (Fig 2B), co pozostaje w korelacji z wynikami otrzymanymi podczas pomiarów transportu glukozy opisanymi powyżej. Po 24h inkubacji podocytów z insuliną nie wykryto różnic w stopniu fosforylacji IR i Akt w porównaniu do komórek kontrolnych, co świadczy o zahamowaniu sygnałowania insulinowego w podocycie. Dodatkowo, zbadano także komórkową lokalizację zarówno receptora insulinowego oraz transportera GLUT 4. Oba te białka ulegały translokacji z błony komórkowej podocyta po 5 min inkubacji z wysokim stężeniem insuliny (Fig 2D). Zjawisko to jest fizjologiczną odpowiedzią komórki na krótkotrwałą stymulację insuliną^{65,66}. Dodatkowo ustalono również, iż po pięciominutowej inkubacji podocytów z insuliną ilość NPP 1 i Pit 1 w błonie komórkowej zmniejsza się odpowiednio o 90% i 83% (Fig. 3B).

We wcześniejszych badaniach ustalono związek między aktywnością NPP1 a jego zdolnością do hamowania IR poprzez bezpośrednią interakcję z podjednostką α^{42} . Dlatego też zbadano, czy NPP1 oddziałuje z IR i Pit 1 w warunkach HI. Dzięki metodzie immunoprecypitacji ustalono formowanie się kompleksów NPP1/IR oraz NPP1/Pit 1 po 24h hodowli podocytów w środowisku HI, kiedy komórki te tracą wrażliwość na insulinę (Fig. 3A). Interakcja NPP1 z IR i Pit 1 była również zbadana poprzez barwienie immunofluorescencyjne. Dzięki analizie współczynników kolokalizacji *k1* oraz *k2* zaobserwowano istotny wzrost w nakładaniu się sygnałów fluorescencji dla par NPP1/IR oraz NPP1/Pit 1 po 24h inkubacji podocytów z insuliną (Fig. 4A-B). Ponadto, dzięki wybarwieniu białka Rab5a

(odpowiedzialnego za fuzję błony komórkowej z wczesnymi endosomami) oraz samych pęcherzyków endosomalnych ustalono, że do szybkiej internalizacji analizowanych białek dochodzi właśnie na drodze endocytozy (Fig. 4C).

Opierając się na wzajemnej interakcji NPP1 i Pit 1 oraz naszych wcześniejszych ustaleniach dotyczących zmniejszenia ilości białka Pit 1 w podocytach hodowanych w warunkach hiperglikemicznych, postanowiono sprawdzić, czy białko Pit 1 jest odpowiedzialne za regulację sygnałowania insulinowego w ludzkich podocytach. W tym celu poprzez transdukcję lentiwirusową do podocytów wprowadzono shRNA wyciszające ekspresję genu *SLC20A1* kodującego transporter Pit 1 (komórki shPit 1). Ekspresja wyciszanego genu zmniejszyła się o 42%, natomiast produkcja białka Pit 1 spadła o 31% (Fig. 5A-B) w porównaniu do komórek kontrolnych (shControl). Kolejnym krokiem było sprawdzenie aktywności eNPP w komórkach shPit 1. W porównaniu do komórek shControl, w komórkach shPit 1 wykazano istotny wzrost aktywności enzymatycznej eNPP, przy czym inkubacja komórek shPit 1 w środowisku HI nie prowadziła do zwiększenia tej aktywności (Fig. 5C). Analogiczne obserwacje poczyniono w przypadku zewnątrzkomórkowego stężenia ATP – wyciszenie ekspresji genu *SLC20A1* spowodowało spadek ilości ATP, lecz było to niezależne od warunków w jakich hodowano podocyty (Fig. 5C). Warto również zauważyć, iż zahamowanie ekspresji *SLC20A1* prowadziło do indukcji stresu oksydacyjnego, na co wskazuje zwiększona aktywność oksydazy NADPH oraz generacja RONS w komórkach shPit 1 (Fig. 5D).

W następnym etapie sprawdzono, czy w komórkach shPit 1 doszło do zmian w ilości lub lokalizacji białka NPP1. W komórkach transdukowanych za pomocą kontrolnego shRNA pięciominutowa inkubacja z insuliną spowodowała niemal całkowitą translokację NPP1 z błony komórkowej (co obserwowano w podocytach, których nie poddawano transdukcji). Taką samą prawidłowość zaobserwowano dla podocytów shPit 1 hodowanych w warunkach SG, jednakże krótkotrwała stymulacja tych komórek insuliną nie wpływała na lokalizację NPP1 (Fig. 6A). Następnie, w komórkach shPit 1 dzięki immunofluorescencji postanowiono wybarwić pęcherzyki endosomalne oraz analizowane wcześniej białko Rab5a (Fig. 6B). W komórkach kontrolnych, pięciominutowa inkubacja w warunkach HI prowadziła do translokacji pęcherzyków endosomalnych w pobliże błony komórkowej podocyta. Natomiast w komórkach shPit 1, niezależnie od działania insuliny, pęcherzyki endosomalne gromadziły się w przestrzeni okołojądrowej. Podobne obserwacje poczyniono dla białka

Rab5a. W podocytach shPit 1 białko Rab5a zlokalizowane było w pobliżu jądra komórkowego, niezależnie od obecności insuliny w środowisku hodowlanym. Powyższe dane sugerują, że procesy endocytozy są tłumione w komórkach z wyciszoną ekspresją genu *SLC20A1*.

Ostatnim elementem, na którym skupiono się w niniejszych badaniach była ocena w jaki sposób wyciszenie ekspresji genu *SLC20A1* wpływa na sygnałowanie insulinowe w podocycie. Analizując stosunek p-IR/IR oraz p-Akt/Akt nie stwierdzono różnic w stopniu fosforylacji tych dwóch białek w komórkach shPit 1 w porównaniu do komórek kontrolnych. Jednakże, krótkotrwała inkubacja podocytów shPit 1 w warunkach HI nie doprowadziła do wzrostu stopnia fosforylacji IR i Akt, a w konsekwencji nie doszło do aktywacji szlaku zależnego od insuliny (Fig. 7A). Warto również zaznaczyć, iż w komórkach shPit 1 zmieniło się także komórkowe rozmieszczenie receptora insulinowego i transportera GLUT 4. Oba analizowane białka były przemieszczane z błony komórkowej podocyta, bez względu na to, czy komórki hodowano w pożywce SG, czy HI (Fig. 7B). Mając na uwadze powyższe obserwacje postanowiono zbadać dokomórkowy transport glukozy. W komórkach shControl pięciominutowa inkubacja z insuliną spowodowała 25% wzrost wychwytu glukozy, podczas gdy w podocytach z wyciszonym genem *SLC20A1* ten efekt insuliny był zniesiony (Fig. 7C).

W niniejszej pracy wykazano, iż zmiany we wrażliwości podocytów na insulinę rozwijają się po 24h inkubacji komórek w środowisku hiperinsulinemicznym. Świadczy o tym zmniejszona fosforylacja białek IR oraz Akt – które są jednymi z kluczowych elementów w kaskadzie sygnalizacyjnej insuliny. Po tym czasie zahamowaniu uległ także insulinozależny dokomórkowy transport glukozy. W podocytach ze zmniejszoną wrażliwością na insulinę stwierdzono również tworzenie się kompleksów NPP1/IR oraz NPP1/Pit 1. Ponadto zaobserwowano, iż wyciszenie genu *SLC20A1* kodującego transporter Pit 1 prowadzi do wystąpienia zmian charakterystycznych dla komórek z wyindukowaną insulinoopornością.

6.3. Podsumowanie wyników

Wyniki prezentowane w niniejszej rozprawie doktorskiej wskazują, iż warunki hiperglikemiczne i hiperinsulinemiczne obserwowane w przebiegu cukrzycy przyczyniają się do rozwoju patologicznej kłębuszkowej kalcyfikacji oraz do zaburzeń sygnalizacji insulinowej w podocycie. W obu tych zjawiskach aktywnie uczestniczą białka i enzymy warunkujące homeostazę fosforanową. Do rozwoju procesów kalcyfikacyjnych prowadzą zmiany w komórkowym rozmieszczeniu transporterów fosforanowych. Środowisko hiperglikemiczne powoduje zwiększenie produkcji jonów Pi oraz ich retencji w przestrzeni zewnątrzkomórkowej z jednoczesną redukcją naturalnie występujących inhibitorów mineralizacji.

Prawidłowe funkcjonowanie komórek podocytarnych ulega zaburzeniu nie tylko przez rozwój kłębuszkowej kalcyfikacji. Białka uczestniczące w homeostazie Pi – w szczególności Pit 1 i NPP1 – przyczyniają się do uniewrażliwienia podocytów na działanie insuliny. Fizjologiczna reakcja podocytów na ten hormon warunkuje zachowanie integralności kłębuszkowej bariery filtracyjnej. Natomiast wedle ustaleń prezentowanych w niniejszej pracy, do insulinooporności podocytów przyczynia się formowanie kompleksów zarówno NPP1/IR oraz NPP1/Pit 1. Skutkiem tegoż zjawiska jest inhibicja sygnalizacji insulinowej w podocycie, a także rozwój stresu oksydacyjnego co upośledza prawidłowe funkcjonowanie tych komórek. Na szczególną uwagę zasługuje fakt, iż zahamowanie ekspresji genu kodującego transporter Pit 1 bezpośrednio przyczynia się do zaburzenia wrażliwości podocytów na działanie insuliny w przebiegu cukrzycowej choroby nerek.

7. Wnioski

1. **W podocytach długotrwanie eksponowanych na wysokie stężenie glukozy, które odzwierciedla warunki panujące w przebiegu cukrzycowej choroby nerek, dochodzi do zmian zarówno w ilości, jak i w komórkowej lokalizacji analizowanych transporterów fosforanowych.** Zmniejszenie błonowej frakcji sodozależnych transporterów Pi przy współistniejącym zwiększeniu ilości białka XPR1 w błonie komórkowej podocyta prowadzi do retencji jonów Pi w przestrzeni zewnątrzkomórkowej, co skutkuje nasileniem procesów mineralizacji. Analogiczne obserwacje poczyniono w badaniach *in vivo* na szczurzym modelu z cukrzycą wyindukowaną podaniem streptozotocyny.
2. **Środowisko hiperglikemiczne powoduje zmiany w aktywności i rozmieszczeniu białek enzymatycznych biorących udział w homeostazie fosforanowej.** Warunki wysokiego stężenia glukozy prowadzą do wzrostu aktywności TNAP, co skutkuje zwiększoną generacją jonów Pi będących podstawowym składnikiem w powstawaniu hydroksyapatytu. Dodatkowo, w omawianych warunkach zmniejsza się ilość enzymu NPP1 w błonie komórkowej podocyta. Prowadzi to do spadku w produkcji P_{PPi} w przestrzeni zewnątrzkomórkowej, będącego jednym z najsilniejszych naturalnych inhibitorów mineralizacji.
3. **Zmniejszenie wrażliwości podocytów na insulinę *in vitro* rozwija się po 24h inkubacji w warunkach hiperinsulinemicznych.** Po tym czasie dochodzi do zahamowania wewnątrzkomórkowej sygnalizacji zależnej od insuliny oraz do wygaszenia insulinozależnego dokomórkowego transportu glukozy. Środowisko hiperinsulinemiczne prowadzi także do rozregulowania metabolizmu oksydacyjnego podocyta, o czym świadczy zwiększona aktywność oksydazy NADPH oraz wzmożona generacja reaktywnych form tlenu i azotu.

4. **W podocytach z zahamowanym sygnałowaniem insulinowym dochodzi do formowania kompleksów enzymu NPP1 zarówno z transporterem Pit 1, jak i receptorem insulinowym.** Bezpośrednia interakcja NPP1 z podjednostką α IR może być jednym z mechanizmów, w wyniku którego w podocycie dochodzi do zahamowania wewnątrzkomórkowej sygnalizacji zależnej od insuliny.

5. **Wyciszenie genu *SLC20A1* kodującego transporter Pit 1 powoduje zmniejszenie wrażliwości podocytów na insulinę.** Zjawisko to objawia się inhibicją szlaku sygnalizacyjnego zależnego od insuliny oraz niemal całkowitą internalizacją IR i transportera glukozy GLUT 4. W rezultacie zmniejszeniu ulega dokomórkowy transport glukozy, a także nasila się stres oksydacyjny spowodowany nadmiernym wytwarzaniem RONS, których jednym z głównych źródeł w podocycie jest oksydaza NADPH. Obserwacje te są analogiczne do tych poczynionych w przypadku komórek podocytarnych stymulowanych insuliną przez 24h.

WNIOSEK KOŃCOWY

Warunki obserwowane w przebiegu cukrzycowej choroby nerek powodują promowanie procesów kalcyfikacji zarówno w kłębuszku nerkowym, jak i w samym podocycie. Patomechanizm tego zjawiska opiera się na zmianach w systemie białek transportujących i enzymatycznych biorących udział w homeostazie fosforanowej. Na szczególną uwagę zasługuje udział transportera Pit 1 i enzymu NPP1 w powstawaniu insulinooporności podocytów w trakcie rozwoju DKD. Otrzymane wyniki sugerują, iż białko Pit 1 jest kluczowym czynnikiem uczestniczącym w NPP1-zależnym hamowaniu wewnątrzkomórkowej sygnalizacji insulinowej, która odgrywa znaczącą rolę w fizjologii nie tylko samego podocyta, ale także kłębuszkowej bariery filtracyjnej.

8. Bibliografia

1. Schmidt AM. Highlighting Diabetes Mellitus. *Arterioscler Thromb Vasc Biol.* 2018;38(1):e1-e8. doi:10.1161/ATVBAHA.117.310221
2. Lee SJ, Lee IK, Jeon JH. Vascular calcification—new insights into its mechanism. *Int J Mol Sci.* 2020;21(8). doi:10.3390/ijms21082685
3. Valencia WM, Florez H. How to prevent the microvascular complications of type 2 diabetes beyond glucose control. *BMJ.* 2017;356. doi:10.1136/bmj.i6505
4. Samsu N. Diabetic Nephropathy: Challenges in Pathogenesis, Diagnosis, and Treatment. *Biomed Res Int.* 2021;2021:1497449. doi:10.1155/2021/1497449
5. Pollak MR, Quaggin SE, Hoenig MP, Dworkin LD. The glomerulus: The sphere of influence. *Clin J Am Soc Nephrol.* 2014;9(8):1461-1469. doi:10.2215/CJN.09400913
6. Pavenstädt H, Kriz W, Kretzler M. Cell biology of the glomerular podocyte. *Physiol Rev.* 2003;83(1):253-307. doi:10.1152/physrev.00020.2002
7. Garg P. A Review of Podocyte Biology. *Am J Nephrol.* 2018;47(suppl 1):3-13. doi:10.1159/000481633
8. Deegens JKJ, Dijkman HBPM, Borm GF, et al. Podocyte foot process effacement as a diagnostic tool in focal segmental glomerulosclerosis. *Kidney Int.* 2008;74(12). doi:10.1038/ki.2008.413
9. Fukasawa H, Bornheimer S, Kudlicka K, Farquhar MG. Slit diaphragms contain tight junction proteins. *J Am Soc Nephrol.* 2009;20(7):1491-1503. doi:10.1681/ASN.2008101117
10. Brinkkoetter PT, Ising C, Benzing T. The role of the podocyte in albumin filtration. *Nat Rev Nephrol.* 2013;9(6). doi:10.1038/nrneph.2013.78
11. Welsh GI, Hale LJ, Eremina V, et al. Insulin signaling to the glomerular podocyte is critical for normal kidney function. *Cell Metab.* 2010;12(4). doi:10.1016/j.cmet.2010.08.015
12. Coward RJM, Welsh GI, Yang J, et al. The human glomerular podocyte is a novel target for insulin action. *Diabetes.* 2005;54(11). doi:10.2337/diabetes.54.11.3095
13. Coward R, Fornoni A. Insulin signaling: Implications for podocyte biology in diabetic kidney disease. *Curr Opin Nephrol Hypertens.* 2015;24(1):104-110. doi:10.1097/MNH.0000000000000078

14. Jankowski M, Piwkowska A, Rogacka D, Audzeyenka I, Janaszak-Jasiecka A, Angielski S. Expression of membrane-bound NPP-type ecto-phosphodiesterases in rat podocytes cultured at normal and high glucose concentrations. *Biochem Biophys Res Commun.* 2011;416(1-2). doi:10.1016/j.bbrc.2011.10.144
15. Piwkowska A, Rogacka D, Audzeyenka I, Jankowski M, Angielski S. High glucose concentration affects the oxidant-antioxidant balance in cultured mouse podocytes. *J Cell Biochem.* 2011;112(6):1661-1672. doi:10.1002/jcb.23088
16. Li C, Siragy HM. High glucose induces podocyte injury via enhanced (Pro)renin receptor-Wnt- β -catenin-snail signaling pathway. *PLoS One.* 2014;9(2). doi:10.1371/journal.pone.0089233
17. Guo W, Gao H, Pan W, Yu P, Che G. High glucose induces Nox4 expression and podocyte apoptosis through the Smad3/ezrin/PKA pathway. *Biol Open.* 2021;10(5). doi:10.1242/BIO.055012
18. Russo D, Palmiero G, De Blasio AP, Balletta MM, Andreucci VE. Coronary artery calcification in patients with CRF not undergoing dialysis. *Am J Kidney Dis.* 2004;44(6):1024-1030. doi:10.1053/j.ajkd.2004.07.022
19. Kramer H, Toto R, Peshock R, Cooper R, Victor R. Association between chronic kidney disease and coronary artery calcification: The Dallas heart study. *J Am Soc Nephrol.* 2005;16(2):507-513. doi:10.1681/ASN.2004070610
20. Azpiazu D, Gonzalo S, González-Parra E, Egido J, Villa-Bellosta R. Role of pyrophosphate in vascular calcification in chronic kidney disease. *Nefrologia.* 2018;38(3):250-257. doi:10.1016/j.nefro.2018.03.003
21. Villa-Bellosta R, Egido J. Phosphate, pyrophosphate, and vascular calcification: A question of balance. *Eur Heart J.* 2017;38(23):1801-1804. doi:10.1093/eurheartj/ehv605
22. Moe SM, Chen NX. Pathophysiology of vascular calcification in chronic kidney disease. *Circ Res.* 2004;95(6):560-567. doi:10.1161/01.RES.0000141775.67189.98
23. Moe SM, Chen NX. Mechanisms of vascular calcification in chronic kidney disease. *J Am Soc Nephrol.* 2008;19(2):213-216. doi:10.1681/ASN.2007080854
24. Villa-Bellosta R. New insights into endogenous mechanisms of protection against arterial calcification. *Atherosclerosis.* 2020;306:68-74. doi:10.1016/j.atherosclerosis.2020.03.007
25. Saleem MA, Zavadil J, Bailly M, et al. The molecular and functional phenotype of

- glomerular podocytes reveals key features of contractile smooth muscle cells. *Am J Physiol - Ren Physiol*. 2008;295(4). doi:10.1152/ajprenal.00559.2007
26. Biber J, Hernando N, Forster I, Murer H. Regulation of phosphate transport in proximal tubules. *Pflugers Arch Eur J Physiol*. 2009;458(1):39-52. doi:10.1007/s00424-008-0580-8
 27. Biber J, Hernando N, Forster I. Phosphate Transporters and Their Function. *Annu Rev Physiol*. 2013;75(1):535-550. doi:10.1146/annurev-physiol-030212-183748
 28. Suzuki A, Ghayor C, Guicheux J, et al. Enhanced expression of the inorganic phosphate transporter Pit-1 is involved in BMP-2-induced matrix mineralization in osteoblast-like cells. *J Bone Miner Res*. 2006;21(5):674-683. doi:10.1359/jbmr.020603
 29. Ansermet C, Moor MB, Centeno G, et al. Renal fanconi syndrome and hypophosphatemic rickets in the absence of xenotropic and polytropic retroviral receptor in the nephron. *J Am Soc Nephrol*. 2017;28(4). doi:10.1681/ASN.2016070726
 30. Lee SY, Müller CE. Nucleotide pyrophosphatase/phosphodiesterase 1 (NPP1) and its inhibitors. *Med Chem Comm*. 2017;8(5):823-840. doi:10.1039/c7md00015d
 31. Mackenzie NCW, Zhu D, Milne EM, et al. Altered bone development and an increase in FGF-23 expression in *Enpp1^{-/-}* mice. *PLoS One*. 2012;7(2). doi:10.1371/journal.pone.0032177
 32. Jansen S, Perrakis A, Ulens C, et al. Structure of NPP1, an ectonucleotide pyrophosphatase/phosphodiesterase involved in tissue calcification. *Structure*. 2012;20(11). doi:10.1016/j.str.2012.09.001
 33. Carr G, Moochhala SH, Eley L, Vandewalle A, Simmons NL, Sayer JA. The pyrophosphate transporter ANKH is expressed in kidney and bone cells and colocalises to the primary cilium/basal body complex. *Cell Physiol Biochem*. 2009;24(5-6). doi:10.1159/000257515
 34. Li X, Yang HY, Giachelli CM. Role of the sodium-dependent phosphate cotransporter, Pit-1, in vascular smooth muscle cell calcification. *Circ Res*. 2006;98:905-912. doi:10.1161/01.RES.0000216409.20863.e7
 35. Masumoto A, Sonou T, Ohya M, et al. Calcium overload accelerates phosphate-induced vascular calcification via pit-1, but not the calcium-sensing receptor. *J Atheroscler Thromb*. 2017;24:716-724. doi:10.5551/jat.36574
 36. Mizobuchi M, Ogata H, Hatamura I, et al. Up-regulation of *Cbfa1* and Pit-1 in calcified

- artery of uraemic rats with severe hyperphosphataemia and secondary hyperparathyroidism. *Nephrol Dial Transplant.* 2006;21(4):911-916. doi:10.1093/ndt/gfk008
37. Sekiguchi S, Suzuki A, Asano S, et al. Phosphate overload induces podocyte injury via type III Na-dependent phosphate transporter. *Am J Physiol - Ren Physiol.* 2011;300(4):848-856. doi:10.1152/ajprenal.00334.2010
 38. Asada Y, Takayanagi T, Kawakami T, et al. Risedronate Attenuates Podocyte Injury in Phosphate Transporter-Overexpressing Rats. *Int J Endocrinol.* 2019;2019:4194853. doi:10.1155/2019/4194853
 39. Forand A, Koumakis E, Rousseau A, et al. Disruption of the Phosphate Transporter Pit1 in Hepatocytes Improves Glucose Metabolism and Insulin Signaling by Modulating the USP7/IRS1 Interaction. *Cell Rep.* 2016;16(10):2736-2748. doi:10.1016/j.celrep.2016.08.012
 40. Maddux BA, Sbraccia P, Kumakura S, et al. Membrane glycoprotein PC-1 and insulin resistance in non-insulin-dependent diabetes mellitus. *Nature.* 1995;373:448-457.
 41. Maddux BA, Goldfine ID. Membrane glycoprotein PC-1 inhibition of insulin receptor function occurs via direct interaction with the receptor alpha-subunit. *Diabetes.* 2000;49(1):13-19. doi:10.2337/diabetes.49.1.13
 42. Chin CN, Dallas-Yang Q, Liu F, et al. Evidence that inhibition of insulin receptor signaling activity by PC-1/ENPP1 is dependent on its enzyme activity. *Eur J Pharmacol.* 2009;606(1-3):17-24. doi:10.1016/j.ejphar.2009.01.016
 43. Tassone EJ, Cimellaro A, Perticone M, et al. Uric acid impairs insulin signaling by promoting ENPP1 binding to insulin receptor in human umbilical vein endothelial cells. *Front Endocrinol (Lausanne).* 2018;9:98. doi:10.3389/fendo.2018.00098
 44. Kasztan M, Piwkowska A, Kreft E, et al. Extracellular purines' action on glomerular albumin permeability in isolated rat glomeruli: insights into the pathogenesis of albuminuria. *Am J Physiol Physiol.* 2016;311(1):F103-F111. doi:10.1152/ajprenal.00567.2015
 45. Ilatovskaya D V., Palygin O, Levchenko V, Staruschenko A. Pharmacological characterization of the p2 receptors profile in the podocytes of the freshly isolated rat glomeruli. *Am J Physiol - Cell Physiol.* 2013;305(10). doi:10.1152/ajpcell.00138.2013
 46. Garland JS, Holden RM, Ross R, et al. Insulin resistance is associated with Fibroblast

- Growth Factor-23 in stage 3-5 chronic kidney disease patients. *J Diabetes Complications*. 2014;28(1). doi:10.1016/j.jdiacomp.2013.09.004
47. Saleem MA, O'Hare MJ, Reiser J, et al. A conditionally immortalized human podocyte cell line demonstrating nephrin and podocin expression. *J Am Soc Nephrol*. 2002;13(3):630-638.
 48. Rogacka D, Piwkowska A, Audzeyenka I, Angielski S, Jankowski M. SIRT1-AMPK crosstalk is involved in high glucose-dependent impairment of insulin responsiveness in primary rat podocytes. *Exp Cell Res*. 2016;349(2):328-338. doi:10.1016/j.yexcr.2016.11.005
 49. Münzel T, Kurz S, Rajagopalan S, et al. Hydralazine prevents nitroglycerin tolerance by inhibiting activation of a membrane-bound NADH oxidase: A new action for an old drug. *J Clin Invest*. 1996;98(6). doi:10.1172/JCI118935
 50. Kulesza T, Typiak M, Rachubik P, et al. Hyperglycemic environment disrupts phosphate transporter function and promotes calcification processes in podocytes and isolated glomeruli. *J Cell Physiol*. 2022;237(5):2478-2491. doi:10.1002/jcp.30700
 51. McIntyre CW. The functional cardiovascular consequences of vascular calcification. *Semin Dial*. 2007;20(2). doi:10.1111/j.1525-139X.2007.00258.x
 52. Rocha-Singh KJ, Zeller T, Jaff MR. Peripheral arterial calcification: Prevalence, mechanism, detection, and clinical implications. *Catheter Cardiovasc Interv*. 2014;83(6). doi:10.1002/ccd.25387
 53. Nordheim E, Jenssen TG. Chronic kidney disease in patients with diabetes mellitus. *Endocr Connect*. 2021;10(5). doi:10.1530/EC-21-0097
 54. Kulesza T, Typiak M, Rachubik P, et al. Pit 1 transporter (SLC20A1) as a key factor in the NPP1-mediated inhibition of insulin signaling in human podocytes. *J Cell Physiol*. 2023:1-16. doi:10.1002/jcp.31051
 55. Audzeyenka I, Rogacka D, Rachubik P, et al. The PKGI α -Rac1 pathway is a novel regulator of insulin-dependent glucose uptake in cultured rat podocytes. *J Cell Physiol*. 2021;236(6):4655-4668. doi:10.1002/jcp.30188
 56. Hale LJ, Coward RJM. The insulin receptor and the kidney. *Curr Opin Nephrol Hypertens*. 2013;22(1). doi:10.1097/MNH.0b013e32835abb52
 57. McMahon GM, Datta D, Bruneau S, et al. Constitutive activation of the mTOR signaling pathway within the normal glomerulus. *Biochem Biophys Res Commun*. 2012;425(2).

doi:10.1016/j.bbrc.2012.07.075

58. Rachubik P, Szrejder M, Rogacka D, et al. The TRPC6-AMPK pathway is involved in insulin-dependent cytoskeleton reorganization and glucose uptake in cultured rat podocytes. *Cell Physiol Biochem*. 2018;51(1):393-410. doi:10.1159/000495236
59. Rogacka D, Audzeyenka I, Rachubik P, et al. Insulin increases filtration barrier permeability via TRPC6-dependent activation of PKGI α signaling pathways. *Biochim Biophys Acta - Mol Basis Dis*. 2017;1863(6):1312-1325. doi:10.1016/j.bbadis.2017.03.002
60. Rachubik P, Szrejder M, Audzeyenka I, et al. The PKGI α /VASP pathway is involved in insulin- And high glucose-dependent regulation of albumin permeability in cultured rat podocytes. *J Biochem*. 2020;168(6):575-588. doi:10.1093/jb/mvaa059
61. Piwkowska A, Rogacka D, Audzeyenka I, Angielski S, Jankowski M. Combined effect of insulin and high glucose concentration on albumin permeability in cultured rat podocytes. *Biochem Biophys Res Commun*. 2015;461(2):383-389. doi:10.1016/j.bbrc.2015.04.043
62. Piwkowska A, Rogacka D, Kasztan M, Angielski S, Jankowski M. Insulin increases glomerular filtration barrier permeability through dimerization of protein kinase G type I α subunits. *Biochim Biophys Acta - Mol Basis Dis*. 2013;1832(6):791-804. doi:10.1016/j.bbadis.2013.02.011
63. Szrejder M, Rachubik P, Rogacka D, et al. Metformin reduces TRPC6 expression through AMPK activation and modulates cytoskeleton dynamics in podocytes under diabetic conditions. *Biochim Biophys Acta - Mol Basis Dis*. 2020;1866(3):165610. doi:10.1016/j.bbadis.2019.165610
64. Zhou HH, Chin C-N, Wu M, et al. Suppression of PC-1/ENPP-1 expression improves insulin sensitivity in vitro and in vivo. *Eur J Pharmacol*. 2009;616(1-3):346-352. doi:10.1016/J.EJP.2009.06.057
65. Fagerholm S, Örtengren U, Karlsson M, Ruishalme I, Strålfors P. Rapid insulin-dependent endocytosis of the insulin receptor by caveolae in primary adipocytes. *PLoS One*. 2009;4(6). doi:10.1371/journal.pone.0005985
66. Fazakerley DJ, Koumanov F, Holman GD. GLUT4 On the move. *Biochem J*. 2022;479(3):445-462. doi:10.1042/BCJ20210073

9. Kopie publikacji będących podstawą rozprawy

9.1. Poświadczony przez Bibliotekę IMDiK PAN pięcioletni impact factor (IF₅) publikacji będących podstawą rozprawy

Lista publikacji będących podstawą rozprawy doktorskiej

1. Kulesza T, Typiak M, Rachubik P, Audzeyenka I, Rogacka D, Angielski S, Saleem MA, Piwkowska A. 2022. Hyperglycemic environment disrupts phosphate transporter function and promotes calcification processes in podocytes and isolated glomeruli. *J Cell Physiol*, 237(5): 2478-2491; **IF₅ = 6,398**
2. Kulesza T, Typiak M, Rachubik P, Rogacka D, Audzeyenka I, Saleem MA, Piwkowska A. 2023. Pit 1 transporter (SLC20A1) as a key factor in the NPP1-mediated inhibition of insulin signaling in human podocytes. *J Cell Physiol*, doi: 10.1002/jcp.31051; **IF₅ = 6,398**
3. Kulesza T, Piwkowska A. 2021. The impact of type III sodium-dependent phosphate transporters (Pit 1 and Pit 2) on podocyte and kidney function. *J Cell Physiol*, 236(10): 7176-7185; **IF₅ = 6,398**

BIBLIOTEKA
Instytut Medycyny Doświadczalnej i Klinicznej
im. Mirosława Mossakowskiego
Polskiej Akademii Nauk
02-106 Warszawa, ul. A. Pawińskiego 5
tel. 22 608-66-11 NIP 525-000-81-69
e-mail: library@indik.pan.pl

KIEROWNIK BIBLIOTEKI
Katarzyna Nieszporska
mgr Katarzyna Nieszporska

9.2. Kopie prac oryginalnych

- 9.2.1. [Kulesza T](#), [Typiak M](#), [Rachubik P](#), [Audzeyenka I](#), [Rogacka D](#), [Angielski S](#), [Saleem MA](#), [Piwkowska A](#). **Hyperglycemic environment disrupts phosphate transporter function and promotes calcification processes in podocytes and isolated glomeruli.** *J Cell Physiol.* 2022; 237(5): 2478-2491.



Received: 22 September 2021 | Accepted: 2 February 2022

DOI: 10.1002/jcp.30700

RESEARCH ARTICLE

Journal of Cellular Physiology WILEY

Hyperglycemic environment disrupts phosphate transporter function and promotes calcification processes in podocytes and isolated glomeruli

Tomasz Kulesza¹ | Marlena Typiak^{1,2} | Patrycja Rachubik¹ | Irena Audzeyenka^{1,3} | Dorota Rogacka^{1,3} | Stefan Angielski¹ | Moin A. Saleem⁴ | Agnieszka Piwkowska^{1,3}

¹Laboratory of Molecular and Cellular Nephrology, Mossakowski Medical Research Institute, Polish Academy of Sciences, Gdansk, Poland

²Department of General and Medical Biochemistry, Faculty of Biology, University of Gdansk, Gdansk, Poland

³Department of Molecular Biotechnology, Faculty of Chemistry, University of Gdansk, Gdansk, Poland

⁴Bristol Renal, University of Bristol, Bristol, UK

Correspondence

Tomasz Kulesza, Laboratory of Molecular and Cellular Nephrology, Mossakowski Medical Research Institute, Polish Academy of Sciences, Wita Stwosza St. 63, Gdansk 80-308, Poland.
Email: tkulesza@imdik.pan.pl

Funding information

Narodowe Centrum Nauki, Grant/Award Number: 2018/29/B/NZ4/02074

Abstract

Soft tissue calcification is a pathological phenomenon that often occurs in end-stage chronic kidney disease (CKD), which is caused by diabetic nephropathy, among other factors. Hyperphosphatemia present during course of CKD contributes to impairments in kidney function, particularly damages in the glomerular filtration barrier (GFB). Essential elements of the GFB include glomerular epithelial cells, called podocytes. In the present study, we found that human immortalized podocytes express messenger RNA and protein of phosphate transporters, including NaPi 2c (SLC34A3), Pit 1 (SLC20A1), and Pit 2 (SLC20A2), which are sodium-dependent and mediate intracellular phosphate (Pi) transport, and XPR1, which is responsible for extracellular Pi transport. We found that cells that were grown in a medium with a high glucose (HG) concentration (30 mM) expressed less Pit 1 and Pit 2 protein than podocytes that were cultured in a standard glucose medium (11 mM). We found that exposure of the analyzed transporters in the cell membrane of the podocyte is altered by HG conditions. We also found that the activity of tissue nonspecific alkaline phosphatase increased in HG, causing a rise in Pi generation. Additionally, HG led to a reduction of the amount of ectonucleotide pyrophosphatase/phosphodiesterase 1 in the cell membrane of podocytes. The extracellular concentration of pyrophosphate also decreased under HG conditions. These data suggest that a hyperglycemic environment enhances the production of Pi in podocytes and its retention in the extracellular space, which may induce glomerular calcification.

KEYWORDS

diabetic nephropathy, glomerular calcification, phosphate homeostasis, phosphate transporters, podocyte

Abbreviations: ALP, alkaline phosphatase; ATP, adenosine triphosphate; BSA, bovine serum albumin; CKD, chronic kidney disease; DN, diabetic nephropathy; eNPP1, ectonucleotide pyrophosphatase/phosphodiesterase 1; ERK1/2, extracellular signal-regulated kinase 1/2; ESRD, end-stage renal disease; FBS, fetal bovine serum; GFB, glomerular filtration barrier; GFR, glomerular filtration rate; HG, high glucose concentration medium (30 mM); IR, insulin receptor; NaPi 2c, type II sodium-dependent phosphate transporter c; PBS, phosphate-buffered saline; PCR, polymerase chain reaction; PFBC, primary familial brain calcification; Pi, phosphate; Pit 1, type III sodium-dependent phosphate transporter 1; Pit 2, type III sodium-dependent phosphate transporter 2; PPI, pyrophosphate; SG, standard glucose concentration medium (11 mM); SLC, solute carrier; STZ, streptozotocin; TNAP, tissue nonspecific alkaline phosphatase; USP7, ubiquitin-specific peptidase 7; VC, vascular calcification; VSMC, vascular smooth muscle cell; XPR1, xenotropic and polytropic retrovirus receptor 1.

1 | INTRODUCTION

Diabetes accounts for up to half of all chronic kidney disease (CKD) cases worldwide (Webster et al., 2017). Although 30%–40% of diabetic patients develop diabetic nephropathy (DN) (Umanath & Lewis, 2018), the consequences of this condition can be end-stage renal disease, the most advanced form of CKD. Diabetic nephropathy affects not only the kidney itself, mainly by damaging the glomerular filtration barrier (GFB) and leading to proteinuria, but also provokes undesirable alterations throughout the body. The most serious complications include the dysregulation of bone and mineral metabolism, manifested by hyperphosphatemia and the calcification of soft tissues, mainly blood vessels, defined as vascular calcification (VC) (Reiss et al., 2018; Webster et al., 2017).

Calcification is the process of depositing calcium phosphate salts in the form of hydroxyapatite [$\text{Ca}_{10}(\text{PO}_4)_6(\text{OH})_2$]. This phenomenon is desirable for bones and teeth but pathological in the case of other tissues. According to numerous studies, as many as 40% of CKD patients develop VC (Russo et al., 2004). Additionally, the positive correlation between VC and renal failure was shown to be stronger in a group of diabetic patients (Kramer et al., 2005). During the course of CKD, hormonal balance is also disrupted, manifested by permanent hyperphosphatemia. High serum inorganic phosphate (Pi) concentrations directly contribute to the intensification of VC and deterioration of the glomerular filtration rate with increasing proteinuria (Cozzolino et al., 2017). Therefore, the presence of calcification inhibitors is crucial, including inorganic pyrophosphate (PPI), osteopontin, fetuin A, and albumin. PPI is the most potent endogenous factor that prevents the formation of hydroxyapatite in vivo and in vitro (Azpiazu et al., 2018; Rutsch et al., 2011; Villa-Bellosta & Sorribas, 2011).

The renal glomerulus contains capillaries and podocytes that are surrounded by the mesangial matrix. Podocytes are terminally differentiated epithelial cells that consist of a cell body, major processes, and foot processes that branch from them. Foot processes tightly entwine capillaries and interlock each other, forming slit diaphragms, which are a crucial element of the GFB (Garg, 2018). The loss of podocyte function and a reduction of their number comprise the first mechanism by which diabetes damages the kidney (Coward & Fornoni, 2015). Podocytes are located in the urinary part of Bowman's capsule, where albumin or osteopontin is missing. Therefore, PPI appears to be one of the main protective factors against glomerular calcification (Fleish & Bisaz, 1962).

Recent research has shed light on membrane phosphate transporters that appear to be involved in the pathomechanism of calcification (Chavkin et al., 2015; Crouthamel et al., 2013; Legati et al., 2015; Li & Giachelli, 2007; Yamada et al., 2018). These include proteins from the solute carrier (SLC) family, including type II (SLC34A1–NaPi 2a and SLC34A3–NaPi 2c) and type III (SLC20A1–Pit 1 and SLC20A2–Pit 2) sodium-dependent phosphate transporters (Kulesza & Piwkowska, 2021). NaPi 2a and NaPi 2c are responsible for the renal reabsorption of phosphate by transferring HPO_4^{2-} ions into the cell. They are located in the proximal tubule and subject to strict hormonal regulation, such as by parathyroid hormone and fibroblast growth factor 23 (Forster

et al., 2013). Pit 1 and Pit 2 are widely expressed throughout the body. Their function includes the intracellular transport of H_2PO_4^- (Forster et al., 2013). In addition to a phosphate transporter role, proteins from the SLC20 family appear to act as Pi sensors and mediate cell signaling (Bon et al., 2018; Chavkin et al., 2015). Pit 1 is also involved in Pi-induced podocyte injury (Sekiguchi et al., 2011). The plasma membrane protein Xenotropic and polytropic retrovirus receptor 1 (XPR1) is responsible for the export of phosphate from the cell (Giovannini et al., 2013). XPR1 may intensify mineralization processes through an increase in Pi efflux into the extracellular space (Legati et al., 2015).

Maintaining a proper balance between Pi (one of the building blocks of hydroxyapatite) and PPI (a mineralization inhibitor) is essential. Two major enzymes are involved in this process: tissue nonspecific alkaline phosphatase (TNAP) and ectonucleotide pyrophosphatase/phosphodiesterase (eNPP). TNAP is an alkaline phosphatase (ALP) isoenzyme that is found mainly in the kidneys, liver, and bones and hydrolyzes phosphorylated substrates. As a result of its activity, inorganic Pi is released (Orimo, 2010). eNPP comprises a group of membrane enzymatic proteins, consisting of seven isoforms (eNPP1–7), of which eNPP1 is the best characterized. The main task of these proteins is to control the turnover of extracellular nucleotides and salvage purines and pyrimidines. eNPP1 mainly hydrolyzes nucleoside triphosphates to PPI and nucleoside monophosphates. The leading substrate for eNPP1 is adenosine triphosphate (ATP), which is broken down into adenosine monophosphate and PPI (Lee & Müller, 2017). A significant pool of extracellular nucleotides in the kidney has been reported (Kasztan et al., 2016; Solini et al., 2015). Thus, optimal activity of these two enzymes appears to protect against undesirable glomerular calcification.

The present study investigated the expression of phosphate transporters in glomeruli in the rat kidneys and immortalized human podocytes that were cultured under standard glucose (SG) and high glucose (HG) conditions. We tested TNAP and eNPP activity in these cells. We also assessed extracellular and intracellular levels of ATP and PPI and examined whether the observed changes influenced the development of glomerular calcification.

2 | MATERIALS AND METHODS

2.1 | Human podocyte cell line

Immortalized human podocytes (provided by Moin A. Saleem) were created as described previously (Saleem et al., 2002). Podocyte-specific markers were checked regularly to ensure purity of the cell line (Audzeyenka, Rachubik, et al., 2020). Podocytes were cultured in RPMI-1640 medium (Thermo Fisher Scientific) with the addition of 10% fetal bovine serum (FBS) (Thermo Fisher Scientific), 100 U/ml penicillin, and 100 mg/ml streptomycin (Sigma Aldrich). Cells were grown to the desired confluence at 33°C and then transferred to 37°C for 10–14 days for differentiation. Subsequently, podocytes were cultured in a medium with a SG concentration (11 mM) and a HG concentration (30 mM) for 5 days. All experiments were

performed after this time. To ensure that high osmolarity did not affect Pi transport system an osmotic control was performed by adding 19 mM L-glucose to SG medium. No changes in analyzed proteins were detected between SG and L-glucose conditions.

2.2 | Experimental animals and ethical approval

Experiments were performed with Wistar male rats that were obtained from the Mossakowski Medical Research Institute, Polish Academy of Sciences, Warsaw, Poland. The rats were maintained on a 12 h light/12 h light/dark cycle with free access to a standard pellet diet and tap water. The experiments were conducted in accordance with directive 2010/63/EU, and the protocol was approved by the local Ethical Commission at the University of Science and Technology in Bydgoszcz (no. 51/2018 and 47/2018 BIS).

The experiments were conducted with male Wistar rats that were subjected to streptozotocin (STZ; 80 mg/kg, i.p.)-induced diabetes and age-matched control (CTRL) Wistar rats. Experiments were performed after 14 days in STZ rats that had a blood glucose concentration >200 mg/dl (Table 1). Rats were kept in separate metabolic cages for 48 h with free access to a regular pellet diet and drinking water. The animals were allowed to habituate to the cages during the first 24 h. During the next 24 h, urine was collected, and urinary albumin and creatinine were measured in an external laboratory. Following an overnight fast, cardiac blood was collected immediately after the rat was euthanized to determine levels of serum phosphate, albumin, and creatinine and activity of ALP, which were assessed by an external laboratory. Fasting blood glucose concentrations were measured in whole blood samples using a glucose oxidase method (Accu-Chek Performa; Roche Diagnostics).

2.3 | Western blot

Cell lysates were generated as described previously (Piwkowska et al., 2012). The samples were heated at 96°C for 2 min, and then equal amounts of total protein (20 or 30 µg per well) were loaded onto 10% sodium dodecyl sulfate (SDS)-polyacrylamide gels and subjected to electrophoresis. Samples were then electrotransferred to polyvinylidene fluoride membranes and incubated overnight at 4°C with primary antibodies (Table 2). Horseradish peroxidase-conjugated anti-mouse (catalog no. A9044; Sigma Aldrich) and anti-rabbit (catalog no. A9169; Sigma Aldrich) secondary antibodies were used to

detect proteins. The resulting bands were densitometrically analyzed with Quantity One software (Bio-Rad).

2.4 | Cell surface biotinylation

To assess cell membrane localization of the analyzed proteins, podocytes were incubated with a 1 mg/ml biotin solution (catalog no. 21338; Thermo Fisher Scientific) in phosphate-buffered saline (PBS), pH 8.0, for 30 min at 4°C. Unbound biotin was removed by washing the cells five times with PBS supplemented with 100 mM glycine, pH 8.3. Podocytes were then lysed as previously described (Piwkowska et al., 2012). Part of the lysate was frozen for evaluation of the total amount of analyzed transporters. The other part of the lysate was incubated with the Neutr/Avidin resin (catalog no. 53150; Thermo Fisher Scientific) on a rotor at 4°C overnight. Biotin-coated membrane proteins bound to the avidin resin. The next day, the samples were washed five times with PBS. Membrane proteins were eluted by heating the lysates at 96°C for 10 min with two-times concentrated loading buffer (0.5 M Tris, 10% SDS, 30% glycerol, 9.3% DL-dithiothreitol, and 0.012% bromophenol blue). Membrane and total lysates were then subjected to Western blot analysis.

2.5 | Real-time polymerase chain reaction

Total RNA was isolated from human podocyte cells using the RNeasy Plus Mini Kit, followed by on-column genomic DNA elimination (Qiagen). Quantity and purity of the RNA were measured using a NanoDrop device (Thermo Fisher Scientific). The isolated RNA was then used as a template for reverse-transcription polymerase chain reaction (PCR). The obtained complementary DNA was subjected to real-time PCR in a LightCycler 480 instrument (Roche) with gene-specific intron-spanning primers and fluorescent hydrolysis probes (Roche; Table 3). We did not establish expression of the SLC34A1 gene that encodes NaPi 2a protein; therefore, this transporter was not analyzed in the studies. Using the $\Delta\Delta C_t$ method, with β -actin as a reference, relative quantification of the initial amount of specific messenger RNA (mRNA) transcripts was performed. The amplification products were separated on 2.5% agarose gel and viewed in a Molecular Imager using Image Lab 6.0 software (Bio-Rad).

2.6 | Immunofluorescent staining

Podocytes were grown on human fibronectin-coated glass coverslips (catalog no. 354088; Corning). Cells were fixed in 4% formaldehyde for 20 min at room temperature, permeabilized for 1 min in 0.1% Triton X-100, and then blocked with PBS that contained 2% FBS, 2% bovine serum albumin (BSA), and 0.2% fish gelatin (blocking solution) for 30 min at 4°C. Subsequently, podocytes were incubated with primary antibodies that were diluted with blocking solution (Table 2) overnight at 4°C. The next day, cells were incubated with secondary

TABLE 1 Characteristics of rats used in metabolic cage studies

Parameter	CTRL (n = 6)	STZ (n = 6)
Body weight	271.8 ± 26.42 g	224.8 ± 5.26 g
Blood glucose	120.3 ± 16.38 mg/dl	386.2 ± 56.28 mg/dl
Urine volume	9.3 ± 1.22 ml/24 h	192.0 ± 6.35 ml/24 h

TABLE 2 Primary antibodies used in the experiments

Antibody	Dilution	Manufacturer
Pit 1	1:4000 (WB), 1:25 (IF), 1:25 (IHC)	Biorbyt, catalog no. orb412245 (WB, IF), catalog no. orb523403 (IHC)
Pit 2	1:1000 (WB), 1:25 (IF), 1:100 (IHC)	Biorbyt, catalog no. orb247601 (WB, IF); Novus Biological, catalog no. NBP1-83360 (IHC)
NaPi 2c	1:500 (WB), 1:30 (IF), 1:100 (IHC)	Novus Biological, catalog no. NBP2-93939 (WB); MyBioSource, catalog no. MBS7108535 (IF); Biorbyt, catalog no. orb254286 (IHC)
XPR1	1:450 (WB), 1:25 (IF), 1:50 (IHC)	Sigma Aldrich, catalog no. SAB2700987 (WB, IF); Novus Biological, catalog no. NBP2-48531 (IHC)
eNPP1	1:100 (WB)	Santa Cruz Biotechnology, catalog no. sc-166649
Actin	1:5000 (WB)	Sigma Aldrich, catalog no. A5441
Nephrin	1:50 (IF)	Santa Cruz Biotechnology, catalog no. sc-376522

Abbreviations: IF, immunofluorescence; IHC, immunohistochemistry; WB, western blot.

TABLE 3 Sequences of primers and fluorescent probes that were used in the experiments

Protein name	Gene name	Accession no. for mRNA sequence	Primer sequence	Probe sequence	Product length (bp)
Pit 1	SLC20A1	NM_005415.5	Forward: CTGCAATGCTGTCTGACC Reverse: ATAAGCAACCAGAGGCCCA	CTCTGCCT	236
Pit 2	SLC20A2	NM_001257180.2	Forward: TGCATACGGAAGAGCACTGTCC Reverse: GCGGTGTAGCAGGTGTAAT	CAGCCAG	246
XPR1	XPR1	NM_001135669.2	Forward: TCGGGGTGGCTTCTTCTGA Reverse: GGCACCACAATATCCCGAGG	CTGTCTCC	170
NaPi 2c	SLC34A3	NM_001177316.2	Forward: AACATCGGCACCACTACCA Reverse: CGGCCAGGTGAAGAAGA	CCAGGGCA	109
TNAP	ALPL	NM_000478.6	Forward: CCTGCCTTACTAATCCTTAGTGC Reverse: CGTTGGTGTGAGCTTCTGA	CCAGGGCA	114
eNPP1	ENPP1	NM_006208.3	Forward: TGGGTAGAAGAACCATGTGAGA Reverse: GAGGGTAGGAGGCGTTTCA	CTGCTGGG	72
β -Actin	ACTB	NM_001101.5	Forward: ATGGCAATGAGCGGTTCC Reverse: GGATGCCACAGGACTCCA	CTCCAGC	76

Abbreviation: mRNA, messenger RNA.

antibodies (catalog no. A11010 or A11059; Thermo Fisher Scientific, 1:200 dilution in blocking solution) for 2 h at 4°C. Podocytes were imaged with a confocal microscope (Eclipse Ti, Nikon Instruments; RCM device, Confocal.nl).

2.7 | Immunohistochemistry

Formalin-fixed and paraffin-embedded kidney sections from CTRL and STZ Wistar rats were deparaffinized and rehydrated by washing with a Histochoice Cleaning Agent (Sigma Aldrich) and a decreasing series of ethanol solutions (100%, 95%, 90%, 70%, and 50%). Heat-induced epitope retrieval was performed by heating the slides in citrate buffer (10 mM, pH 6) at 99–100°C for 20 min. Samples were

then blocked in 5% BSA in PBS (blocking solution) for 1 h at room temperature. The slides were then incubated with primary antibodies (Table 2) that were diluted in blocking solution overnight at 4°C. The next day, kidney sections were incubated with secondary antibodies (catalog no. 8114S; Cell Signaling Technology) at room temperature for 30 min. Afterward, the slides were incubated with Signal Stain DAB Substrate (Cell Signaling Technology) for 2 min and quickly washed in double-distilled water. Samples were counterstained for 5 s with hematoxylin and dehydrated in ethanol and Histochoice Cleaning Agent. Tissue sections were imaged with a light microscope (Eclipse Ti; Nikon Instruments). Quantitative analysis of the studied proteins in renal glomeruli was performed using ImageJ 1.52a software (National Institutes of Health, Bethesda, MD, USA).

2.8 | Determination of TNAP and eNPP activity

TNAP activity was determined using the SteamTAG Alkaline Phosphatase Activity Assay Kit (catalog no. CBA-301-CB, BioCat) according to the manufacturer's instructions. eNPP activity was assessed using *p*-nitrophenyl thymidine 5'-monophosphate (pNTMP) as a substrate. Briefly, podocytes were lysed in buffer that contained 1% Triton X-100, 200 mM Tris-HCl (pH 8), and 1.6 mM MgCl₂. Lysates were incubated with 1 mg/ml substrate solution for 20 min at room temperature. Absorbance of the resulting yellow product was measured at $\lambda = 405$ nm. The activity of both TNAP and eNPP is presented as nmol of the product that formed within 1 min and was related to protein content of the lysate (nmol/min/mg protein).

2.9 | Determination of intracellular and extracellular ATP levels

Extracellular and intracellular ATP levels were assessed using the ATP Determination Kit (catalog no. A22066; Invitrogen), which uses an enzymatic reaction with luciferase and luciferin as a substrate.

To assess the extracellular concentration of ATP, podocytes were incubated with the medium without the addition of FBS and antibiotics for 2 h. The medium was then harvested from the cells, heated at 96°C for 3 min, and briefly centrifuged. Luminescence measurements were performed at room temperature according to the kit's instructions.

Intracellular ATP levels were determined by incubating podocytes with 6% HClO₄ for 30 min at 4°C on a shaker. Afterward, the resulting supernatant was adjusted to pH 7.8 with KOH and K₂CO₃, followed by luminescence assessment.

2.10 | Determination of intracellular and extracellular PPI levels

The Pyrophosphate Assay Kit (catalog no. K568; BioVision) was used to determine the amount of intracellular and extracellular PPI. To establish the intracellular amount of PPI, cell lysates were prepared using reaction buffer that was provided in the kit. Lysates were deproteinized with Amicon Ultra Centrifugal Filters (catalog no. UFC500396; Millipore), and measurements were performed according to the manufacturer's instructions. PPI content was related to protein concentration in the lysate (nmol PPI/mg protein).

To assess the extracellular concentration of PPI, podocytes were cultured for 2 h in PBS supplemented with MgCl₂, CaCl₂, and an appropriate amount of glucose. Afterward, PBS was harvested from the cells and deproteinized using Amicon Ultra Centrifugal Filters (catalog no. UFC500396; Millipore). The assay was then performed according to the manufacturer's instructions.

2.11 | Evaluation of calcification intensity in human podocytes and rat kidney

Podocytes were washed twice with PBS and fixed in 4% formaldehyde for 20 min at 4°C. Cells were then incubated with 0.1% Triton X-100 for 2 min to permeabilize the cell membrane. Podocytes were then stained with 2% Alizarin Red S (catalog no. A5533; Sigma Aldrich), pH 4.2, for 1 h at room temperature. Afterward, excess dye was rinsed off with double-distilled water.

Rat kidney sections were dewaxed and rehydrated as described above. The samples were then stained with 2% Alizarin Red S (catalog no. A5533; Sigma Aldrich), pH 4.2, for 1 h and counterstained with hematoxylin. Cells and kidney sections were imaged with a light microscope (Eclipse Ti; Nikon Instruments). ImageJ 1.52a software (National Institutes of Health) was used to quantify the intensity of calcification.

2.12 | Rat serum and urine biochemistry analysis

Evaluations of biochemical parameters in rat blood and urine were performed in an external diagnostic laboratory using Alinity devices (Abbott Laboratories). The tests that were used are summarized in Table 4.

2.13 | Statistical analysis

Data were analyzed using Prism 5.03 software (GraphPad). The Shapiro-Wilk test was used to check normality of the data distribution. If the data were normally distributed, then the parametric unpaired *t* test was performed. Otherwise, the nonparametric Mann-Whitney test was implemented. Statistical significance was assumed at values of $p \leq 0.05$. The results are presented as mean \pm SEM.

TABLE 4 Tests used to determine biochemical parameters in rat serum and urine

Parameter	Measurement principle
Serum albumin	Absorbance of albumin-bromocresol green complex
Serum/urine creatinine	Absorbance of creatinine-picrate complex
Serum calcium	Absorbance of Arsenazo III dye
Serum phosphate	Absorbance of phosphomolybdate
Serum alkaline phosphatase activity	Absorbance of <i>p</i> -nitrophenol
Microalbuminuria	Immunoturbidimetric with antibodies to albumin

3 | RESULTS

3.1 | Phosphate balance is disturbed in rats with STZ-induced diabetes

To assess phosphate metabolism, we performed biochemical studies of serum and urine from STZ rats and age-matched CTRL rats. The results are shown in Table 5. Renal function was impaired in STZ rats, reflected by an almost 17-fold increase in the daily excretion of albumin, 95% reduction in urinary creatinine concentration, 17% decrease in serum albumin concentration, and 26% increase in serum creatinine concentration. We also found a 44% rise in Pi concentration and an almost twofold increase in ALP activity in STZ rats. These results suggest that diabetes led to the dysregulation of phosphate balance in STZ rats.

We also assessed the intensity of renal calcification in CTRL and STZ rats (Figure 1a). We used Alizarin Red S staining, which is commonly used to visualize calcium complexes. In STZ rats, calcification processes were more apparent than in CTRL rats (integrated density in STZ rats vs. CTRL rats: $1.782 \times 10^7 \pm 0.03 \times 10^7 \mu\text{m}^2$ vs. $0.645 \times 10^7 \pm 0.03 \times 10^7 \mu\text{m}^2$; Figure 1c).

3.2 | Amount of phosphate transporters in glomeruli in rats with STZ-induced diabetes differs from their healthy counterparts

To evaluate whether the changes in biochemical parameters were related to disturbances in phosphate transporters, we performed

immunohistochemical staining of kidney tissue from Wistar STZ and CTRL rats. The density of brown staining was directly proportional to the amount of examined transporters. There were clear differences in the intensity of brown staining between glomeruli in STZ and CTRL rats (Figure 2a,b). We detected a 62% reduction of Pit 1 levels in glomeruli in STZ rats (integrated density in STZ rats vs. CTRL rats: $30.253 \pm 3.002 \mu\text{m}^2$ vs. $80.515 \pm 7.358 \mu\text{m}^2$; Figure 2c). A similar decrease in Pit 2 levels (60%) was found in STZ rats compared with their healthy counterparts (integrated density in STZ rats vs. CTRL rats: $18.862 \pm 1.792 \mu\text{m}^2$ vs. $46.764 \pm 3.528 \mu\text{m}^2$; Figure 2d). This confirmed our findings of disturbances in SLC20 family transporters under hyperglycemic conditions in vitro. We also found a 35% decrease in NaPi 2c levels in glomeruli in STZ rats (integrated density in STZ rats vs. CTRL rats: $23.413 \pm 1.259 \mu\text{m}^2$ vs. $36.205 \pm 3.434 \mu\text{m}^2$; Figure 2e), but no significant differences in the amount of XPR1 were found (Figure 2f).

3.3 | Immortalized human podocytes express membrane phosphate transporters

To verify our findings in an in vivo model, we evaluated the expression of the studied proteins in vitro. Using real-time PCR, we found that human immortalized podocytes expressed mRNA of the *SLC20A1*, *SLC20A2*, *SLC34A3*, and *XPR1* genes, which encode Pit 1, Pit 2, NaPi 2c, and XPR1 phosphate transporters, respectively. By designing specific primers, we observed distinct bands after electrophoretic separation of the PCR product (Figure 3a). We then performed immunofluorescence staining to assess the expression and cellular localization of these proteins in human

TABLE 5 Biochemical analysis of serum and urine samples from CTRL and STZ rats

Parameter	CTRL	STZ	
Serum albumin	27.75 ± 0.95 g/L	23.00 ± 0.93 g/L	* $p = 0.024$, $n = 4-6$, Mann-Whitney test
Serum creatinine	0.55 ± 0.02 mg/dl	0.69 ± 0.05 mg/dl	* $p = 0.042$, $n = 4-6$, Mann-Whitney test
Serum phosphate	9.05 ± 0.65 mg/dl	13.07 ± 1.43 mg/dl	* $p = 0.038$, $n = 4-6$, Mann-Whitney test
Serum ALP activity	271.5 ± 33.0 U/L	515.8 ± 78.8 U/L	* $p = 0.032$, $n = 4-6$, Mann-Whitney test
Urine albumin	0.14 ± 0.02 mg/24 h	2.46 ± 0.33 mg/24 h	** $p = 0.002$, $n = 6$, Mann-Whitney test
Urine creatinine	110.4 ± 11.37 mg/dl	6.3 ± 0.23 mg/dl	** $p = 0.004$, $n = 5-6$, Mann-Whitney test

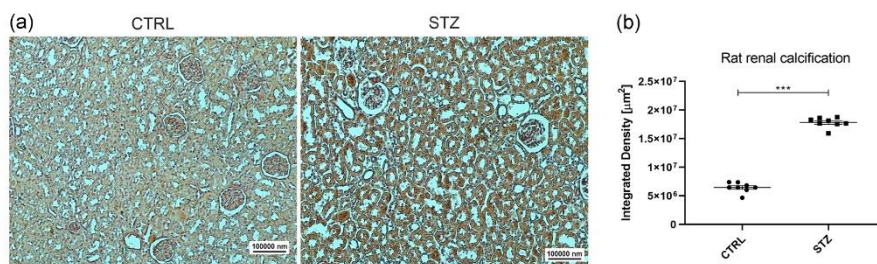


FIGURE 1 Renal calcification occurs in Wistar rats with streptozotocin-induced diabetes. (a) Kidney sections stained with Alizarin Red S solution in CTRL and STZ rats (scale bar = 100 μm , $\times 10$ magnification). (b) Increases in calcification in kidney sections in STZ rats (** $p < 0.0001$, unpaired t test, $n = 8$).

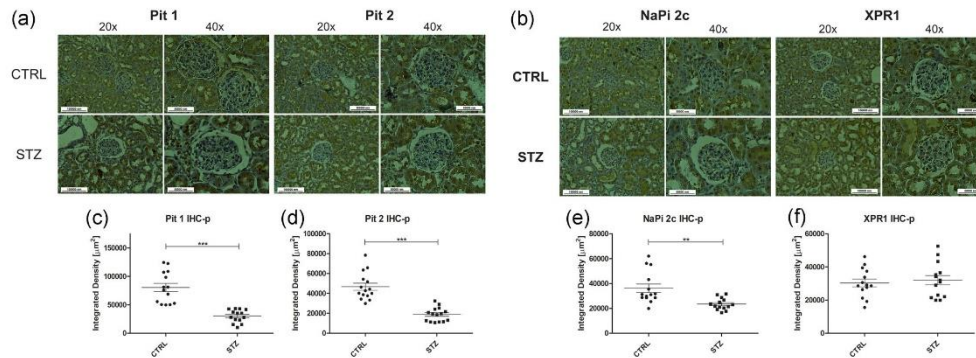


FIGURE 2 Immunohistochemistry of kidney sections exhibited differences in glomerular phosphate transporters in diabetic rats compared with control rats. (a, b) Images of renal tissue samples from CTRL and STZ rats with visible brown-stained phosphate transporters (scale bar = 100 μm for $\times 20$ magnification, scale bar = 50 μm for $\times 40$ magnification). (c) Decline in the amount of Pit 1 in glomeruli in STZ rats versus CTRL rats ($***p < 0.0001$, unpaired t test, $n = 14$). (d) Pit 2 deteriorates in renal glomeruli under diabetic conditions ($***p < 0.0001$, unpaired t test, $n = 15$). (e) Decrease in NaPi 2c levels in glomeruli in STZ rat ($**p = 0.002$, Mann-Whitney test, $n = 14$). (f) No differences in XPR1 transporter levels between STZ and CTRL rats

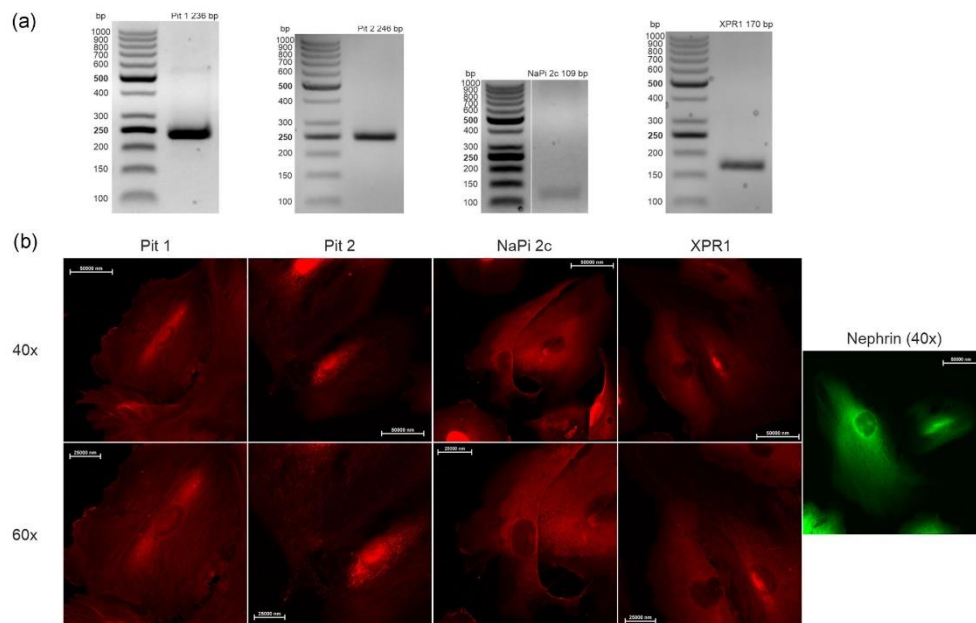


FIGURE 3 Expression of phosphate transporters in immortalized human podocytes. (a) Real-time PCR products electrophoresed on a 2.5% agarose gel. The resulting bands correspond to the amplified mRNA of Pit 1, Pit 2, NaPi 2c, and XPR1, respectively. (b) Confocal images of Pit 1, Pit 2, NaPi 2c, XPR1, and the podocyte marker nephrin in human podocytes (scale bar = 50 μm for $\times 40$ magnification, scale bar = 25 μm for $\times 60$ magnification). mRNA, messenger RNA

podocytes. The analyzed transporters exhibited intense fluorescence in the podocyte cell membrane and foot processes that they formed with adjacent cells (Figure 3b).

3.4 | HG concentration affects the amount of Pit 1 and Pit 2 but not NaPi 2c or XPR1

Because phosphate metabolism is disturbed during the course of DN and CKD (Kulesza & Piwkowska, 2021), we investigated whether the expression of phosphate transporters changes in podocytes that are cultured under HG conditions. We found that in HG concentrations, among the four analyzed proteins, only Pit 1 mRNA expression significantly decreased (by 19%) relative to the SG concentration (HG: 0.79 ± 0.05 vs. SG: 0.97 ± 0.03 ; Figure 4a-d). This finding was confirmed by Western blot analysis, in which the amount of Pit 1 protein decreased in HG by 48% (HG: 0.60 ± 0.04 vs. SG: 1.16 ± 0.06) compared with podocytes that were cultured in SG (Figure 4e). We demonstrated a similar relationship for Pit 2, which deteriorated by 34% in HG (HG: 0.41 ± 0.07 vs. SG: 0.62 ± 0.05 ; Figure 4f). We observed no alterations of the amount of NaPi 2c or XPR1 in podocytes that were cultured in HG (Figure 4g,h).

3.5 | Cellular localization of phosphate transporters in human podocytes changes under HG conditions

All of the tested proteins perform their function in the cell membrane. Therefore, the next phase of the present study was to examine

whether the HG environment influences the cellular localization of the analyzed transporters. We used a cell surface biotinylation method and found that all sodium-dependent phosphate transporters were depleted in the podocyte plasma membrane under HG conditions compared with the SG control. The most significant decline (60%) was observed for Pit 1 (HG: 0.29 ± 0.10 vs. SG: 0.73 ± 0.07 ; Figure 5a). NaPi 2c was reduced by 41% in HG (HG: 0.39 ± 0.06 vs. SG: 0.66 ± 0.06 ; Figure 5c). The amount of Pit 2 in the cell membrane declined by 36% under HG conditions (HG: 0.27 ± 0.03 vs. SG: 0.42 ± 0.03 ; Figure 5b). We detected an opposite trend for XPR1, which is responsible for the Pi surge from the cell. Despite the lack of differences in total levels of this transporter between the SG and HG conditions, translocation to the podocyte cell membrane increased by 359% under HG conditions (HG: 0.78 ± 0.04 vs. SG: 0.17 ± 0.07 ; Figure 5d). To visualize our findings, we immunofluorescently stained podocytes under SG and HG conditions (Figure 5e). The most redundant decrease in fluorescence intensity under HG conditions was observed for Pit 1 and Pit 2, but no significant differences were found for NaPi 2c or XPR1.

3.6 | HG conditions affect eNPP1 expression and cellular distribution and TNAP activity in human podocytes

eNPP1 and TNAP are key enzymes that participate in the maintenance of proper phosphate/pyrophosphate balance. We evaluated their expression and activity under HG conditions. Using specific primers, we found that HG influenced only eNPP1 mRNA levels, resulting in a 14% decline (HG: 0.85 ± 0.03 vs. SG: 0.99 ± 0.03 ;

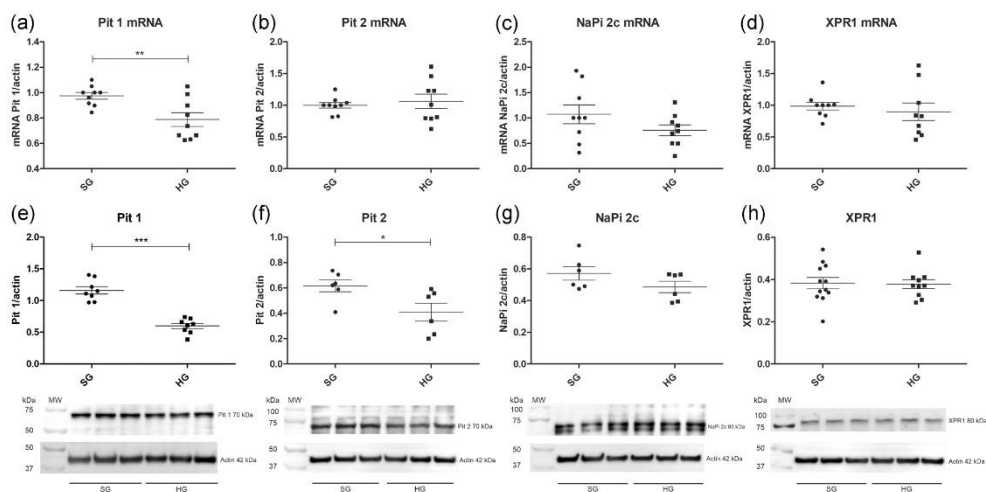


FIGURE 4 High glucose concentration alters the expression of only some phosphate transporters. (a) Pit 1 mRNA decreased under high glucose (HG) conditions (30 mM, 5 days) compared with standard glucose (SG) conditions (11 mM) (** $p = 0.006$, unpaired t test, $n = 9$). (b-d) Pit 2, NaPi 2c, and XPR1 mRNA levels did not vary between SG and HG conditions. (e) Significant reduction of Pit 1 levels under HG conditions, determined by Western blot (** $p < 0.0001$, unpaired t test, $n = 8$). (f) Decrease in Pit 2 levels under HG conditions (* $p = 0.026$, Mann-Whitney test, $n = 6$). (g, h) No differences in NaPi 2c or XPR1 levels were observed between the SG and HG conditions. mRNA, messenger RNA

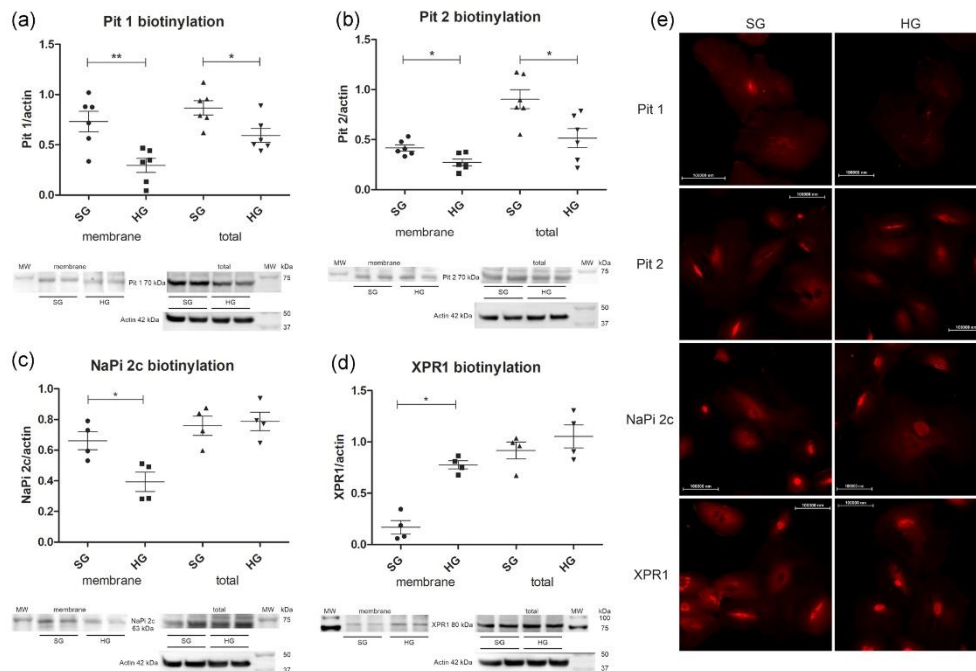


FIGURE 5 Cellular localization of phosphate transporters changes under high glucose conditions. (a) Pit 1 content deteriorates in the podocyte membrane (** $p = 0.005$, unpaired t test, $n = 6$) and whole-cell lysates (* $p = 0.020$, unpaired t test, $n = 6$) under HG conditions. (b) Pit 2 levels in the plasma membrane (* $p = 0.010$, unpaired t test, $n = 6$) and total Pit 2 levels (* $p = 0.018$, unpaired t test, $n = 6$) decreased under HG conditions compared with SG conditions. (c) NaPi 2c is less present in the plasma membrane under HG conditions (* $p = 0.029$, Mann–Whitney test, $n = 4$), but total NaPi 2c levels remained unchanged. (d) XPR1 levels increased 3.5-fold in the podocyte plasma membrane under HG conditions (* $p = 0.029$, Mann–Whitney test, $n = 4$), but total XPR1 levels remained unchanged. (e) Immunofluorescence labeling of Pit 1, Pit 2, NaPi 2c, and XPR1 in podocytes that were cultured under SG and HG conditions (scale bar = 100 μm , $\times 20$ magnification). HG, high glucose; SG, standard glucose

Figure 6a). No changes in TNAP mRNA levels were found (Figure 6b). We established that HG caused a 24% increase in TNAP activity (HG: 0.21 ± 0.003 nmol/min/mg protein vs. SG: 0.17 ± 0.007 nmol/min/mg protein; Figure 6d), whereas eNPP activity remained intact (Figure 6c). Because of the lack of a specific substrate for eNPP1, the overall activity of ectonucleotide pyrophosphatases/phosphodiesterases was assessed. eNPP1 is a membrane protein. Thus, we evaluated its cellular distribution. We found no alterations of the total amount of this protein between the SG and HG conditions but noted a 63% decrease in its expression in the podocyte cell membrane under HG conditions (HG: 0.48 ± 0.12 vs. SG: 1.29 ± 0.13 ; Figure 6e).

3.7 | Intracellular and extracellular ATP concentration and extracellular PPI concentrations are affected by HG in human immortalized podocytes

Considering the disturbances in the activity and expression of the tested enzymes, we investigated the amount of intracellular and

extracellular ATP (which is hydrolyzed by eNPP1 mainly to PPI) and PPI (which is the most potent calcification inhibitor and can be hydrolyzed by TNAP to Pi). We detected a two-fold decline in extracellular ATP levels (HG: 0.07 ± 0.01 μM vs. SG: 0.14 ± 0.01 μM ; Figure 7a) and 37% decrease in intracellular ATP levels (HG: 10.1 ± 1.3 μM vs. SG: 15.9 ± 1.7 ; Figure 7b) in podocytes that were cultured under HG conditions. We also observed a 22% reduction of extracellular PPI levels under HG conditions (HG: 15.5 ± 1.0 μM vs. SG: 19.8 ± 1.7 μM ; Figure 7c). No significant changes in intracellular PPI were detected between the SG and HG conditions (Figure 7d).

3.8 | HG conditions increased calcification process in human podocytes

To investigate whether changes in phosphate transporter level induce calcification in podocytes, we performed Alizarin Red S staining (Figure 8a). We observed an increase in calcification intensity in podocytes that were cultured under HG conditions (integrated

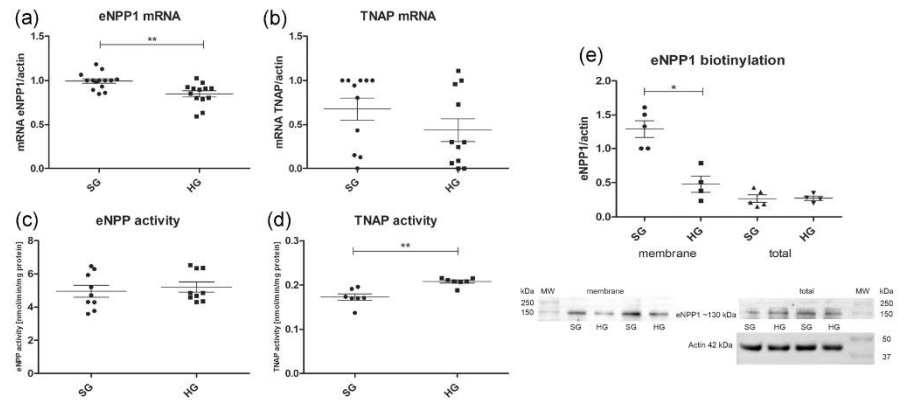


FIGURE 6 High glucose changes eNPP1 expression and its cellular distribution and increases TNAP activity. (a) eNPP1 mRNA levels decreased under HG conditions (** $p = 0.002$, unpaired t test, $n = 13$ – 14). (b) No changes in TNAP mRNA levels under HG conditions compared with SG conditions. (c) Overall eNPP activity remained the same under SG and HG conditions. (d) TNAP activity significantly escalates under HG conditions (** $p = 0.005$, Mann–Whitney test, $n = 7$). (e) Biotinylation of eNPP1 revealed a decrease in levels in the plasma membrane under HG conditions (* $p = 0.020$, Mann–Whitney test, $n = 4$ – 5), but total eNPP1 levels remained unchanged. eNPP1, ectonucleotide pyrophosphatase/phosphodiesterase 1; HG, high glucose; SG, standard glucose; TNAP, tissue nonspecific alkaline phosphatase

density in HG vs. SG: $3.77 \times 10^6 \pm 0.225 \times 10^6 \mu\text{m}^2$ vs. $0.595 \times 10^6 \pm 0.085 \times 10^6 \mu\text{m}^2$; Figure 8b).

4 | DISCUSSION

The present study, for the first time, demonstrated the presence of sodium-dependent phosphate transporters in podocytes and found that HG affects their amount and distribution in the cell. The in vitro observations were confirmed by in vivo studies in rats with STZ-induced diabetes, in which we observed a decrease in the amount of sodium-dependent transporters in glomeruli. We also observed an escalation in TNAP activity in human podocytes, which generates Pi, and a decrease in extracellular P_i levels. These alterations may contribute to an increase in calcification processes in both human podocytes under HG conditions and kidneys in STZ rats.

To date, little information has been reported on the role of the analyzed proteins, mainly type III sodium-dependent transporters, in kidney damage and pathological calcification (Asada et al., 2019; Sekiguchi et al., 2011; Tsuchiya et al., 2004). Conversely, the negative influence of chronic hyperphosphatemia on glomerular calcification is well known. The treatment of rats with dibasic sodium phosphate for 14 days resulted in the deposition of calcium phosphate salts in the glomerulus (Tsuchiya et al., 2004). During plasma filtration, glomerular epithelial cells were overloaded with high doses of phosphate. Dense granules that were stained with von Kossa dye (which is used to visualize calcium complexes) were observed in podocytes (Tsuchiya et al., 2004). This led to the fusion and detachment of foot processes, thickening of the glomerular basement membrane, and

consequently overt proteinuria that resembled nephrotic syndrome (Tsuchiya et al., 2009). These abnormalities may result from the influx of Pi into podocytes, with the participation of phosphate co-transporters. Furthermore, the overexpression of Pit 1 protein in rats led to glomerular sclerotic changes that were nearly identical to those described above (Sekiguchi et al., 2011). Additionally, the expression of markers of podocyte damage, such as desmin and connexin-43, was elevated. These changes were manifested by proteinuria, which was proportional to the amount of phosphate in the diet. However, administration of the bisphosphonate drug risedronate in transgenic rats, resulted in abnormalities that were much less severe (Asada et al., 2019). Bisphosphonates show similarity to phosphate ions and compete with them for the transition to the podocyte via the Pit 1 transporter and thus protect it from Pi-induced damage. Deterioration in the amount of SLC20 proteins that was observed in the present study under diabetic conditions does not exclude their participation in podocyte injury and glomerular calcification. Further studies of this issue are required.

Several mechanisms by which Pit 1, Pit 2, and XPR1 proteins contribute to calcification in other tissues, mainly blood vessels and the brain, have been discovered. The use of phosphonoformic acid on vascular smooth muscle cells (VSMCs), which is an inhibitor of sodium-dependent phosphate transporters, resulted in the abolition of calcification processes in these cells (Chen et al., 2002). This confirms the participation of proteins from the SLC20 family in this phenomenon. Silencing of the *SLC20A1* gene, which encodes Pit 1 protein, by small interfering RNA abolished mineralization (Li et al., 2006). Additionally, the targeted deletion of Pit 1 in VSMCs in mice resulted in a twofold increase in Pit 2 expression and calcification retention, suggesting compensatory mechanisms

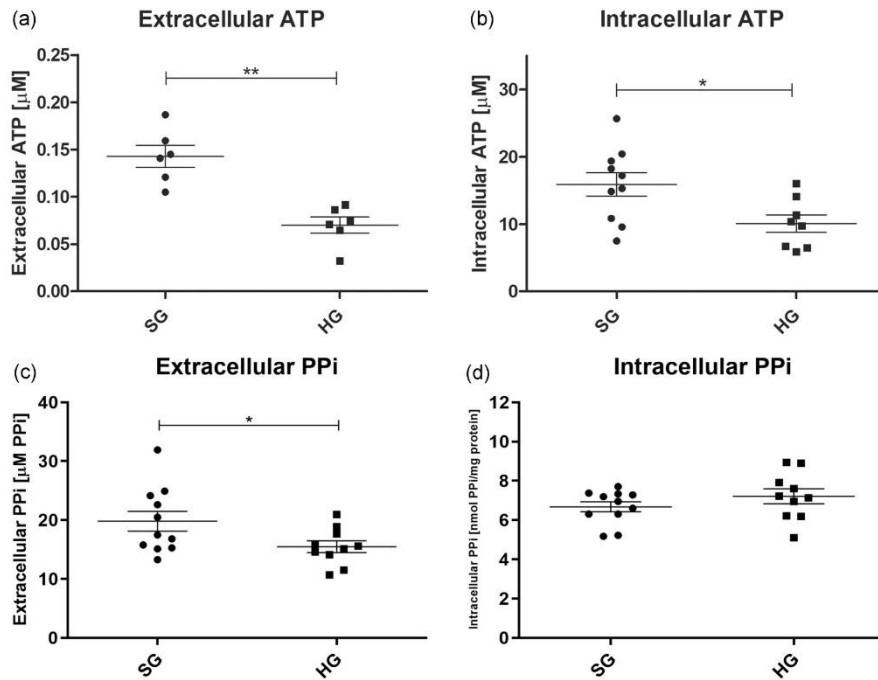


FIGURE 7 Levels of intracellular/extracellular ATP and PPI are altered in podocytes under high glucose conditions. (a) Decrease in extracellular ATP levels in podocytes that were cultured under HG conditions (** $p = 0.002$, Mann-Whitney test, $n = 6$). (b) A similar regularity was observed in the case of the intracellular amount of ATP (* $p = 0.021$, unpaired t test, $n = 8-10$). (c) Extracellular PPI levels decreased in podocytes under HG conditions (* $p = 0.045$, unpaired t test, $n = 10-11$). (d) Intracellular PPI levels did not change under HG conditions. ATP, adenosine triphosphate; HG, high glucose

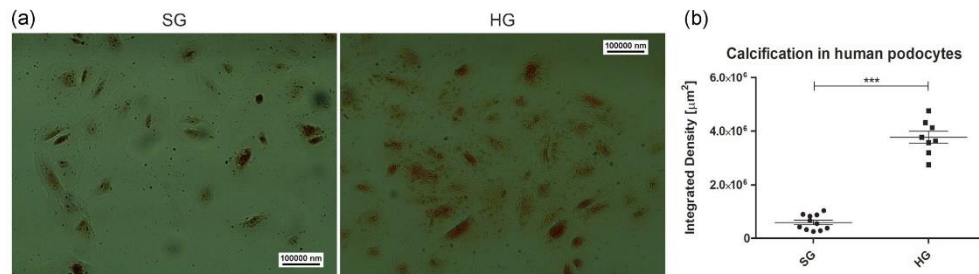


FIGURE 8 Calcification intensifies in human podocytes under high glucose conditions. (a) Light microscopy images show an increase in orange-red Alizarin Red staining in podocytes under HG conditions (scale bar = $100 \mu\text{m}$, $\times 10$ magnification). (b) Quantification of dye intensity in HG compared with SG (*** $p < 0.0001$, unpaired t test, $n = 8-11$). HG, high glucose; SG, standard glucose

(Crouthamel et al., 2013). Yamada et al. (2018) reported that VSMC calcification was induced by a high-phosphate diet in mice with global Pit 2 haploinsufficiency. These findings demonstrate the dual nature of Pit 2 in mineralization. In the present study, we observed a reduction of the total amount and membrane localization of both Pit 1

and Pit 2 under diabetic conditions. We did not recognize any compensatory mechanisms at the level of mRNA or protein expression. Pit 1 and Pit 2 have been reported to form homo- or heterodimers that are Pi-sensitive sensors, and these heterodimers can mediate extracellular signal-regulated kinase 1/2 (ERK1/2) signaling (Bon

et al., 2018). In podocytes, this signaling pathway plays a crucial role mainly through interactions with TRPC6 calcium channels (Farmer et al., 2019). Our group's previous studies established that TRPC6 participates in insulin-dependent actin cytoskeleton rearrangement and glucose transport (Rachubik et al., 2018; Rogacka et al., 2017). The upregulation of ERK signaling by Pit 1/Pit 2 heterodimers may enhance TRPC6 activity, possibly resulting in podocyte injury, which has been observed in other diseases (Yu et al., 2018).

Disturbances in the transport of phosphates have recently started to be associated with the pathogenesis of Fahr's disease, also known as primary familial brain calcification (PFBC) (Legati et al., 2015). Mutations of the *SLC20A2* and *XPR1* genes, which encode Pit 2 and XPR1 transporters, respectively, contribute to calcification of the basal ganglia. Some of these mutations are loss-of-function mutations, in which improperly produced proteins are unable to act as a phosphate transporter (Hsu et al., 2013; López-Sánchez et al., 2020). The precipitation of calcium phosphate in brain tissue that is detected in PFBC results from the accumulation of phosphate ions in the cell through the ineffective export and retention of Pi in the extracellular space (Anheim et al., 2016; Taglia et al., 2018). In the present study, we noticed a slightly different tendency. We observed a reduction of the amount of proteins in the podocyte cell membrane by which Pi is transported into the cell. The amount of membrane XPR1 and Pi-producing activity of TNAP increased, suggesting the retention of phosphate ions in the extracellular space.

Apart from hepatocytes, myocytes, and adipocytes, podocytes are insulin-sensitive cells (Lay & Coward, 2018). Changes in podocyte permeability to albumin and reorganization of the actin cytoskeleton are closely related to insulin signaling and insulin-dependent glucose transport, as confirmed by our previous research (Audzeyenka, Rogacka, et al., 2020; Piwkowska et al., 2013, 2015; Rachubik et al., 2018). Recent studies reported an effect of Pit 1 on insulin signaling (Forand et al., 2016). In hepatocytes, Pit 1 deletion led to a prolonged interaction between ubiquitin-specific peptidase 7 (USP7) and insulin receptor (IR) substrate 1, protecting it against proteasomal degradation and prolonging insulin signaling (Forand et al., 2016). We observed a decrease in Pit 1 under hyperglycemic conditions, but Pit 1-induced podocyte injury could be mediated by an interaction with USP7 and result in impairments in insulin signaling. Another protein that influences insulin-dependent signaling is eNPP1. In addition to its function of purifying the extracellular space of nucleotides, eNPP1 directly interacts with IR, specifically the α subunit. This phenomenon leads to inhibition of the activity of IR tyrosine kinase and consequently insulin resistance (Dong et al., 2005; Maddux & Goldfine, 2000). IR inhibition depends on the enzymatic activity of eNPP1 (Chin et al., 2009). We observed interesting regularities for the eNPP1 protein during our research. Although HG conditions did not alter the activity of eNPP1, the amount of mRNA and content of this protein in the cell membrane of podocytes were reduced under HG conditions. Thus, eNPP1 appeared to contribute to the intensification of calcification processes that we observed under HG conditions through a decrease in the production of protective PPI that we noted in the extracellular space. The amount of eNPP1 in the

podocyte cell membrane decreased while the total amount of this protein remained unaffected. There was an eNPP1 translocation which did not have to affect its overall activity.

In conclusion, the present study established the presence of phosphate transporters in human podocytes and observed rearrangements of their distribution in the cell under diabetic conditions. We recognized an increase in calcification processes both in vitro and in vivo. Our results shed new light on the pathophysiology of renal calcification in DN, but more research is required to understand the detailed implications.

ACKNOWLEDGEMENT

This study was supported by Grant 2018/29/B/NZ4/02074 to Agnieszka Piwkowska from the National Science Center in Poland.

CONFLICT OF INTERESTS

The authors declare no conflict of interests.

AUTHOR CONTRIBUTIONS

Tomasz Kulesza: prepared the original draft of the manuscript. **Agnieszka Piwkowska:** designed the study and obtained funding and managed the project. **Tomasz Kulesza, Marlena Typiak, Patrycja Rachubik, and Agnieszka Piwkowska:** performed the experiments and analyzed the data. **Agnieszka Piwkowska, Dorota Rogacka, Irena Audzeyenka, Marlena Typiak, Stefan Angielski, and Moin A. Saleem:** revised the manuscript. **Moin A. Saleem and Irena Audzeyenka:** provided materials and methods. All authors approved the final version of the manuscript.

DATA AVAILABILITY STATEMENT

The data that support the findings of this study are available from the corresponding author upon reasonable request.

ORCID

Tomasz Kulesza  <http://orcid.org/0000-0001-5166-7444>
Marlena Typiak  <http://orcid.org/0000-0002-9687-1016>
Patrycja Rachubik  <http://orcid.org/0000-0002-7691-8243>
Dorota Rogacka  <http://orcid.org/0000-0001-6242-0324>
Agnieszka Piwkowska  <http://orcid.org/0000-0002-0086-7777>

REFERENCES

- Anheim, M., López-Sánchez, U., Giovannini, D., Richard, A. C., Touhami, J., N'Guyen, L., Rudolf, G., Thibault-Stoll, A., Frebourg, T., Hannequin, D., Campion, D., Battini, J. L., Sitbon, M., & Nicolas, G. (2016). XPR1 mutations are a rare cause of primary familial brain calcification. *Journal of Neurology*, 263(8), 1559–1564. <https://doi.org/10.1007/s00415-016-8166-4>
- Asada, Y., Takayanagi, T., Kawakami, T., Tomatsu, E., Masuda, A., Yoshino, Y., Sekiguchi-Ueda, S., Shibata, M., Ide, T., Niimi, H., Yaoita, E., Seino, Y., Sugimura, Y., & Suzuki, A. (2019). Risedronate attenuates podocyte injury in phosphate transporter-overexpressing rats. *International Journal of Endocrinology*, 2019, 4194853. <https://doi.org/10.1155/2019/4194853>
- Audzeyenka, I., Rachubik, P., Rogacka, D., Typiak, M., Kulesza, T., Angielski, S., Rychtowski, M., Wysocka, M., Gruba, N., Lesner, A.,

- Saleem, M. A., & Piwkowska, A. (2020). Cathepsin C is a novel mediator of podocyte and renal injury induced by hyperglycemia. *Biochimica et Biophysica Acta-Molecular Cell Research*, 1867(8), 118723. <https://doi.org/10.1016/j.bbamcr.2020.118723>
- Audzeyenka, I., Rogacka, D., Rachubik, P., Typiak, M., Rychłowski, M., Angielski, S., & Piwkowska, A. (2020). The PKG α -Rac1 pathway is a novel regulator of insulin-dependent glucose uptake in cultured rat podocytes. *Journal of Cellular Physiology*, 236(6), 4655–4668. <https://doi.org/10.1002/jcp.30188>
- Azpiazu, D., Gonzalo, S., González-Parra, E., Egido, J., & Villa-Belosta, R. (2018). Role of pyrophosphate in vascular calcification in chronic kidney disease. *Nefrología : publicación oficial de la Sociedad Española Nefrología*, 38, 250–257. <https://doi.org/10.1016/j.nefroe.2018.03.003>
- Bon, N., Couasnay, G., Bourguin, A., Sourice, S., Beck-Cormier, S., Guicheux, J., & Beck, L. (2018). Phosphate (Pi)-regulated heterodimerization of the high-affinity sodium-dependent Pi transporters Pit1/SLC20A1 and Pit2/SLC20A2 underlies extracellular Pi sensing independently of Pi uptake. *Journal of Biological Chemistry*, 293(6), 2102–2114. <https://doi.org/10.1074/jbc.M117.807339>
- Chavkin, N. W., Chia, J. J., Crouthamel, M. H., & Giachelli, C. M. (2015). Phosphate uptake-independent signaling functions of the type III sodium-dependent phosphate transporter, PIT-1, in vascular smooth muscle cells. *Experimental Cell Research*, 333(1), 39–48. <https://doi.org/10.1016/j.yexcr.2015.02.002>
- Chen, N. X., O'Neill, K. D., Duan, D., & Moe, S. M. (2002). Phosphorus and uremic serum up-regulate osteopontin expression in vascular smooth muscle cells. *Kidney International*, 62, 1724–1731. <https://doi.org/10.1046/j.1523-1755.2002.00625.x>
- Chin, C. N., Dallas-Yang, Q., Liu, F., Ho, T., Ellsworth, K., Fischer, P., Natasha, T., Ireland, C., Lu, P., Li, C., Wang, I. M., Strohl, W., Berger, J. P., An, Z., Zhang, B. B., & Jiang, G. (2009). Evidence that inhibition of insulin receptor signaling activity by PC-1/ENPP1 is dependent on its enzyme activity. *European Journal of Pharmacology*, 606(1–3), 17–24. <https://doi.org/10.1016/j.ejphar.2009.01.016>
- Coward, R., & Fornoni, A. (2015). Insulin signaling: Implications for podocyte biology in diabetic kidney disease. *Current Opinion in Nephrology and Hypertension*, 24(1), 104–110. <https://doi.org/10.1097/MNH.0000000000000078>
- Cozzolino, M., Foque, D., Ciceri, P., & Galassi, A. (2017). Phosphate in chronic kidney disease progression. *Contributions to Nephrology*, 190, 71–82. <https://doi.org/10.1159/000468915>
- Crouthamel, M. H., Lau, W. L., Leaf, E. M., Chavkin, N. W., Wallingford, M. C., Peterson, D. F., Li, X., Liu, Y., Chin, M. T., Levi, M., & Giachelli, C. M. (2013). Sodium-dependent phosphate cotransporters and phosphate-induced calcification of vascular smooth muscle cells: Redundant roles for PIT-1 and PIT-2. *Arteriosclerosis, Thrombosis, and Vascular Biology*, 33(11), 2625–2632. <https://doi.org/10.1161/ATVBAHA.113.302249>
- Dong, H., Maddux, B. A., Altomonte, J., Meseck, M., Accili, D., Terkeltaub, R., Johnson, K., Youngren, J. F., & Goldfine, I. D. (2005). Increased hepatic levels of the insulin receptor inhibitor, PC-1/NPP1, induce insulin resistance and glucose intolerance. *Diabetes*, 54(2), 367–372. <https://doi.org/10.2337/diabetes.54.2.367>
- Farmer, L. K., Rollason, R., Whitcomb, D. J., Ni, L., Goodliff, A., Lay, A. C., Birnbaumer, L., Heeson, K. J., Xu, S. Z., Saleem, M. A., & Welsh, G. I. (2019). TRPC6 Binds to and activates calpain, independent of its channel activity, and regulates podocyte cytoskeleton, cell adhesion, and motility. *Journal of the American Society of Nephrology*, 30(10), 1910–1924. <https://doi.org/10.1681/ASN.2018070729>
- Fleisch, H., & Bisaz, S. (1962). Isolation from urine of pyrophosphate, a calcification inhibitor. *American Journal of Physiology-Legacy Content*, 203(4), 671–675. <http://dx.doi.org/10.1152/ajplegacy.1962.203.4.671>
- Forand, A., Koumakis, E., Rousseau, A., Sossier, Y., Journe, C., Merlin, J. F., Leroy, C., Boitez, V., Codogno, P., Friedlander, G., & Cohen, I. (2016). Disruption of the phosphate transporter Pit1 in hepatocytes improves glucose metabolism and insulin signaling by modulating the USP7/IRS1 interaction. *Cell Reports*, 16(10), 2736–2748. <https://doi.org/10.1016/j.celrep.2016.08.012>
- Forster, I. C., Hernando, N., Biber, J., & Murer, H. (2013). Phosphate transporters of the SLC20 and SLC34 families. *Molecular Aspects of Medicine*, 34(2–3), 386–395. <https://doi.org/10.1016/j.mam.2012.07.007>
- Garg, P. (2018). A review of podocyte biology. *American Journal of Nephrology*, 47(suppl 1), 3–13. <https://doi.org/10.1159/000481633>
- Giovannini, D., Touhami, J., Charnet, P., Sitbon, M., & Battini, J. L. (2013). Inorganic phosphate export by the retrovirus receptor XPR1 in metazoans. *Cell Reports*, 3(6), 1866–1873. <https://doi.org/10.1016/j.celrep.2013.05.035>
- Hsu, S. C., Sears, R. L., Lemos, R. R., Quintáns, B., Huang, A., Spiteri, E., Nevarez, L., Mamah, C., Zatz, M., Pierce, K. D., Fullerton, J. M., Adair, J. C., Berner, J. E., Bower, M., Brodaty, H., Carmona, O., Dobricic, V., Fogel, B. L., García-Estevez, D., ... Coppola, G. (2013). Mutations in SLC20A2 are a major cause of familial idiopathic basal ganglia calcification. *Neurogenetics*, 14(1), 11–22. <https://doi.org/10.1007/s10048-012-0349-2>
- Kasztan, M., Piwkowska, A., Kreft, E., Rogacka, D., Audzeyenka, I., Szczepanska-Konkel, M., & Jankowski, M. (2016). Extracellular purines' action on glomerular albumin permeability in isolated rat glomeruli: insights into the pathogenesis of albuminuria. *American Journal of Physiology-Renal Physiology*, 311(1), F103–F111. <https://doi.org/10.1152/ajprenal.00567.2015>
- Kramer, H., Toto, R., Peshock, R., Cooper, R., & Victor, R. (2005). Association between chronic kidney disease and coronary artery calcification: The Dallas heart study. *Journal of the American Society of Nephrology*, 16(2), 507–513. <https://doi.org/10.1681/ASN.2004070610>
- Kulesza, T., & Piwkowska, A. (2021). The impact of type III sodium-dependent phosphate transporters (Pit 1 and Pit 2) on podocyte and kidney function. *Journal of Cellular Physiology*, 236(10), 7176–7185. <https://doi.org/10.1002/jcp.30368>
- Lay, A. C., & Coward, R. J. M. (2018). The evolving importance of insulin signaling in podocyte health and disease. *Frontiers in Endocrinology*, 9, 693. <https://doi.org/10.3389/fendo.2018.00693>
- Lee, S. Y., & Müller, C. E. (2017). Nucleotide pyrophosphatase/phosphodiesterase 1 (NPP1) and its inhibitors. *MedChemComm*, 8(5), 823–840. <http://doi.org/10.1039/c7md00015d>
- Legati, A., Giovannini, D., Nicolas, G., López-Sánchez, U., Quintáns, B., Oliveira, J. R., Sears, R. L., Ramos, E. M., Spiteri, E., Sobrido, M. J., Carracedo, A., Castro-Fernández, C., Cubizolle, S., Fogel, B. L., Goizet, C., Jen, J. C., Kirdlar, S., Lang, A. E., Miedzybrodzka, Z., ... Coppola, G. (2015). Mutations in XPR1 cause primary familial brain calcification associated with altered phosphate export. *Nature Genetics*, 47(6), 579–581. <https://doi.org/10.1038/ng.3289>
- Li, X., & Giachelli, C. M. (2007). Sodium-dependent phosphate cotransporters and vascular calcification. *Current Opinion in Nephrology & Hypertension*, 16(4), 325–328. <http://dx.doi.org/10.1097/mnh.0b013e3281c55ef1>
- Li, X., Yang, H. Y., & Giachelli, C. M. (2006). Role of the sodium-dependent phosphate cotransporter, Pit-1, in vascular smooth muscle cell calcification. *Circulation Research*, 98, 905–912. <https://doi.org/10.1161/01.RES.0000216409.20863.e7>
- López-Sánchez, U., Tury, S., Nicolas, G., Wilson, M. S., Jurici, S., Ayrignac, X., Courgnaud, V., Saiardi, A., Sitbon, M., & Battini, J. L. (2020). Interplay between primary familial brain calcification-associated SLC20A2 and XPR1 phosphate transporters requires inositol polyphosphates for control of cellular phosphate

- homeostasis. *Journal of Biological Chemistry*, 295(28), 9366–9378. <https://doi.org/10.1074/JBC.RA119.011376>
- Maddux, B. A., & Goldfine, I. D. (2000). Membrane glycoprotein PC-1 inhibition of insulin receptor function occurs via direct interaction with the receptor alpha-subunit. *Diabetes*, 49(1), 13–19. <https://doi.org/10.2337/diabetes.49.1.13>
- Orimo, H. (2010). The mechanism of mineralization and the role of alkaline phosphatase in health and disease. *Journal of Nippon Medical School*, 77(Issue 1), 4–12. <https://doi.org/10.1272/jnms.77.4>
- Piwkowska, A., Rogacka, D., Angielski, S., & Jankowski, M. (2012). Hydrogen peroxide induces activation of insulin signaling pathway via AMP-dependent kinase in podocytes. *Biochemical and Biophysical Research Communications*, 428(1), 167–172. <https://doi.org/10.1016/j.bbrc.2012.10.033>
- Piwkowska, A., Rogacka, D., Audzeyenka, I., Angielski, S., & Jankowski, M. (2015). Combined effect of insulin and high glucose concentration on albumin permeability in cultured rat podocytes. *Biochemical and Biophysical Research Communications*, 461(2), 383–389. <https://doi.org/10.1016/j.bbrc.2015.04.043>
- Piwkowska, A., Rogacka, D., Kasztan, M., Angielski, S., & Jankowski, M. (2013). Insulin increases glomerular filtration barrier permeability through dimerization of protein kinase G type Ia subunits. *Biochimica et Biophysica Acta - Molecular Basis of Disease*, 1832(6), 791–804. <https://doi.org/10.1016/j.bbdis.2013.02.011>
- Rachubik, P., Szejder, M., Rogacka, D., Audzeyenka, I., Rychłowski, M., Angielski, S., & Piwkowska, A. (2018). The TRPC6-AMPK pathway is involved in insulin-dependent cytoskeleton reorganization and glucose uptake in cultured rat podocytes. *Cellular Physiology and Biochemistry*, 51(1), 393–410. <https://doi.org/10.1159/000495236>
- Reiss, A. B., Miyawaki, N., Moon, J., Kasselmann, L. J., Voloshyna, I., D'Avino, R., & De Leon, J. (2018). CKD, arterial calcification, atherosclerosis and bone health: Inter-relationships and controversies. *Atherosclerosis*, 278(November 2017), 49–59. <https://doi.org/10.1016/j.atherosclerosis.2018.08.046>
- Rogacka, D., Audzeyenka, I., Rachubik, P., Rychłowski, M., Kasztan, M., Jankowski, M., Angielski, S., & Piwkowska, A. (2017). Insulin increases filtration barrier permeability via TRPC6-dependent activation of PKG α signaling pathways. In *Biochimica et Biophysica Acta-Molecular Basis of Disease*, 1863(Issue 6), 1312–1325. <https://doi.org/10.1016/j.bbdis.2017.03.002>
- Russo, D., Palmiero, G., De Blasio, A. P., Balletta, M. M., & Andreucci, V. E. (2004). Coronary artery calcification in patients with CRF not undergoing dialysis. *American Journal of Kidney Diseases*, 44(6), 1024–1030. <https://doi.org/10.1053/j.ajkd.2004.07.022>
- Rutsch, F., Nitschke, Y., & Terkeltaub, R. (2011). Genetics in arterial calcification: Pieces of a puzzle and cogs in a wheel. In *Circulation Research*, 109(Issue 5), 578–592. <https://doi.org/10.1161/CIRCRESAHA.111.247965>
- Saleem, M. A., O'Hare, M. J., Reiser, J., Coward, R. J., Inward, C. D., Farren, T., Chang, Y. X., Ni, L., Mathieson, P. W., & Mundel, P. (2002). A conditionally immortalized human podocyte cell line demonstrating nephrin and podocin expression. *Journal of the American Society of Nephrology*, 13(3), 630–638.
- Sekiguchi, S., Suzuki, A., Asano, S., Nishiwaki-Yasuda, K., Shibata, M., Nagao, S., Yamamoto, N., Matsuyama, M., Sato, Y., Yan, K., Yaoita, E., & Itoh, M. (2011). Phosphate overload induces podocyte injury via type III Na-dependent phosphate transporter. *American Journal of Physiology-Renal Physiology*, 300(4), F848–F856. <http://dx.doi.org/10.1152/ajprenal.00334.2010>
- Solini, A., Uselli, V., & Fiorina, P. (2015). The dark side of extracellular ATP in kidney diseases. *Journal of the American Society of Nephrology*, 26(5), 1007–1016. <https://doi.org/10.1681/ASN.2014070721>
- Taglia, I., Formichi, P., Battisti, C., Peppoloni, G., Barghigiani, M., Tessa, A., & Federico, A. (2018). Primary familial brain calcification with a novel SLC20A2 mutation: Analysis of PIT-2 expression and localization. *Journal of Cellular Physiology*, 233(3), 2324–2331. <https://doi.org/10.1002/jcp.26104>
- Tsuchiya, N., Matsushima, S., Takasu, N., Kyokawa, Y., & Torii, M. (2004). Glomerular calcification induced by bolus injection with dibasic sodium phosphate solution in sprague-dawley rats. *Toxicologic Pathology*, 32(4), 408–412. <https://doi.org/10.1080/01926230490452490>
- Tsuchiya, N., Torii, M., Narama, I., & Matsui, T. (2009). Nephrotic syndrome induced by dibasic sodium phosphate injections for twenty-eight days in rats. *Toxicologic Pathology*, 37(3), 270–279. <https://doi.org/10.1177/0192623309332996>
- Umanath, K., & Lewis, J. B. (2018). Update on diabetic nephropathy: Core curriculum 2018. *American Journal of Kidney Diseases*, 71(6), 884–895. <https://doi.org/10.1053/j.ajkd.2017.10.026>
- Villa-Belostta, R., & Sorribas, V. (2011). Calcium Phosphate Deposition With Normal Phosphate Concentration-Role of Pyrophosphate. *Circulation Journal*, 75(11), 2705–2710. <http://dx.doi.org/10.1253/circj.cj-11-0477>
- Webster, A. C., Nagler, E. V., Morton, R. L., & Masson, P. (2017). Chronic kidney disease. *The Lancet*, 389(10075), 1238–1252. [https://doi.org/10.1016/S0140-6736\(16\)32064-5](https://doi.org/10.1016/S0140-6736(16)32064-5)
- Yamada, S., Leaf, E. M., Chia, J. J., Cox, T. C., Speer, M. Y., & Giachelli, C. M. (2018). PIT-2, a type III sodium-dependent phosphate transporter, protects against vascular calcification in mice with chronic kidney disease fed a high-phosphate diet. *Kidney International*, 94, 716–727. <https://doi.org/10.1016/j.kint.2018.05.015>
- Yu, Y., Zhang, L., Xu, G., Wu, Z., Li, Q., Gu, Y., & Niu, J. (2018). Angiotensin II Type I receptor agonistic autoantibody induces podocyte injury via activation of the TRPC6-Calcium/calineurin pathway in pre-eclampsia. *Kidney and Blood Pressure Research*, 43(5), 1666–1676. <https://doi.org/10.1159/000494744>

SUPPORTING INFORMATION

Additional supporting information may be found in the online version of the article at the publisher's website.

How to cite this article: Kulesza, T., Typiak, M., Rachubik, P., Audzeyenka, I., Rogacka, D., Angielski, S., Saleem, M. A., & Piwkowska, A. (2022). Hyperglycemic environment disrupts phosphate transporter function and promotes calcification processes in podocytes and isolated glomeruli. *Journal of Cellular Physiology*, 1–14. <https://doi.org/10.1002/jcp.30700>

9.2.2. Kulesza T, Typiak M, Rachubik P, Rogacka D, Audzeyenka I, Saleem MA, Piwkowska A. **Pit 1 transporter (SLC20A1) as a key factor in the NPP1-mediated inhibition of insulin signaling in human podocytes.** *J Cell Physiol.* 2023; doi: 10.1002/jcp.31051

Received: 23 March 2023 | Accepted: 16 May 2023
DOI: 10.1002/jcp.31051

RESEARCH ARTICLE

Journal of Cellular Physiology WILEY

Pit 1 transporter (SLC20A1) as a key factor in the NPP1-mediated inhibition of insulin signaling in human podocytes

Tomasz Kulesza¹ | Marlena Typiak^{1,2} | Patrycja Rachubik¹ |
Dorota Rogacka^{1,3} | Irena Audzeyenka^{1,3} | Moin A. Saleem⁴ |
Agnieszka Piwkowska^{1,3}

¹Laboratory of Molecular and Cellular Nephrology, Mossakowski Medical Research Institute, Polish Academy of Sciences, Gdansk, Poland

²Department of General and Medical Biochemistry, Faculty of Biology, University of Gdansk, Gdansk, Poland

³Department of Molecular Biotechnology, Faculty of Chemistry, University of Gdansk, Gdansk, Poland

⁴Bristol Renal, University of Bristol, Bristol, UK

Correspondence

Tomasz Kulesza, Laboratory of Molecular and Cellular Nephrology, Mossakowski Medical Research Institute, Polish Academy of Sciences, Wita Stwosza St. 63, Gdansk 80-308, Poland.
Email: tkulesza@imdik.pan.pl

Funding information

Narodowe Centrum Nauki

Abstract

Podocytes are crucially involved in blood filtration in the glomerulus. Their proper function relies on efficient insulin responsiveness. The insulin resistance of podocytes, defined as a reduction of cell sensitivity to this hormone, is the earliest pathomechanism of microalbuminuria that is observed in metabolic syndrome and diabetic nephropathy. In many tissues, this alteration is mediated by the phosphate homeostasis-controlling enzyme nucleotide pyrophosphatase/phosphodiesterase 1 (NPP1). By binding to the insulin receptor (IR), NPP1 inhibits downstream cellular signaling. Our previous research found that hyperglycemic conditions affect another protein that is involved in phosphate balance, type III sodium-dependent phosphate transporter 1 (Pit 1). In the present study, we evaluated the insulin resistance of podocytes after 24 h of incubation under hyperinsulinemic conditions. Thereafter, insulin signaling was inhibited. The formation of NPP1/IR complexes was observed at that time. A novel finding in the present study was our observation of an interaction between NPP1 and Pit 1 after the 24 h stimulation of podocytes with insulin. After downregulation of the *SLC20A1* gene, which encodes Pit 1, we established insulin resistance in podocytes that were cultured under native conditions, manifested as a lack of intracellular insulin signaling and the inhibition of glucose uptake via the glucose transporter type 4. These findings suggest that Pit 1 might be a major factor that participates in the NPP1-mediated inhibition of insulin signaling.

KEYWORDS

diabetic nephropathy, insulin resistance, insulin signaling, phosphate transporters, podocyte

Abbreviations: Akt (PKB), protein kinase B; ATP, adenosine triphosphate; DCF, 2',7'-dichlorodihydrofluorescein; FBS, fetal bovine serum; GFB, glomerular filtration barrier; GLUT4, glucose transporter type 4; HG, high glucose (30 mM); IR, insulin receptor; IRS1/2, insulin receptor substrates 1 and 2; NPP1, nucleotide pyrophosphatase/phosphodiesterase 1; PCR, polymerase chain reaction; Pi, phosphate; Pit 1, type III sodium-dependent phosphate transporter 1; PPI, pyrophosphate; p-Akt, phosphorylated protein kinase B; p-IR, phosphorylated insulin receptor; RONS, reactive oxygen/nitrogen species; SG, standard glucose (11 mM); USP, ubiquitin-specific peptidase.

1 | INTRODUCTION

Insulin resistance can be considered a cornerstone in the development of various disorders of the body's energy homeostasis, such as metabolic syndrome and type II diabetes. Insulin resistance is defined as a decrease in the sensitivity of insulin-dependent tissues to this hormone, despite its normal or even elevated level (Yaribeygi et al., 2019). Insulin-sensitive cells, in addition to myocytes, hepatocytes, and adipocytes, include podocytes, specialized epithelial cells of the glomerulus (Rogacka, 2021). Interlocking foot processes of podocytes form slit diaphragms, the most dynamic part of the glomerular filtration barrier (GFB). This structure prevents proteins from entering the ultrafiltrate (Garg, 2018). The loss of podocyte function through the effacement of foot processes, destruction of slit diaphragms, and finally the detachment of podocytes from capillary walls occurs in early stages of diabetes, manifesting as microalbuminuria, which is often overlooked in routine urinalysis (Brinkkoetter et al., 2013; Pagtalunan et al., 1997; Weil et al., 2012; Wolf et al., 2005). In recent years, many studies have suggested that impairments in insulin signaling and the insulin resistance of podocytes are the main reasons for faulty GFB function in diabetic nephropathy (Lu et al., 2021; Rousseau et al., 2022; Welsh et al., 2010).

Under physiological conditions, insulin acts on podocytes directly through insulin receptors (IRs) that are present on their cell membrane. Upon binding of the insulin molecule to the α subunit of IRs, the β subunit undergoes autophosphorylation, which initiates intracellular downstream signaling that involves insulin receptor substrates 1 and 2 (IRS1/2), phosphoinositide-3-kinase, phosphoinositide-dependent kinase 1, and protein kinase B (PKB/Akt), which triggers the shift of glucose transporter type 4 (GLUT4) vesicles to the cell membrane and glucose influx (Rogacka, 2021). Notably, podocytes are the most insulin-sensitive cells in the glomerulus, reflected by profoundly higher IR expression than in mesangial and endothelial cells (Mima et al., 2011).

Harmful effects of diabetes, apart from a decrease in insulin sensitivity, include long-lasting high glucose (HG) concentrations, which further exacerbates insulin resistance. The common denominator of podocyte injury that is caused by the aforementioned pathophysiological conditions is oxidative stress and the generation of reactive oxygen/nitrogen species (RONS) (Piwkowska et al., 2011; Whaley-Connell et al., 2007), whereas an increase in NADPH oxidase activity is responsible for RONS production (Piwkowska et al., 2010). The HG-induced generation of RONS directly alters podocyte function, which initially leads to microalbuminuria and over time transforms into overt proteinuria during the course of diabetic nephropathy (Susztak et al., 2006). Interestingly, podocytes appear to be insulin resistant before the occurrence of microalbuminuria, thus demonstrating the fragility of these cells to fluctuations in carbohydrate metabolism (Tejada et al., 2008).

Our recent studies demonstrated that HG conditions alter podocyte function by decreasing the amount of type III

sodium-dependent phosphate transporter (Pit 1) and nucleotide pyrophosphatase/phosphodiesterase 1 (NPP1) (Kulesza et al., 2022). Pit 1 belongs to the solute carrier family of proteins, and its crucial function is the transport of phosphate (Pi) into the cell (Kulesza & Piwkowska, 2021). In turn, NPP1 is a membrane enzyme whose essential function is to cleanse nucleotides from the extracellular space. The main substrate of NPP1 is adenosine triphosphate (ATP), which is hydrolyzed to adenosine monophosphate and pyrophosphate (PPi) (Lee & Müller, 2017). Our research established that hyperglycemia causes a decrease in the total amount and plasma membrane exposure of the Pit 1 transporter. NPP1 also abates from the membrane of podocytes, resulting in Pi retention in the extracellular space and a decrease in extracellular PPi concentrations, thereby promoting ectopic calcification in the glomerulus (Kulesza et al., 2022).

In addition to its catalytic functions, NPP1 is known to participate in the development of insulin resistance (Dong et al., 2005). This protein directly binds to the α subunit of the IR, which causes conformational changes in the β subunit. Structural modifications impair the function of tyrosine kinase and IR autophosphorylation is blocked, which inhibits further steps of insulin signaling (Lee & Müller, 2017; Maddux & Goldfine, 2000). These actions appear to be associated with the pyrophosphatase/phosphodiesterase activity of NPP1 (Chin et al., 2009). Pit 1 also appears to mediate insulin-dependent glucose transport. The specific knockout of Pit 1 in hepatocytes improves glucose management and sensitizes these cells to insulin (Forand et al., 2016). However, the deletion of Pit 1 in macrophages impairs their function by weakening the inflammatory response, reflected by reductions of RONS generation and wound healing ability (Koumakis et al., 2019). Therefore, the role of the Pit 1 transporter in different tissues is ambiguous, and further studies of the function of this protein in podocytes are necessary.

The present study sheds new light on the involvement of NPP1 and Pit 1 proteins in insulin signaling in podocytes. We examined the activity of ectonucleotide pyrophosphatase/phosphodiesterase (eNPP) and the amount of extracellular ATP. We also assessed the cellular localization of Pit 1 and NPP1 after insulin stimulation. We established the degree of interaction between Pit 1 and NPP1 under the influence of insulin. Moreover, insulin signaling was verified by analyzing IR and Akt phosphorylation and measuring intracellular glucose transport. We also downregulated the SLC20A1 gene, which encodes Pit 1, and assessed effects on the insulin response of podocytes.

2 | MATERIALS AND METHODS

2.1 | Podocyte cell line

Development of the immortalized human podocyte cell line (provided by Moin A. Saleem) was described previously (Saleem et al., 2002). Cell purity was checked systematically (Audzeyenka et al., 2020).

Podocytes were cultured in RPMI-1640 medium (Catalog No. 21875059; Thermo Fisher Scientific) that was supplemented with 10% fetal bovine serum (FBS; Catalog No. 10270106; Thermo Fisher Scientific), 100 U/mL penicillin, and 100 mg/mL streptomycin (Catalog No. 15140122; Thermo Fisher Scientific). After reaching the desired confluence at 33°C and 5% CO₂, podocytes were cultured at 37°C and 5% CO₂ for 10–14 days for differentiation. Afterward, the cells were cultured with 100 nM insulin solution (Catalog No. I9278; Sigma-Aldrich) for 24 h, 1 h, or 5 min. RPMI-1640 medium with a standard glucose (SG) concentration (1 mM) without the addition of insulin served as a control.

2.2 | Lentiviral transduction and gene silencing

To silence the *SLC20A1* gene, which encodes Pit 1 protein, podocytes were infected with GIPZ *SLC20A1* short hairpin RNA (shRNA) viral particles (shPit 1) and GIPZ nonsilencing shRNA viral particles (shControl; Dharmacon) as a negative control. To enhance transduction, polybrene (Catalog No. H9268; Sigma-Aldrich) was added to proliferating cells at 33°C. The selection of shRNA-expressing podocytes was conducted with puromycin. Podocytes were then cultured at 37°C for differentiation. Gene silencing was assessed using real-time polymerase chain reaction (PCR) and immunofluorescence.

2.3 | Western blot

Cell lysates and Western blot analysis were performed as previously described (Kulesza et al., 2022). Primary antibodies that were used in the experiments are listed in Table 1. The density of emerging bands was analyzed using Quantity One software (Bio-Rad).

2.4 | Cell surface biotinylation

The biotinylation of cell membrane proteins was performed as previously described (Kulesza et al., 2022; Typiak et al., 2021). Briefly, podocytes were incubated with 1 mg/mL biotin solution (Catalog No. 21338; Thermo Fisher Scientific) for 30 min at 4°C. Next, cell lysates were generated and then incubated with Neutr/Avidin resin (Catalog No. 53150; Thermo Fisher Scientific) on a rotor at 4°C overnight. The next day, membrane samples (which bound to Avidin) and total samples were subjected to Western blot analysis.

2.5 | Immunoprecipitation

Cell lysates were precleared using Protein G PLUS-Agarose (Catalog No. sc-2002; Santa Cruz Biotechnology) on a rotor at 4°C for 30 min. Next, cell extracts were incubated with IP/WB Optima B or IP/WB Optima C (Catalog No. sc-45039/45040; Santa Cruz Biotechnology) supplemented with anti-NPP1 antibodies (Table 1) on a rotor at 4°C overnight. To elute protein complexes, lysates were heated in sodium dodecyl sulfate loading buffer at 96°C for 10 min. The eluate was then subjected to Western blot analysis.

2.6 | Real-time PCR

Podocyte total RNA was isolated using the RNeasy Plus Mini Kit and subsequent on-column genomic DNA eradication (Qiagen). The purity and concentration of RNA were assessed using a NanoDrop device (Thermo Fisher Scientific). Next, isolated RNA was subjected to reverse-transcription PCR. The resulting complementary DNA was analyzed by real-time PCR in a LightCycler 480 instrument (Roche) using gene-specific

TABLE 1 Primary antibodies used in the experiments.

Antibody	Dilution	Source
Actin	1:10,000 (WB)	Sigma-Aldrich; Catalog No. A5441
NPP1	1:100 (WB), 1:15 (IF)	Santa Cruz Biotechnology; Catalog No. sc-166649
IR β	1:250 (WB), 1:20 (IF)	Santa Cruz Biotechnology; Catalog No. sc-81465
p-IR β (Tyr 1150/1151)	1:250 (WB)	Santa Cruz Biotechnology; Catalog No. sc-81500
IR α	1:1500 (WB), 1:30 (IF)	Thermo Fisher Scientific; Catalog No. bs-0047R
Akt	1:350 (WB)	Santa Cruz Biotechnology; Catalog No. sc-8144
p-Akt (Ser 473)	1:350 (WB)	Santa Cruz Biotechnology; Catalog No. sc-7985
Rab5a	1:50 (IF)	ABClonal; Catalog No. A1180
GLUT4	1:300 (WB)	Santa Cruz Biotechnology; Catalog No. sc-53566
Pit 1	1:20,000 (WB), 1:200 (IF)	Biorbyt; Catalog No. orb412245

Abbreviations: Akt, protein kinase B; GLUT4, glucose transporter type 4; IF, immunofluorescence; IR, insulin receptor; NPP1, nucleotide pyrophosphatase/phosphodiesterase 1; p-IR, phosphorylated insulin receptor; Pit 1, type III sodium-dependent phosphate transporter 1; WB, Western blot.

intron-spanning primers and fluorescent hydrolysis probes (Table 2; Roche). The $\Delta\Delta C_t$ method, with β -actin as the reference gene, was used to determine the relative quantification of specific messenger RNA (mRNA) transcripts.

2.7 | Immunofluorescent staining and endosome imaging

Cells were grown on glass coverslips that were coated with human fibronectin (Catalog No. 354088; Corning). Podocytes were fixed in 4% formaldehyde for 15 min at room temperature, permeabilized in 0.1% Triton X-100, and incubated with blocking solution (2% FBS, 2% bovine serum albumin, and 0.2% fish gelatin) for 1 h at room temperature. Cells were then incubated with primary antibodies (Table 1) overnight at 4°C. The next day, the cells were immersed in secondary antibody solution (1:200 dilution in blocking solution; Catalog No. A11010 or A11059; Thermo Fisher Scientific) for 2 h at 4°C. To detect endosomal vesicles, pHrodo Green Dextran/pHrodo Red Dextran (Catalog No. P35368/P10361; Thermo Fisher Scientific) was used according to the manufacturer's protocol. Fluorescence imaging was performed using a confocal microscope (Eclipse Ti; Nikon Instruments; RCM device, Confocal.nl).

2.8 | eNPP activity

eNPP activity was measured using *p*-nitrophenyl thymidine 5'-monophosphate as a substrate. Podocytes were lysed in 200 mM Tris-HCl buffer (pH 8) with the addition of 1% Triton X-100 and 1.6 mM MgCl₂. After incubation with 1 mg/mL substrate solution for 20 min, the absorbance of yellow product was measured at $\lambda = 405$ nm. The activity of eNPP is expressed as nmol of the product catalyzed in 1 min relative to protein amount in the lysate (nmol/min/mg protein).

2.9 | Extracellular ATP levels

To measure extracellular ATP levels, podocytes were grown in serum-free medium for at least 2 h before the experiment. The medium was collected from the cells and heated at 96°C for 3 min. Measurements were performed using the ATP Determination Kit (Catalog No. A22066; Invitrogen) according to the manufacturer's instructions. The resulting luminescence was detected with a Sirius 2 luminometer (Berthold Technologies).

2.10 | Glucose uptake measurement

Glucose transport was assessed as previously described (Rogacka et al., 2018, 2010) with slight modifications. Briefly, 24 h before the experiment, podocytes were incubated in a medium without FBS or antibiotics. Two hours before the measurements, the cells were grown in a glucose-free medium. The assessment was conducted with the addition of 1 μ Ci/well of (1,2-³H)-deoxy-D-glucose diluted in isotope-free glucose at a final concentration of 50 μ M. Extracellular radioactivity was measured in medium harvested from the cells. Next, podocytes were lysed in 0.5 M NaOH for intracellular radioactivity analysis. Both evaluations were performed using a MicroBeta2 Microplate Counter (Perkin Elmer).

2.11 | NADPH oxidase activity and RONS levels

To assess NADPH oxidase activity, lucigenin-enhanced chemiluminescence was measured with a Sirius 2 luminometer (Berthold Technologies) as described previously (Piwkowska et al., 2010). The method consisted of integration of the area under the curve to determine the amount of superoxide with reference to a previously characterized standard curve (Münzel et al., 1996).

The fluoroprobe 2',7'-dichlorodihydrofluorescein diacetate (H₂DCFDA) was used to assess RONS generation as previously

TABLE 2 Sequences of primers and fluorescent probes for real-time PCR analysis.

Protein name	Gene name	Accession no. for mRNA sequence	Primer sequence	Probe sequence	Product length (bp)
Pit 1	SLC20A1	NM_005415.5	Forward: CTGCAATGCTGTGTCTGACC Reverse: ATAAAGCAACCAGAGGCCCA	CTCTGCCT	236
GLUT4	SLC2A4	NM_001042.3	Forward: ACTGGCCATTGTTATCGGCA Reverse: AGGCGCTTCAGACTCTTCTGG	CTGCTGCC	210
NPP1	ENPP1	NM_006208.3	Forward: TGGGTAGAAGAACCATGTGAGA Reverse: GAGGGTAGGAGGCGTTTCA	CTGCTGGG	72
β -Actin	ACTB	NM_001101.5	Forward: ATGGCAATGAGCGGTTC Reverse: GGATGCCACAGGACTCCA	CTTCCAGC	76

Abbreviations: bp, base pair; GLUT4, glucose transporter type 4; mRNA, messenger RNA; NPP1, nucleotide pyrophosphatase/phosphodiesterase 1; PCR, polymerase chain reaction; Pit 1, type III sodium-dependent phosphate transporter 1.

described (Piwkowska et al., 2011). H_2DCFDA was transformed intracellularly to 2',7'-dichlorodihydrofluorescein (DCF). To evade light-induced DCF degradation, the samples were incubated in the dark. The measurement of DCF fluorescence was performed with an EnSpire Multimode Plate Reader (Perkin Elmer) at excitation and emission wavelengths of 485 and 525 nm, respectively.

2.12 | Statistical analysis

The statistical analysis was performed using Prism 8.4.3 software (GraphPad). All data are presented as the mean \pm SEM. Values of $p \leq 0.05$ were considered statistically significant. The Shapiro–Wilk test was used to check normality of the data distribution. If the data passed the Shapiro–Wilk test, then unpaired t-test (for two groups) or one-way analysis of variance followed by Dunnett's or Sidak's post hoc test (for more than two groups) was performed. For data that did not meet a normal distribution, nonparametric tests were used.

3 | RESULTS

3.1 | Insulin affects the amount and function of NPP1 and Pit 1 proteins and oxidative balance in human podocytes

In our previous research, we established the presence of specific Pi transporters in human podocytes and decreases in NPP1 and Pit 1 membrane content under hyperglycemic conditions that mimicked insulin resistance (Kulesza et al., 2022). Therefore, we assessed the ways in which these proteins respond to the direct stimulation of podocytes with insulin.

We first evaluated expression of the *ENPP1* and *SLC20A1* genes, which encode NPP1 and Pit 1 proteins, respectively. All analyzed genes are visualized in Figure 1b. A 22% increase in *ENPP1* expression was observed after 1 h of incubation with insulin, which increased to 30% after 24 h of incubation (SG: 0.98 ± 0.05 , culture medium supplemented with 100 nM insulin [INS] 1 h: 1.19 ± 0.07 , INS 24 h: 1.26 ± 0.06 ; Figure 1a). Pit 1 mRNA expression increased by 30% 5 min after exposure to insulin, and this 30% increase lasted up to 24 h (SG: 0.94 ± 0.06 , INS 5 min: 1.20 ± 0.08 , INS 1 h: 1.26 ± 0.06 , INS 24 h: 1.23 ± 0.06 ; Figure 1a). However, we observed the opposite trend at the protein level. Insulin caused a 43% reduction of NPP1 protein levels after 5 min (SG: 0.41 ± 0.03 , INS 5 min: 0.24 ± 0.01 ; Figure 1c). Pit 1 levels also decreased by 29% after 5 min and 1 h of incubation with insulin (SG: 0.78 ± 0.04 , INS 5 min: 0.56 ± 0.03 , INS 1 h: 0.52 ± 0.08 ; Figure 1c). The observed increase in mRNA expression may be a mechanism that compensates for lower levels of the analyzed proteins.

Next, we evaluated whether insulin influences eNPP activity by direct measurement and indirectly by assessing levels of ATP (a main substrate of NPP1). eNPP activity increased after 5 min of incubating podocytes with insulin and remained at this level up to 1 h (SG: 2.99 ± 0.08 nmol/min/mg protein, INS 5 min: 3.38 ± 0.07 nmol/min/mg

protein, INS 1 h: 3.25 ± 0.04 nmol/min/mg protein; Figure 1d). Extracellular ATP levels decreased by 40% after 5 min of incubation with insulin (SG: 1.14 ± 0.09 nmol/mg protein, INS 5 min: 0.68 ± 0.11 nmol/mg protein; Figure 1d), which was consistent with higher eNPP activity.

We also found that insulin increased oxidative stress in podocytes. Measurements of NADPH oxidase activity revealed a 48% increase after 5 min of incubation, with an increasing trend up to 24 h (SG: 15.52 ± 1.41 nmol/min/mg protein, INS 5 min: 22.61 ± 0.83 nmol/min/mg protein, INS 1 h: 24.23 ± 0.121 nmol/min/mg protein, INS 24 h: 24.51 ± 2.26 nmol/min/mg protein; Figure 1e). We confirmed this effect by evaluating RONS levels. In podocytes that were cultured with insulin, RONS levels were 46% higher than in control cells and remained at this level throughout the studied period of time (SG: 795 ± 53 RLU/ μ g protein, INS 5 min: 1160 ± 51 RLU/ μ g protein, INS 1 h: 1070 ± 37 RLU/ μ g protein, INS 24 h: 1039 ± 24 RLU/ μ g protein; Figure 1e).

3.2 | Short-term incubation with insulin reduces plasma membrane exposure of IRs and GLUT4

NPP1 is responsible for inhibiting IRs and downstream insulin signaling (Maddux & Goldfine, 2000). Therefore, in the next experiments, we evaluated insulin-dependent glucose uptake via GLUT4. We first confirmed that insulin stimulation increased glucose uptake in human podocytes, with a 24% increase after 5 min of incubation and 13% increase after 1 h of incubation (SG: 1731 ± 58 pmol/15 min/mg protein, INS 5 min: 2145 ± 59 pmol/15 min/mg protein, INS 1 h: 1962 ± 67 pmol/15 min/mg protein; Figure 2a). After 24 h under hyperinsulinemic conditions, glucose uptake was at a similar level to the cells not stimulated with insulin, which indicated the insulin resistance of podocytes. We also observed an increase in phosphorylated insulin receptor (p-IR) and phosphorylated protein kinase B (p-Akt) proteins, indicating active downstream insulin signaling. The p-IR/IR ratio increased nearly 1.5-fold after 5 min (SG: 0.36 ± 0.10 , INS 5 min: 0.85 ± 0.06 ; Figure 2b), whereas a 25% increase in the p-Akt/Akt ratio lasted up to 1 h of incubation with insulin (SG: 0.83 ± 0.04 , INS 5 min: 1.07 ± 0.03 , INS 1 h: 1.028 ± 0.04 ; Figure 2b). In contrast, a 50% decrease in GLUT4 mRNA levels was observed after 5 min of incubation with insulin (SG: 1.07 ± 58 , INS 5 min: 0.59 ± 0.11 ; Figure 2c). A significant reduction of the plasma membrane presence of the IR and GLUT4 was observed. The amount of IRs decreased by nearly 100% (SG: 0.83 ± 0.10 , INS 5 min: 0.04 ± 0.01 ; Figure 2d), and the amount of GLUT4 decreased by 63% after 5 min of incubation with insulin (SG: 0.28 ± 0.04 , INS 5 min: 0.10 ± 0.01 ; Figure 2d).

3.3 | NPP1 forms complexes with IR α subunit and Pit 1

In earlier studies, the relationship between NPP1 activity and its ability to inhibit IRs through a direct interplay with the α subunit of

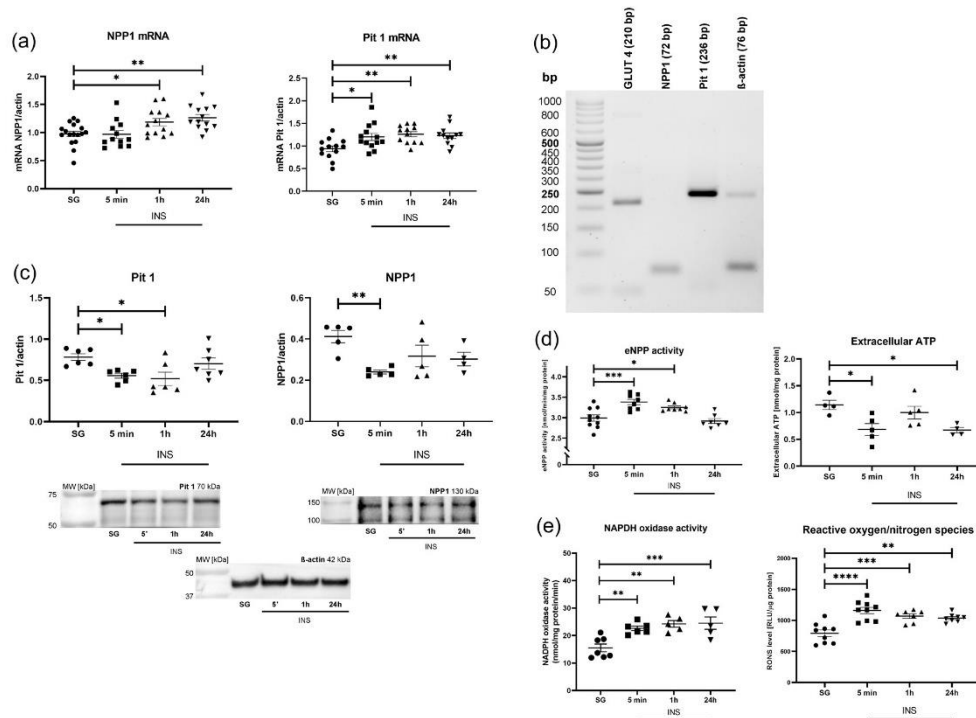


FIGURE 1 Insulin alters NPP1 and Pit 1 expression in human podocytes, eNPP activity, and oxidative balance. (a) Real-time PCR analysis of the *ENPP1* gene, which encodes NPP1 protein ($*p < 0.05$, $**p < 0.01$, Dunnett's multiple-comparison post hoc test, $n = 12-17$), and the *SLC20A1* gene, which encodes Pit 1 protein ($*p < 0.05$, $**p < 0.01$, Dunnett's multiple-comparison post hoc test, $n = 12-13$). (b) Visualization of real-time PCR products subjected to electrophoresis on 2.5% agarose gel. (c) Amount of NPP1 protein ($**p < 0.01$, Dunnett's multiple-comparison post hoc test, $n = 4-5$) and Pit 1 protein ($*p < 0.05$, Dunnett's multiple-comparison post hoc test, $n = 6-7$) in podocytes that were incubated with insulin. (d) Changes in eNPP activity ($*p < 0.05$, $***p < 0.001$, Dunnett's multiple-comparison post hoc test, $n = 7-10$) and extracellular ATP levels ($*p < 0.05$, Dunnett's multiple-comparison post hoc test, $n = 4-5$). (e) Oxidative stress in podocytes under conditions of insulin stimulation, represented as an increase in NADPH oxidase activity ($**p < 0.01$, $***p < 0.001$, Dunnett's multiple-comparison post hoc test, $n = 5-7$) and an increase in RONS levels ($**p < 0.01$, $***p < 0.001$, $****p < 0.0001$, Dunnett's multiple-comparison post hoc test, $n = 7-9$). ATP, adenosine triphosphate; eNPP, ectonucleotide pyrophosphatase/phosphodiesterase; NPP1, nucleotide pyrophosphatase/phosphodiesterase 1; PCR, polymerase chain reaction; Pit 1, type III sodium-dependent phosphate transporter 1; SG, standard glucose (11 mM).

the IR was established (Chin et al., 2009). Therefore, we investigated whether NPP1 interacts with IRs and Pit 1 under conditions of insulin stimulation. We found that NPP1 forms a complex with the IR after incubation with insulin, and this effect was most pronounced within 24 h (SG: 0.11 ± 0.06 , INS 5 min: 0.17 ± 0.07 , INS 24 h: 0.56 ± 0.11 ; Figure 3a). We observed similar regularity for Pit 1. Similar to the complex with the IR, the interaction between NPP1 and Pit 1 intensified after 5 min of insulin stimulation, reaching more than a fivefold increase after 24 h compared with control cells (SG: 0.05 ± 0.01 , INS 5 min: 0.14 ± 0.05 , INS 24 h: 0.33 ± 0.07 ; Figure 3a).

Based on the observed formation of Pit 1/NPP1 complexes, we checked the membrane distributions of both proteins under the examined conditions. We observed a 83% reduction of Pit 1 levels in the plasma membrane after 5 min of incubation with insulin (SG:

0.37 ± 0.03 , INS 5 min: 0.06 ± 0.01 ; Figure 3b). Analogous findings were noted for NPP1, with a 90% decrease in the membrane fraction of NPP1 after 5 min of insulin stimulation. In contrast, we observed a 30% increase in the plasma membrane distribution of this protein after 24 h of insulin stimulation (SG: 0.78 ± 0.05 , INS 5 min: 0.07 ± 0.03 , INS 24 h: 1.01 ± 0.05 ; Figure 3b).

3.4 | NPP1 colocalizes with both the IR α subunit and Pit 1

The interaction between NPP1 and both the IR and Pit 1 was also investigated using immunofluorescent analyses of their mutual localization (Figure 4a,b). Differences in Mander's overlap coefficient

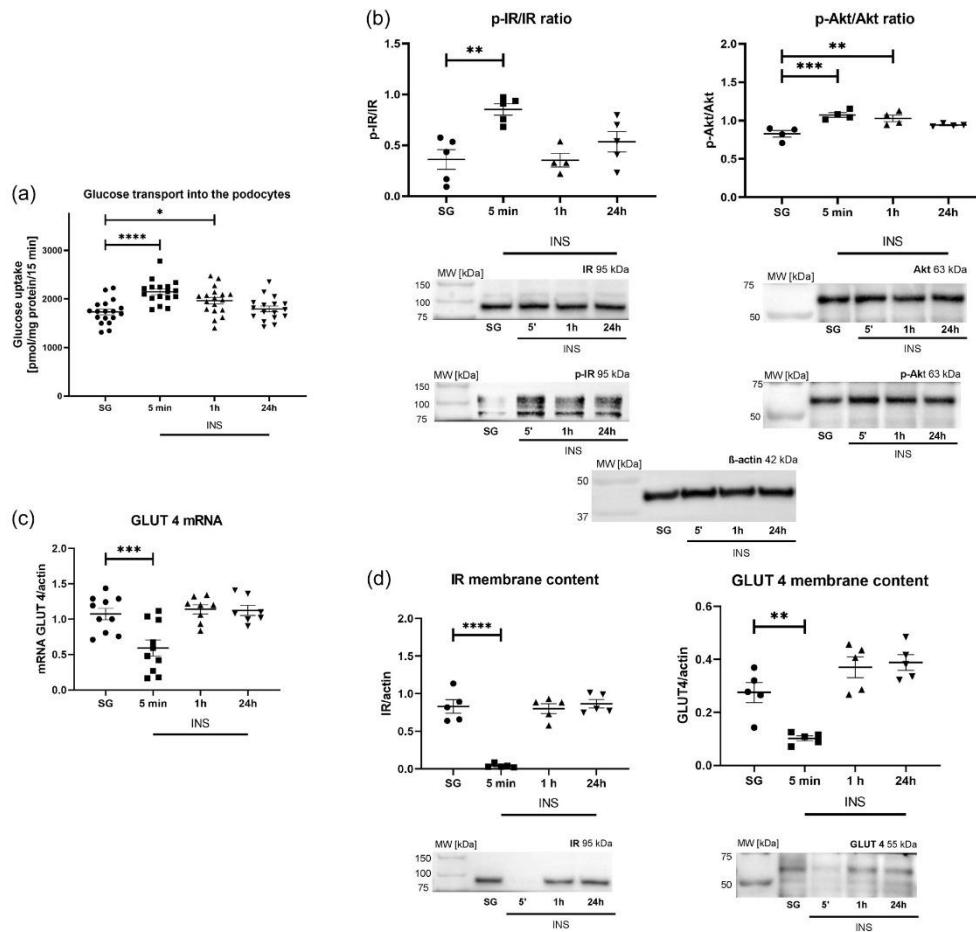


FIGURE 2 Incubation of podocytes with insulin leads to an enhancement of insulin signaling and glucose uptake. (a) Increase in glucose transport into cells after insulin stimulation ($*p < 0.05$, $****p < 0.0001$, Dunnett's multiple-comparison post hoc test, $n = 17-18$). (b) Increase in phosphorylated form of IR and Akt proteins, suggesting active insulin signaling ($**p < 0.01$, $***p < 0.001$, Dunnett's multiple-comparison post hoc test, $n = 4-5$). (c) Reduction of GLUT4 mRNA levels after 5 min of incubation with insulin ($***p < 0.001$, Dunnett's multiple-comparison post hoc test, $n = 7-10$). (d) Translocation of GLUT4 and the IR from the plasma membrane after 5 min of podocyte culture with insulin ($**p < 0.01$, $****p < 0.0001$, Dunnett's multiple-comparison post hoc test, $n = 4-5$). Akt, protein kinase B; GLUT4, glucose transporter type 4; IR, insulin receptor; mRNA, messenger RNA.

for NPP1/IR and NPP1/Pit 1 were not significant, but we observed changes in $k1$ and $k2$ overlap coefficients that clearly indicated that the contribution of the IR and Pit 1 prevailed in their colocalization with NPP1. An increase in the $k2$ coefficient after 24 h of incubation with insulin indicated a greater contribution of NPP1 to the colocalization of NPP1/IR, indicated by yellow coloring in the merged fluorescence images. These findings demonstrated that the inhibitory effect of NPP1 on the IR might occur via their direct interaction. After 24 h of stimulating podocytes with insulin, the input of Pit 1

transporter in mutual localization with NPP1 was elevated, reflected by changes in $k1$ coefficient values. This was confirmed by the detection of NPP1/Pit 1 complexes in immunoprecipitation after insulin treatment that was observed previously.

To evaluate the dynamics of endocytosis, we stained podocytes with dextran reagent, which visualizes endocytic vesicles and Ras-related protein Rab5a, which is responsible for the fusion of plasma membranes and early endosomes (Hoffenberg et al., 2000) (Figure 4c). After 5 min of treatment with insulin, the profound

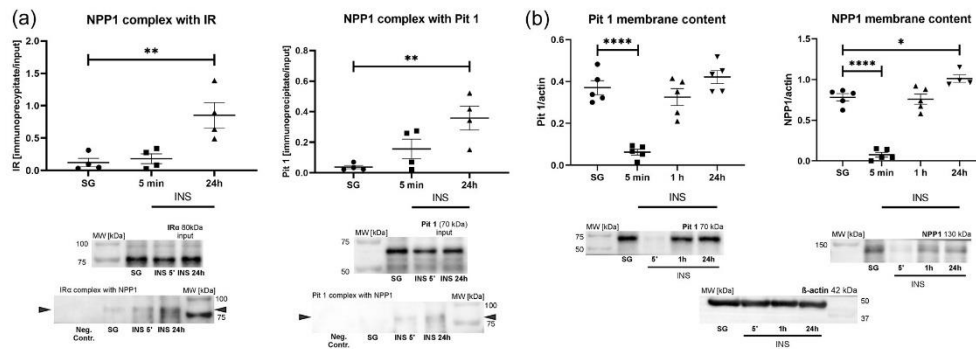


FIGURE 3 Interaction between NPP1 and IR α and between NPP1 and Pit 1 under conditions of insulin stimulation. (a) The formation of NPP1/IR α and NPP1/Pit 1 complexes under the influence of insulin is directly proportional to the incubation time of podocytes with insulin (** $p < 0.01$, Dunnett's multiple-comparison post hoc test, $n = 4$). Representative membranes show the amount of IR α and Pit 1 (blue arrows) that interacted with NPP1 under examined conditions. (b) Membrane content of NPP1 and Pit 1 significantly decreased after podocyte culture with insulin for 5 min (* $p < 0.05$, **** $p < 0.0001$, Dunnett's multiple-comparison post hoc test, $n = 4-5$). IR α , insulin receptor α ; NPP1, nucleotide pyrophosphatase/phosphodiesterase 1; Pit 1, type III sodium-dependent phosphate transporter 1.

recruitment of endocytic vesicles was present near the podocyte plasma membrane. Furthermore, Rab5a staining showed that after 5 min of incubation with insulin, vesicle-like structures were observed in the plasma membrane region. Intensely fluorescent granules were also present in the cell body. We did not observe these changes after 24 h of incubation with insulin. These findings suggest that endocytosis might be involved in the instantaneous NPP1-mediated inhibition of IRs.

3.5 | Silencing of Pit 1 affects eNPP activity and causes oxidative stress

Based on the colocalization of Pit 1 and NPP1 and our previous findings of a decrease in the amount of Pit 1 in podocytes under hyperglycemic conditions with insulin resistance (Kulesza et al., 2022), we tested whether Pit 1 is responsible for the regulation of insulin signaling. We silenced the *SLC20A1* gene, which encodes Pit 1 protein. We observed a 42% decrease in *SLC20A1* expression compared with control cells (shControl: 1.01 ± 0.01 , shPit 1: 0.58 ± 0.06 ; Figure 5a). The silencing was also confirmed by immunofluorescence analysis, in which we observed a 31% decrease in intensity in shPit 1 cells (shControl: 20.29 ± 0.96 , shPit 1: 14.09 ± 0.87 ; Figure 5b).

Next, we investigated the way in which Pit 1 downregulation affects eNPP activity and extracellular ATP levels. In shControl podocytes, an increase in eNPP activity was observed after 5 min of insulin stimulation, whereas in shPit 1 cells, eNPP activity was also significantly higher, but 5 min of insulin stimulation did not cause significant changes (shControl SG: 2.71 ± 0.15 nmol/min/mg protein, shControl INS 5 min: 3.84 ± 0.31 nmol/min/mg protein, shPit 1 SG: 3.42 ± 0.10 nmol/min/mg protein, shPit 1 INS 5 min: 3.57 ± 0.15 nmol/min/mg protein; Figure 5c).

The 66% reduction of extracellular ATP levels in shControl podocytes was observed after 5 min of incubation with insulin. We observed a decrease in extracellular ATP levels in shPit 1 cells compared with shControl podocytes, but insulin did not affect ATP concentrations in the medium (shControl SG: 2.27 ± 0.42 nmol/mg protein, shControl INS 5 min: 0.77 ± 0.08 nmol/mg protein, shPit 1 SG: 1.12 ± 0.27 nmol/mg protein, shPit 1 INS 5 min: 0.93 ± 0.16 nmol/mg protein; Figure 5c).

Silencing of the *SLC20A1* gene likewise resulted in an increase in oxidative stress, manifested by a 83% increase in NADPH oxidase activity in shPit 1 podocytes (shControl SG: 8.82 ± 1.15 nmol/min/mg protein, shControl INS 5 min: 13.61 ± 1.00 nmol/min/mg protein, shPit 1 SG: 16.07 ± 1.53 nmol/min/mg protein, shPit 1 INS 5 min: 15.55 ± 0.59 nmol/min/mg protein; Figure 5d). These relationships were confirmed by a 35% increase in RONS levels in shPit 1 podocytes. Additionally, 5 min of incubation with insulin caused a 22% increase in RONS formation compared with Pit 1-silenced cells that were cultured in SG (shControl SG: 867 ± 38 RLU/ μ g protein, shControl INS 5 min: 1205 ± 50 RLU/ μ g protein, shPit 1 SG: 1174 ± 55 RLU/ μ g protein, shPit 1 INS 5 min: 1428 ± 140 RLU/ μ g protein; Figure 5d).

3.6 | Downregulation of Pit 1 reduces membrane exposure of NPP1

Next, we determined whether the silencing of Pit 1 protein impacts the membrane distribution of NPP1. In shControl cells, 5 min of incubation with insulin caused the nearly complete translocation of NPP1 from the cell membrane. The same regularity was observed for shPit 1 podocytes that were cultured in SG medium, in which stimulation with insulin did not cause any changes (shControl SG: 0.90 ± 0.02 , shControl INS 5 min: 0.11 ± 0.05 , shPit 1 SG: 0.03 ± 0.01 ,

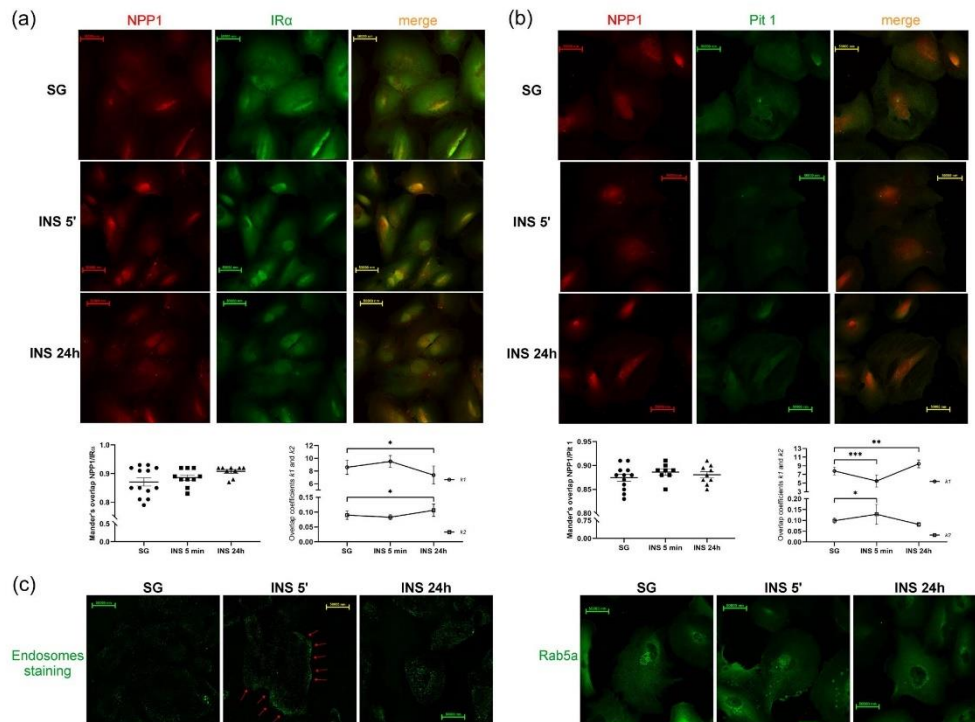


FIGURE 4 Colocalization of NPP1 with Pit 1 and the IR increases under the influence of insulin. (a) Confocal images of the colocalization of NPP1 and the IR α subunit, which reached its highest level after 24 h of incubation with insulin. Scale bar = 50 μ m. $k1$ and $k2$ overlap coefficients indicate the contribution of both proteins to their colocalization (* p < 0.05, Dunnett's multiple-comparison post hoc test, n = 9–13). (b) Similar observations as in (a) for the colocalization of NPP1 and Pit 1. Scale bar = 50 μ m (* p < 0.05, ** p < 0.01, *** p < 0.001, Dunnett's multiple-comparison test, n = 8–12). (c) Dextran Green staining of the distribution of endosomes. Red arrows mark a clearly outlined podocyte cell membrane after 5 min of incubation with insulin. The immunofluorescent staining of Rab5a protein showed vesicle-like structures in the podocyte plasma membrane after 5 min of insulin treatment. Scale bar = 50 μ m. IR, insulin receptor; NPP1, nucleotide pyrophosphatase/phosphodiesterase 1; Pit 1, type III sodium-dependent phosphate transporter 1; SG, standard glucose (11 mM).

shPit 1 INS 5 min: 0.04 ± 0.01 ; Figure 6a). Furthermore, we observed a similar tendency in shControl cells with regard to the total amount of NPP1 protein after 5 min of stimulation with insulin. These alterations were not present in Pit 1-depleted podocytes (shControl SG: 0.50 ± 0.05 , shControl INS 5 min: 0.20 ± 0.04 , shPit 1 SG: 0.41 ± 0.05 , shPit 1 INS 5 min: 0.39 ± 0.06 ; Figure 6a).

Next, we fluorescently stained endosomes and Rab5a protein in Pit 1-silenced podocytes (Figure 6b). In shControl cells, after 5 min of incubation with insulin, we confirmed the observations from nontransduced cells (i.e., the translocation of endosomal vesicles near the podocyte cell membrane). In contrast, in shPit 1 cells, regardless of the action of insulin, endosomal vesicles accumulated perinuclearly. We observed a similar finding for Rab5a protein. When shControl cells were treated with insulin, intense fluorescence was noted in the cytoplasm, whereas in Pit 1-depleted podocytes, Rab5a localized near the nucleus, regardless of whether podocytes were

incubated with insulin. These findings suggest that endocytosis processes are suppressed in Pit 1-downregulated cells, but further research is required to confirm this possibility.

3.7 | Downregulation of the SLC20A1 gene alters insulin signaling pathway in human podocytes

Based on the increases in RONS generation and eNPP activity and the translocation of NPP1 from the plasma membrane in Pit 1-depleted podocytes, we investigated the way in which SLC20A1 silencing affects the insulin signaling pathway. The p-IR/IR ratio increased by 43% in shControl cells that were treated with insulin for 5 min, whereas such an effect was not observed in Pit 1-depleted podocytes (shControl SG: 0.36 ± 0.03 , shControl INS 5 min: 0.51 ± 0.03 , shPit 1 SG: 0.42 ± 0.03 , shPit 1 INS 5 min: 0.39 ± 0.05 ;

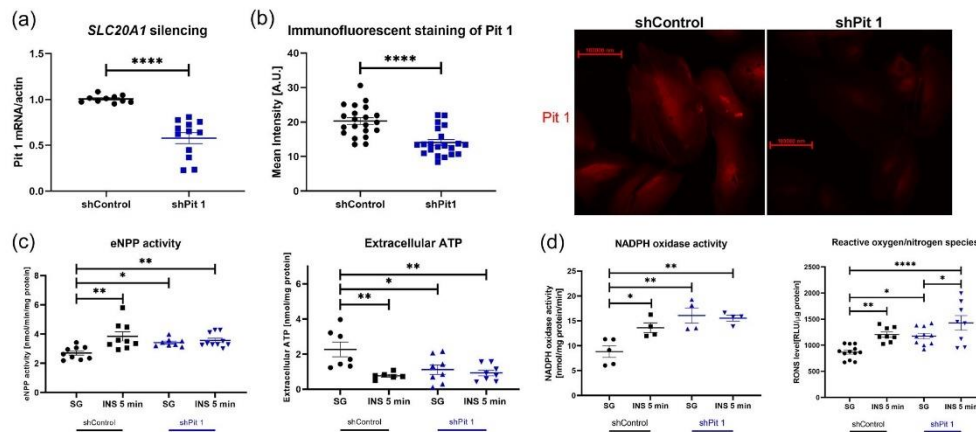


FIGURE 5 eNPP activity and RONS levels depend on Pit 1 expression. (a) Silencing of *SLC20A1* gene examined by real-time PCR (**** $p < 0.0001$, unpaired t -test, $n = 10-12$). (b) Downregulation of Pit 1 visualized by immunofluorescent staining (**** $p < 0.0001$, Mann-Whitney test, $n = 21$). Scale bar = 100 μm . (c) Changes in eNPP activity (* $p < 0.05$, ** $p < 0.01$, Dunn's multiple-comparison post hoc test, $n = 8-10$) and extracellular ATP levels (* $p < 0.05$, ** $p < 0.01$, Dunnett's multiple-comparison post hoc test, $n = 6-8$) in Pit 1-silenced podocytes. (d) Intensification of oxidative stress, expressed as an increase in NADPH oxidase activity (* $p < 0.05$, ** $p < 0.01$, Dunnett's multiple-comparison post hoc test, $n = 4-5$) and RONS generation (* $p < 0.05$, ** $p < 0.01$, **** $p < 0.0001$, Sidak's multiple-comparison post hoc test, $n = 8-12$) in podocytes with the suppression of *SLC20A1* gene expression. ATP, adenosine triphosphate; eNPP, ectonucleotide pyrophosphatase/phosphodiesterase; PCR, polymerase chain reaction; Pit 1, type III sodium-dependent phosphate transporter 1; RONS, reactive oxygen/nitrogen species.

Figure 7a). Similar regularity was found for the p-Akt/Akt ratio, which increased by 28% in shControl cells that were incubated with insulin for 5 min (shControl SG: 1.02 ± 0.03 , shControl INS 5 min: 1.30 ± 0.08 , shPit 1 SG: 1.00 ± 0.07 , shPit 1 INS 5 min: 1.11 ± 0.02 ; Figure 7a).

Next, we established the membrane presence of the IR and GLUT4 in Pit 1-downregulated cells. In shControl podocytes, 5 min of insulin stimulation led to the nearly complete translocation of the IR from the plasma membrane, whereas in shPit 1 cells, the reduction of the membrane amount of the IR was independent of incubation with insulin (shControl SG: 0.84 ± 0.05 , shControl INS 5 min: 0.07 ± 0.03 , shPit 1 SG: 0.01 ± 0.003 , shPit 1 INS 5 min: 0.01 ± 0.003 ; Figure 7b). GLUT4 decreased by 47% in the cellular membrane of shControl cells after 5 min of insulin treatment. The 77% reduction was more severe in shPit 1 podocytes, and incubation with insulin did not affect its intensity (shControl SG: 0.26 ± 0.04 , shControl INS 5 min: 0.14 ± 0.04 , shPit 1 SG: 0.06 ± 0.01 , shPit 1 INS 5 min: 0.05 ± 0.01 ; Figure 7b).

Lastly, we determined whether the aforementioned findings alter insulin-dependent glucose uptake into podocytes. In shControl cells, 5 min of insulin stimulation caused a 25% increase in glucose uptake, whereas glucose transport did not vary in shPit 1 podocytes, regardless of whether the cells were incubated with insulin (shControl SG: 1141 ± 49 pmol/15 min/mg protein, shControl INS 5 min: 1431 ± 70 pmol/15 min/mg protein, shPit 1 SG: 1174 ± 49 pmol/15 min/mg protein, shPit 1 INS 5 min: 1029 ± 48 pmol/15 min/mg protein; Figure 7c).

4 | DISCUSSION

In the present study, we demonstrated the insulin resistance of human podocytes after 1 day of incubation under hyperinsulinemic conditions. This was demonstrated by the inhibition of insulin signaling, reflected by a decrease in IR and Akt phosphorylation and the inhibition of intracellular glucose transport. Insulin also caused oxidative stress and the generation of RONS, which contribute to podocyte injury. We also found an interplay between NPP1 and Pit 1 in insulin-resistant podocytes. Moreover, we found that after silencing the gene that encodes Pit 1 protein, podocytes immediately became insulin resistant, without the involvement of any other factors.

During our research, we encountered an interesting dynamic of the response of human podocytes to incubation in a hyperinsulinemic environment. After 5 min of insulin treatment, intracellular glucose transport increased (which depends on the insulin signaling pathway), and both the IR and GLUT4 translocated from the plasma membrane. In 1982, Fan et al. (1982) reported that insulin that was labeled with ^{125}I cleaved from the surface of adipocytes within 2–6 min, which was attributable to endocytosis that was mediated by a ligand–receptor interaction. Moreover, internalization of the IR is possible when β subunit autophosphorylation occurs, with a $\tau_{1/2}$ of this event of approximately 3 min (Fagerholm et al., 2009). Additionally, Hunker et al. (2006) reported that the participation of proteins from the Rab5 family is essential for IR endocytosis. Our observations are consistent with the above findings. The detected dynamics of

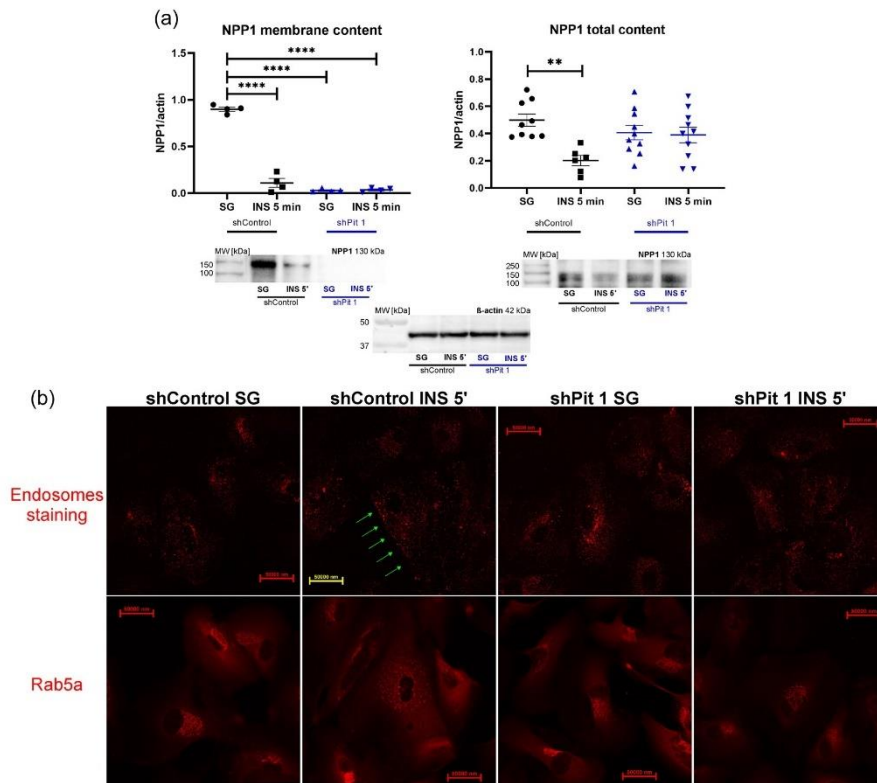


FIGURE 6 Silencing of Pit 1 alters NPP1 cellular localization and affects endocytosis in human podocytes. (a) Decrease in NPP1 protein in the plasma membrane after 5 min of the insulin stimulation of shControl podocytes and a decrease in the membrane amount of NPP1 in shPit 1 cells, regardless of the addition of insulin to the culture medium ($****p < 0.0001$, Dunnett's multiple-comparison post hoc test, $n = 4$). A decrease in the amount of NPP1 was observed in shControl cells that were stimulated with insulin for 5 min, whereas no changes were observed in shPit 1 podocytes ($**p < 0.01$, Dunnett's multiple-comparison post hoc test, $n = 6-10$). (b) Confocal images of endosomes that were stained with Dextran Red. Green arrows indicate the outline of the plasma membrane in shControl cells that were treated with insulin for 5 min, whereas no such changes were observed in shPit 1 podocytes. Five minutes of the insulin stimulation of shControl podocytes also caused a diffused arrangement of Rab5a in the cell body, which was not present in Pit 1-depleted podocytes. NPP1, nucleotide pyrophosphatase/phosphodiesterase 1; Pit 1, type III sodium-dependent phosphate transporter 1; SG, standard glucose (11 mM).

GLUT4 trafficking under conditions of insulin stimulation appeared to be consistent with other cell types. In adipocytes, the two-phase turnover of GLUT4 was observed (Fazakerley et al., 2022). In the rapid phase, which occurs 3 min after the beginning of insulin signaling, nearly half of the total GLUT4 pool is transported to the plasma membrane. In the long-term phase, the translocation of GLUT4 storage vesicles to the plasma membrane is maintained for several hours, with a turnover half time of less than 10 min (Fazakerley et al., 2022). Thus, in the present study, we might have captured the transition between the fast and long-term phases in human podocytes. This may also be a defense mechanism of these cells against the rapid influx of glucose.

Although alterations of NPP1 function are highly connected to ectopic calcification, several reports suggest its participation in the development of insulin resistance (Mackenzie et al., 2012). Nearly 30 years ago, the relationship between insulin resistance and higher NPP1 activity was established (Maddux et al., 1995). Later, Chin et al. (2009) reported that the catalytic activity of NPP1 is necessary for the inhibition of IRs by this enzyme. In contrast, the downregulation of *ENPP1* improves glucose tolerance and enhances insulin signaling both in vitro and in vivo, which prevents the onset of type II diabetes (Zhou et al., 2009). In the present study, insulin resistance developed after 24 h of incubation under hyperinsulinemic conditions. After this time, we did not observe a significant elevation of eNPP activity, as

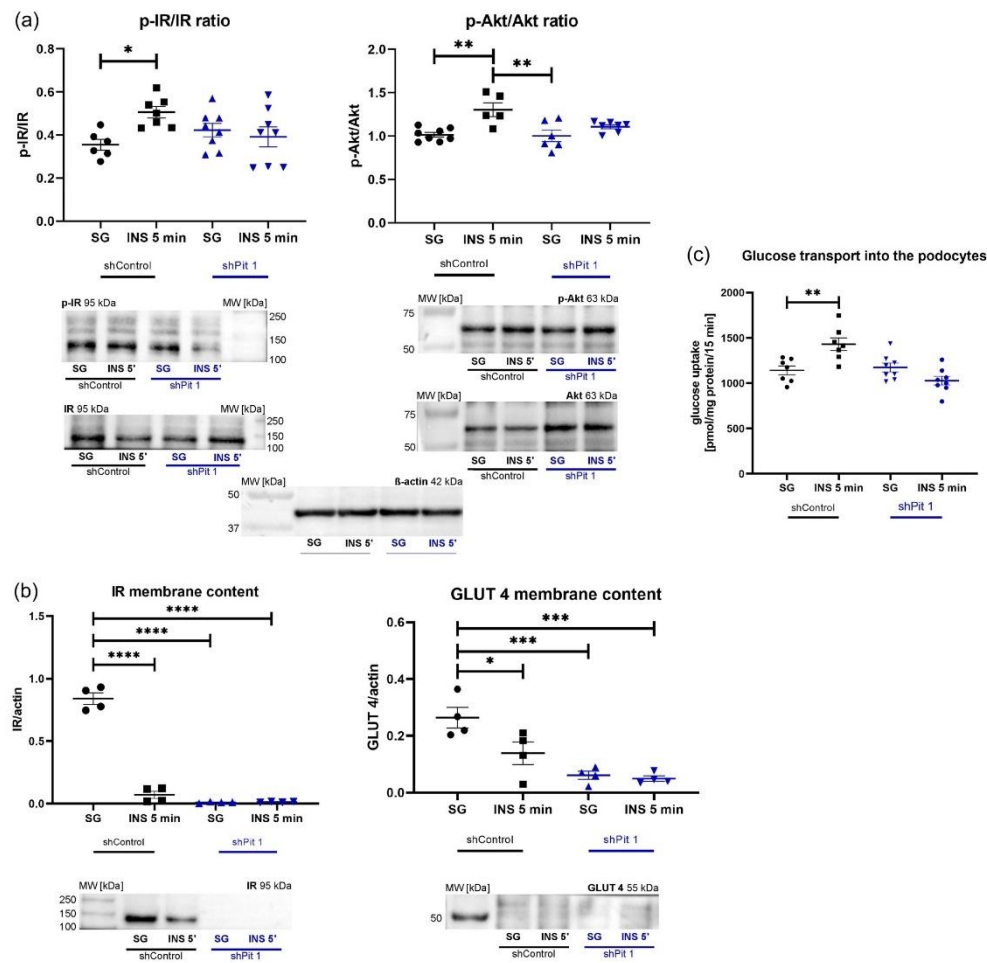


FIGURE 7 Alterations of insulin-dependent glucose uptake in Pit 1-downregulated human podocytes. (a) Insulin insensitivity in shPit 1 cells, expressed as decreases in the p-IR/IR ratio ($*p < 0.05$, Dunnett's multiple-comparison post hoc test, $n = 6-8$) and p-Akt/Akt ratio ($**p < 0.01$, Sidak's multiple-comparison post hoc test, $n = 5-8$) compared with shControl cells that were cultured in SG medium. (b) shPit 1 podocytes expose a lower amount of the IR ($****p < 0.0001$, Dunnett's multiple-comparison post hoc test, $n = 4$) and GLUT4 ($*p < 0.05$, $***p < 0.001$, Dunnett's multiple-comparison post hoc test, $n = 4$) in the plasma membrane compared with shControl podocytes. (c) No increase in glucose uptake into shPit 1 podocytes in response to insulin ($**p < 0.01$, Sidak's multiple-comparison post hoc test, $n = 7-8$). Akt, protein kinase B; GLUT4, glucose transporter type 4; IR, insulin receptor; p-Akt, phosphorylated protein kinase B; p-IR, phosphorylated insulin receptor; Pit 1, type III sodium-dependent phosphate transporter 1; SG, standard glucose (11 mM).

was observed after 5 min and 1 h of insulin stimulation. Thus, in human podocytes, NPP1 appears to contribute to their insulin resistance by interacting with the IR, which we confirmed in the immunoprecipitation and immunofluorescence assays. Notably, preservation of the enzymatic activity of NPP1 per se is necessary to maintain the ability to inhibit IRs (Chin et al., 2009), but changes in

this activity are not always observed, as Dong et al. proved in their work on hepatocytes (Dong et al., 2005).

Since the beginning of the 21st century, many reports have indicated that Pit 1, in addition to its function as a Pi transporter, is involved in the pathomechanism of soft tissue calcification (Li & Giachelli, 2007; Li et al., 2006; Masumoto et al., 2017;

Suzuki et al., 2006). The overexpression of Pit 1 in rat podocytes has also been shown to contribute to the loss of their function, manifested by the appearance of markers of podocyte damage, dysregulation of the GFB, albuminuria, and hypoalbuminemia (Asada et al., 2019; Sekiguchi et al., 2011). In the present study, we investigated the physiological response of Pit 1 to insulin stimulation. We also confirmed our previous observations, in which under HG conditions that mimicked insulin resistance, the amount and membrane exposure of Pit 1 decreased (Kulesza et al., 2022). Therefore, because of the systemic presence of Pit 1 in the body, its dysfunction appears to affect individual tissues differently. For example, Pit 1 may participate in vascular calcification, but this transporter is necessary for the proper action of macrophages (Koumakis et al., 2019), is necessary for the maintenance of normal cell proliferation and adhesion (Beck et al., 2009; Byskov et al., 2012; Kongsfelt et al., 2014), and participates in tumor necrosis factor α -induced apoptosis (Salaün et al., 2010) and hematopoiesis (Forand et al., 2013). Hence, based on our results, the physiological role of Pit 1 in podocytes appears to be crucial for the proper function of these cells, which is disturbed in type II diabetes. Nonetheless, the mechanism by which this occurs is not fully understood.

Studies by Forand et al. (2016), Lamb et al. (2010), and Sadler et al. (2019) are helpful for understanding why Pit 1 silencing contributes to the development of insulin resistance in podocytes. Pit 1 influences insulin signaling in hepatocytes (Forand et al., 2016). In mice with liver-specific Pit 1 knockout, insulin sensitivity increased, and carbohydrate metabolism significantly improved (Forand et al., 2016). Pit 1 was shown to interact with ubiquitin-specific peptidase 7 (USP7), which is a ubiquitin-cleaving enzyme that protects the target protein from proteasomal destruction. One substrate of USP7 is IRS1. With Pit 1 deletion, USP7 can cleave ubiquitin residues from IRS1, resulting in elevation of the half-life of IRS1, which in turn prolongs insulin signaling. However, when USP7 interacts with Pit 1, it cannot perform its actions on IRS1, which contributes to insulin resistance. In turn, in experiments on 3T3-L1 adipocytes, Lamb et al. (2010) found that GLUT4 must be ubiquitinated to be sorted into insulin-sensitive GLUT4 storage vesicles. Nonubiquitinated GLUT4 failed to fuse with the cell membrane and fulfill its role (Lamb et al., 2010). Subsequent studies established that GLUT4 ubiquitination is a dynamic process, in which after translocation to the membrane, GLUT4 must be deubiquitinated to prevent its lysosomal degradation and ensure its recirculation

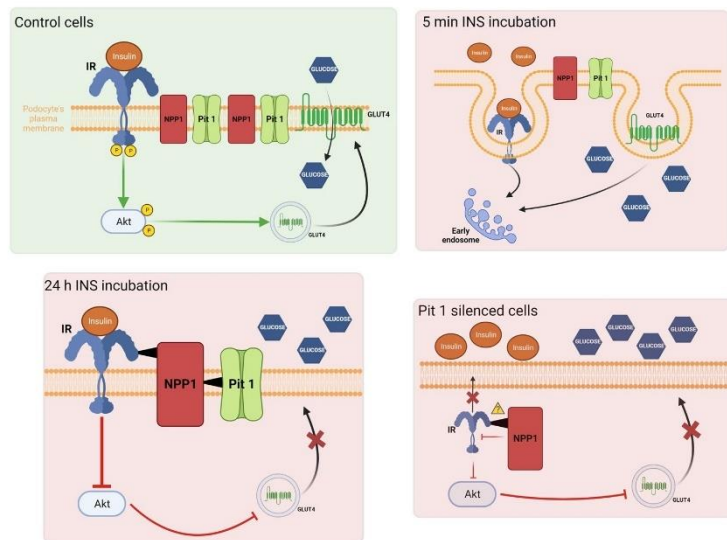


FIGURE 8 Summary of our observations and proposed mechanism of insulin resistance in Pit 1-silenced cells. In healthy podocytes, the binding of insulin to the IR causes its autophosphorylation and further downstream insulin signaling, one of the last stages of which is the phosphorylation of Akt and translocation of GLUT4 storage vesicles to the plasma membrane. This results in intracellular glucose influx via GLUT4. A 5 min incubation of podocytes with insulin leads to the internalization of IR and GLUT4 via early endosomes recruitment. The amount of NPP1 and Pit 1 in the podocyte cell membrane is also reduced. After 24 h of the treatment of podocytes with insulin, IR autophosphorylation does not occur, which inhibits further insulin signaling. The interaction between the IR and NPP1 may be responsible for the loss of its tyrosine kinase activity. Under these conditions, Pit 1 also appears to interact with NPP1, but the implications of this phenomenon are not yet established. Our findings suggest that in Pit 1-depleted podocytes, the IR does not translocate to the plasma membrane where it could bind to insulin, which precludes insulin-dependent glucose uptake. Akt, protein kinase B; GLUT4, glucose transporter type 4; IR, insulin receptor; NPP1, nucleotide pyrophosphatase/phosphodiesterase 1; Pit 1, type III sodium-dependent phosphate transporter 1.

(Sadler et al., 2019). Another ubiquitin-specific protease, USP25, is involved in this process. Therefore, we presume that a similar regularity may occur in podocytes because they are also insulin-dependent cells, such as adipocytes or hepatocytes. After Pit 1 depletion, there is no interaction of this protein with USPs. Thus, USPs might deubiquitinate GLUT4, thereby preventing its trafficking to the plasma membrane and resulting in insulin resistance. Further research is needed to elucidate the role of Pit 1 downregulation and the Pit 1/NPP1 interaction in the development of insulin resistance in podocytes.

In conclusion, our research revealed that the NPP1-mediated inhibition of insulin signaling appears to occur through an interaction between IR and NPP1 proteins as described in previous studies. To our knowledge, this is the first demonstration of an interplay between NPP1 and Pit 1. Furthermore, the downregulation of Pit 1 increased NPP1 activity and promoted the occurrence of mechanisms that are characteristic of insulin-resistant cells. These findings are summarized in Figure 8 and suggest that Pit 1 may be a factor that attenuates NPP1-mediated IR inhibition.

AUTHOR CONTRIBUTIONS

Tomasz Kulesza prepared the original draft of the manuscript. Agnieszka Piwkowska designed the study. Tomasz Kulesza, Marlena Typiak, Patrycja Rachubik, Dorota Rogacka, and Agnieszka Piwkowska performed the experiments and analyzed the data. Agnieszka Piwkowska, Dorota Rogacka, Irena Audzeyenka, Marlena Typiak, and Moin A. Saleem revised the manuscript. Moin A. Saleem and Irena Audzeyenka provided materials and methods. Agnieszka Piwkowska obtained funding and managed the project. All authors approved the final version of the manuscript.

ACKNOWLEDGMENTS

This study was supported by grant 2018/29/B/NZ4/02074 to Agnieszka Piwkowska from the National Science Center in Poland.

CONFLICT OF INTEREST STATEMENT

The authors declare no conflict of interest.

ORCID

Tomasz Kulesza  <http://orcid.org/0000-0001-5166-7444>
 Patrycja Rachubik  <http://orcid.org/0000-0002-7691-8243>
 Dorota Rogacka  <http://orcid.org/0000-0001-6242-0324>
 Agnieszka Piwkowska  <http://orcid.org/0000-0002-0086-7777>

REFERENCES

- Asada, Y., Takayanagi, T., Kawakami, T., Tomatsu, E., Masuda, A., Yoshino, Y., Sekiguchi-Ueda, S., Shibata, M., Ide, T., Niimi, H., Yaoita, E., Seino, Y., Sugimura, Y., & Suzuki, A. (2019). Risedronate attenuates podocyte injury in phosphate transporter-overexpressing rats. *International Journal of Endocrinology*, 2019, 1–10. <https://doi.org/10.1155/2019/4194853>
- Audzeyenka, I., Rachubik, P., Rogacka, D., Typiak, M., Kulesza, T., Angielski, S., Rychłowski, M., Wysocka, M., Gruba, N., Lesner, A., Saleem, M. A., & Piwkowska, A. (2020). Cathepsin C is a novel mediator of podocyte and renal injury induced by hyperglycemia. *Biochimica et Biophysica Acta (BBA) - Molecular Cell Research*, 1867(8), 118723. <https://doi.org/10.1016/j.bbamcr.2020.118723>
- Beck, L., Leroy, C., Salaün, C., Margall-Ducos, G., Desdouets, C., & Friedlander, G. (2009). Identification of a novel function of PIT1 critical for cell proliferation and independent of its phosphate transport activity. *Journal of Biological Chemistry*, 284(45), 31363–31374. <https://doi.org/10.1074/jbc.M109.053132>
- Brinkkoetter, P. T., Ising, C., & Benzing, T. (2013). The role of the podocyte in albumin filtration. *Nature Reviews Nephrology*, 9(6), 328–336. <https://doi.org/10.1038/nrneph.2013.78>
- Byсков, K., Jensen, N., Kongsfelt, I. B., Wielsøe, M., Pedersen, L. E., Haldrup, C., & Pedersen, L. (2012). Regulation of cell proliferation and cell density by the inorganic phosphate transporter PIT1. *Cell Division*, 7, 7. <https://doi.org/10.1186/1747-1028-7-7>
- Chin, C. N., Dallas-Yang, Q., Liu, F., Ho, T., Ellsworth, K., Fischer, P., Natasha, T., Ireland, C., Lu, P., Li, C., Wang, I. M., Strohl, W., Berger, J. P., An, Z., Zhang, B. B., & Jiang, G. (2009). Evidence that inhibition of insulin receptor signaling activity by PC-1/ENPP1 is dependent on its enzyme activity. *European Journal of Pharmacology*, 606(1–3), 17–24. <https://doi.org/10.1016/j.ejphar.2009.01.016>
- Dong, H., Maddux, B. A., Altomonte, J., Meseck, M., Accili, D., Terkeltaub, R., Johnson, K., Youngren, J. F., & Goldfine, I. D. (2005). Increased hepatic levels of the insulin receptor inhibitor, PC-1/NPP1, induce insulin resistance and glucose intolerance. *Diabetes*, 54(2), 367–372. <https://doi.org/10.2337/diabetes.54.2.367>
- Fagerholm, S., Örtengren, U., Karlsson, M., Ruishalme, I., & Strålfors, P. (2009). Rapid insulin-dependent endocytosis of the insulin receptor by caveolae in primary adipocytes. *PLoS One*, 4(6), e5985. <https://doi.org/10.1371/journal.pone.0005985>
- Fan, J. Y., Carpentier, J. L., Gordon, P., Van Obberghen, E., Blackett, N. M., Grunfeld, C., & Orci, L. (1982). Receptor-mediated endocytosis of insulin: Role of microvilli, coated pits, and coated vesicles. *Proceedings of the National Academy of Sciences of the United States of America*, 79(24), 7788–7791. <https://doi.org/10.1073/pnas.79.24.7788>
- Fazakerley, D. J., Koumanov, F., & Holman, G. D. (2022). GLUT4 on the move. *Biochemical Journal*, 479(3), 445–462. <https://doi.org/10.1042/BCJ20210073>
- Forand, A., Beck, L., Leroy, C., Rousseau, A., Boitez, V., Cohen, I., Courtois, G., Hermine, O., & Friedlander, G. (2013). EKLf-driven PIT1 expression is critical for mouse erythroid maturation *in vivo* and *in vitro*. *Blood*, 121(4), 666–678. <https://doi.org/10.1182/blood-2012-05-427302>
- Forand, A., Koumakis, E., Rousseau, A., Sassier, Y., Journe, C., Merlin, J. F., Leroy, C., Boitez, V., Codogno, P., Friedlander, G., & Cohen, I. (2016). Disruption of the phosphate transporter Pit1 in hepatocytes improves glucose metabolism and insulin signaling by modulating the USP7/IRS1 interaction. *Cell Reports*, 16(10), 2736–2748. <https://doi.org/10.1016/j.celrep.2016.08.012>
- Garg, P. (2018). A review of podocyte biology. *American Journal of Nephrology*, 47(Suppl. 1), 3–13. <https://doi.org/10.1159/000481633>
- Hoffenberg, S., Liu, X., Nikolova, L., Hall, H. S., Dai, W., Baughn, R. E., Dickey, B. F., Barbieri, M. A., Aballay, A., Stahl, P. D., & Knoll, B. J. (2000). A novel membrane-anchored Rab5 interacting protein required for homotypic endosome fusion. *Journal of Biological Chemistry*, 275(32), 24661–24669. <https://doi.org/10.1074/jbc.M909600199>
- Hunker, C. M., Kruk, I., Hall, J., Giambini, H., Veisaga, M. L., & Barbieri, M. A. (2006). Role of Rab5 in insulin receptor-mediated endocytosis and signaling. *Archives of Biochemistry and Biophysics*, 449(1–2), 130–142. <https://doi.org/10.1016/j.abb.2006.01.020>
- Kongsfelt, I. B., Byskov, K., Pedersen, L. E., & Pedersen, L. (2014). High levels of the type III inorganic phosphate transporter PIT1

- (SLC20A1) can confer faster cell adhesion. *Experimental Cell Research*, 326(1), 57–67. <https://doi.org/10.1016/j.yexcr.2014.05.014>
- Koumakis, E., Millet-Botti, J., Benna, J. E., Leroy, C., Boitez, V., Codogno, P., Friedlander, G., & Forand, A. (2019). Novel function of PIT1/SLC20A1 in LPS-related inflammation and wound healing. *Scientific Reports*, 9(1), 1808. <https://doi.org/10.1038/s41598-018-37551-1>
- Kulesza, T., & Piwkowska, A. (2021). The impact of type III sodium-dependent phosphate transporters (Pit 1 and Pit 2) on podocyte and kidney function. *Journal of Cellular Physiology*, 236(10), 7176–7185. <https://doi.org/10.1002/jcp.30368>
- Kulesza, T., Typiak, M., Rachubik, P., Audzeyenka, I., Rogacka, D., Angielski, S., Saleem, M. A., & Piwkowska, A. (2022). Hyperglycemic environment disrupts phosphate transporter function and promotes calcification processes in podocytes and isolated glomeruli. *Journal of Cellular Physiology*, 237(5), 2478–2491. <https://doi.org/10.1002/jcp.30700>
- Lamb, C. A., McCann, R. K., Stöckli, J., James, D. E., & Bryant, N. J. (2010). Insulin-regulated trafficking of GLUT4 requires ubiquitination. *Traffic*, 11(11), 1445–1454. <https://doi.org/10.1111/j.1600-0854.2010.01113.x>
- Lee, S. Y., & Müller, C. E. (2017). Nucleotide pyrophosphatase/phosphodiesterase 1 (NPP1) and its inhibitors. *Med Chem Comm*, 8(5), 823–840. <https://doi.org/10.1039/c7md00015d>
- Li, X., & Giachelli, C. M. (2007). Sodium-dependent phosphate cotransporters and vascular calcification. *Current Opinion in Nephrology & Hypertension*, 16, 325–328. <https://doi.org/10.1097/MNH.0b013e3281c55ef1>
- Li, X., Yang, H. Y., & Giachelli, C. M. (2006). Role of the sodium-dependent phosphate cotransporter, Pit-1, in vascular smooth muscle cell calcification. *Circulation Research*, 98, 905–912. <https://doi.org/10.1161/01.RES.0000216409.20863.e7>
- Lu, J., Chen, P. P., Zhang, J. X., Li, X. Q., Wang, G. H., Yuan, B. Y., Huang, S. J., Liu, X. Q., Jiang, T. T., Wang, M. Y., Liu, W. T., Ruan, X. Z., Liu, B. C., & Ma, K. L. (2021). GPR43 deficiency protects against podocyte insulin resistance in diabetic nephropathy through the restoration of AMPK α activity. *Theranostics*, 11(10), 4728–4742. <https://doi.org/10.7150/tno.56598>
- Mackenzie, N. C. W., Huesa, C., Rutsch, F., & MacRae, V. E. (2012). New insights into NPP1 function: Lessons from clinical and animal studies. *Bone*, 51(5), 961–968. <https://doi.org/10.1016/j.bone.2012.07.014>
- Maddux, B. A., & Goldfine, I. D. (2000). Membrane glycoprotein PC-1 inhibition of insulin receptor function occurs via direct interaction with the receptor α -subunit. *Diabetes*, 49(1), 13–19. <https://doi.org/10.2337/diabetes.49.1.13>
- Maddux, B. A., Sbraccia, P., Kumakura, S., Sasson, S., Youngren, J., Fisher, A., Spencer, S., Grupe, A., Henzel, W., Stewart, T. A., Reaven, G. M., & Goldfine, I. D. (1995). Membrane glycoprotein PC-1 and insulin resistance in non-insulin-dependent diabetes mellitus. *Nature*, 373, 448–451. <https://doi.org/10.1038/474448a0>
- Masumoto, A., Sonou, T., Ohya, M., Yashiro, M., Nakashima, Y., Okuda, K., Iwashita, Y., Mima, T., Negi, S., & Shigematsu, T. (2017). Calcium overload accelerates phosphate-induced vascular calcification via Pit-1, but not the calcium-sensing receptor. *Journal of Atherosclerosis and Thrombosis*, 24, 716–724. <https://doi.org/10.5551/jat.36574>
- Mima, A., Ohshiro, Y., Kitada, M., Matsumoto, M., Geraldine, P., Li, C., Li, Q., White, G. S., Cahill, C., Rask-Madsen, C., & King, G. L. (2011). Glomerular-specific protein kinase C- β -induced insulin receptor substrate-1 dysfunction and insulin resistance in rat models of diabetes and obesity. *Kidney International*, 79(8), 883–896. <https://doi.org/10.1038/ki.2010.526>
- Münzel, T., Kurz, S., Rajagopalan, S., Thoenes, M., Berrington, W. R., Thompson, J. A., Freeman, B. A., & Harrison, D. G. (1996). Hydralazine prevents nitroglycerin tolerance by inhibiting activation of a membrane-bound NADH oxidase: A new action for an old drug. *Journal of Clinical Investigation*, 98(6), 1465–1470. <https://doi.org/10.1172/JCI118935>
- Pagtalunan, M. E., Miller, P. L., Jumping-Eagle, S., Nelson, R. G., Myers, B. D., Renke, H. G., Coplon, N. S., Sun, L., & Meyer, T. W. (1997). Podocyte loss and progressive glomerular injury in type II diabetes. *Journal of Clinical Investigation*, 99(2), 342–348. <https://doi.org/10.1172/JCI119163>
- Piwkowska, A., Rogacka, D., Audzeyenka, I., Jankowski, M., & Angielski, S. (2011). High glucose concentration affects the oxidant-antioxidant balance in cultured mouse podocytes. *Journal of Cellular Biochemistry*, 112(6), 1661–1672. <https://doi.org/10.1002/jcb.23088>
- Piwkowska, A., Rogacka, D., Jankowski, M., Dominiczak, M. H., Stepiński, J. K., & Angielski, S. (2010). Metformin induces suppression of NAD(P)H oxidase activity in podocytes. *Biochemical and Biophysical Research Communications*, 393(2), 268–273. <https://doi.org/10.1016/j.bbrc.2010.01.119>
- Rogacka, D. (2021). Insulin resistance in glomerular podocytes: Potential mechanisms of induction. *Archives of Biochemistry and Biophysics*, 710, 109005. <https://doi.org/10.1016/j.abb.2021.109005>
- Rogacka, D., Audzeyenka, I., Rychtowski, M., Rachubik, P., Szejder, M., Angielski, S., & Piwkowska, A. (2018). Metformin overcomes high glucose-induced insulin resistance of podocytes by pleiotropic effects on SIRT1 and AMPK. *Biochimica et Biophysica Acta (BBA) - Molecular Basis of Disease*, 1864(1), 115–125. <https://doi.org/10.1016/j.bbadis.2017.10.014>
- Rogacka, D., Piwkowska, A., Jankowski, M., Kocbuch, K., Dominiczak, M. H., Stepiński, J. K., & Angielski, S. (2010). Expression of GFAT1 and OGT in podocytes: Transport of glucosamine and the implications for glucose uptake into these cells. *Journal of Cellular Physiology*, 225(2), 577–584. <https://doi.org/10.1002/jcp.22242>
- Rousseau, M., Denhez, B., Spino, C., Lizotte, F., Guay, A., Côté, A. M., Burger, D., & Galdes, P. (2022). Reduction of DUSP4 contributes to podocytes oxidative stress, insulin resistance and diabetic nephropathy. *Biochemical and Biophysical Research Communications*, 624, 127–133. <https://doi.org/10.1016/j.bbrc.2022.07.067>
- Sadler, J. B. A., Lamb, C. A., Welburn, C. R., Adamson, I. S., Kioumourtzoglou, D., Chi, N. W., Gould, G. W., & Bryant, N. J. (2019). The deubiquitinating enzyme USP25 binds tankyrase and regulates trafficking of the facilitative glucose transporter GLUT4 in adipocytes. *Scientific Reports*, 9(1), 4710. <https://doi.org/10.1038/s41598-019-40596-5>
- Salaün, C., Leroy, C., Rousseau, A., Boitez, V., Beck, L., & Friedlander, G. (2010). Identification of a novel transport-independent function of PIT1/SLC20A1 in the regulation of TNF-induced apoptosis. *Journal of Biological Chemistry*, 285(45), 34408–34418. <https://doi.org/10.1074/jbc.M110.130989>
- Saleem, M. A., O'Hare, M. J., Reiser, J., Coward, R. J., Inward, C. D., Farren, T., Xing, C. Y., Ni, L., Mathieson, P. W., & Mundel, P. (2002). A conditionally immortalized human podocyte cell line demonstrating nephrin and podocin expression. *Journal of the American Society of Nephrology*, 13(3), 630–638.
- Sekiguchi, S., Suzuki, A., Asano, S., Nishiwaki-Yasuda, K., Shibata, M., Nagao, S., Yamamoto, N., Matsuyama, M., Sato, Y., Yan, K., Yaoita, E., & Itoh, M. (2011). Phosphate overload induces podocyte injury via type III Na-dependent phosphate transporter. *American Journal of Physiology-Renal Physiology*, 300(4), F848–F856. <https://doi.org/10.1152/ajprenal.00334.2010>
- Susztak, K., Raff, A. C., Schiffer, M., & Böttinger, E. P. (2006). Glucose-induced reactive oxygen species cause apoptosis of podocytes and podocyte depletion at the onset of diabetic nephropathy. *Diabetes*, 55(1), 225–233. <https://doi.org/10.2337/diabetes.55.01.06.db05-0894>
- Suzuki, A., Ghayor, C., Guicheux, J., Magne, D., Quillard, S., Kakita, A., Ono, Y., Miura, Y., Oiso, Y., Itoh, M., & Caverzasio, J. (2006).

- Enhanced expression of the inorganic phosphate transporter Pit-1 is involved in BMP-2-induced matrix mineralization in osteoblast-like cells. *Journal of Bone and Mineral Research*, 21(5), 674–683. <https://doi.org/10.1359/jbmr.020603>
- Tejada, T., Catanuto, P., Ijaz, A., Santos, J. V., Xia, X., Sanchez, P., Sanabria, N., Lenz, O., Elliot, S. J., & Fornoni, A. (2008). Failure to phosphorylate AKT in podocytes from mice with early diabetic nephropathy promotes cell death. *Kidney International*, 73(12), 1385–1393. <https://doi.org/10.1038/ki.2008.109>
- Typiak, M., Kulesza, T., Rachubik, P., Rogacka, D., Audzeyenka, I., Angielski, S., Saleem, M. A., & Piwkowska, A. (2021). Role of Klotho in hyperglycemia: Its levels and effects on fibroblast growth factor receptors, glycolysis, and glomerular filtration. *International Journal of Molecular Sciences*, 22(15), 7867. <https://doi.org/10.3390/ijms22157867>
- Weil, E. J., Lemley, K. V., Mason, C. C., Yee, B., Jones, L. I., Blouch, K., Lovato, T., Richardson, M., Myers, B. D., & Nelson, R. G. (2012). Podocyte detachment and reduced glomerular capillary endothelial fenestration promote kidney disease in type 2 diabetic nephropathy. *Kidney International*, 82(9), 1010–1017. <https://doi.org/10.1038/ki.2012.234>
- Welsh, G. I., Hale, L. J., Eremina, V., Jeansson, M., Maezawa, Y., Lennon, R., Pons, D. A., Owen, R. J., Satchell, S. C., Miles, M. J., Caunt, C. J., McArdle, C. A., Pavenstädt, H., Tavaré, J. M., Herzenberg, A. M., Kahn, C. R., Mathieson, P. W., Quaggin, S. E., Saleem, M. A., & Coward, R. J. M. (2010). Insulin signaling to the glomerular podocyte is critical for normal kidney function. *Cell Metabolism*, 12(4), 329–340. <https://doi.org/10.1016/j.cmet.2010.08.015>
- Whaley-Connell, A., Demarco, V. G., Lastra, G., Manrique, C., Nistala, R., Cooper, S. A., Westerly, B., Hayden, M. R., Wiedmeyer, C., Wei, Y., & Sowers, J. R. (2007). Insulin resistance, oxidative stress, and podocyte injury: Role of rosuvastatin modulation of filtration barrier injury. *American Journal of Nephrology*, 28(1), 67–75. <https://doi.org/10.1159/000109394>
- Wolf, G., Chen, S., & Ziyadeh, F. N. (2005). From the periphery of the glomerular capillary wall toward the center of disease: Podocyte injury comes of age in diabetic nephropathy. *Diabetes*, 54(6), 1626–1634. <https://doi.org/10.2337/diabetes.54.6.1626>
- Yaribeygi, H., Farrokhi, F. R., Butler, A. E., & Sahebkar, A. (2019). Insulin resistance: Review of the underlying molecular mechanisms. *Journal of Cellular Physiology*, 234(6), 8152–8161. <https://doi.org/10.1002/jcp.27603>
- Zhou, H. H., Chin, C. N., Wu, M., Ni, W., Quan, S., Liu, F., Dallas-Yang, Q., Ellsworth, K., Ho, T., Zhang, A., Natasha, T., Li, J., Chapman, K., Strohl, W., Li, C., Wang, I. M., Berger, J., An, Z., Zhang, B. B., & Jiang, G. (2009). Suppression of PC-1/ENPP-1 expression improves insulin sensitivity *in vitro* and *in vivo*. *European Journal of Pharmacology*, 616(1–3), 346–352. <https://doi.org/10.1016/J.EJP.2009.06.057>

How to cite this article: Kulesza, T., Typiak, M., Rachubik, P., Rogacka, D., Audzeyenka, I., Saleem, M. A., & Piwkowska, A. (2023). Pit 1 transporter (SLC20A1) as a key factor in the NPP1-mediated inhibition of insulin signaling in human podocytes. *Journal of Cellular Physiology*, 1–16. <https://doi.org/10.1002/jcp.31051>

9.3. Kopia pracy przeglądowej

- 9.3.1. **Kulesza T, Piwkowska A. The impact of type III sodium-dependent phosphate transporters (Pit 1 and Pit 2) on podocyte and kidney function. *J Cell Physiol.* 2021; 236(10): 7176-7185.**



Received: 21 December 2020 | Revised: 26 February 2021 | Accepted: 4 March 2021
DOI: 10.1002/jcp.30368

REVIEW ARTICLE

Journal of Cellular Physiology WILEY

The impact of type III sodium-dependent phosphate transporters (Pit 1 and Pit 2) on podocyte and kidney function

Tomasz Kulesza | Agnieszka Piwkowska

Laboratory of Molecular and Cellular Nephrology, Mossakowski Medical Research Institute, Polish Academy of Sciences, Gdansk, Poland

Correspondence

Tomasz Kulesza, Laboratory of Molecular and Cellular Nephrology, Mossakowski Medical Research Institute, Polish Academy of Sciences, Wita Stwosza St. 63, Gdansk 80-308, Poland.
Email: tkulesza@imdik.pan.pl

Funding information

Narodowe Centrum Nauki,
Grant/Award Number: 2018/29/B/NZ4/02074

Abstract

The sodium-dependent phosphate transporters Pit 1 and Pit 2 belong to the solute carrier 20 (SLC20) family of membrane proteins. They are ubiquitously distributed in the human body. Their crucial function is the intracellular transport of inorganic phosphate (Pi) in the form of $H_2PO_4^-$. They are one of the main elements in maintaining physiological phosphate homeostasis. Recent data have emerged that indicate novel roles of Pit 1 and Pit 2 proteins besides the well-known function of Pi transporters. These membrane proteins are believed to be precise phosphate sensors that mediate Pi-dependent intracellular signaling. They are also involved in insulin signaling and influence cellular insulin sensitivity. In diseases that are associated with hyperphosphatemia, such as diabetes and chronic kidney disease (CKD), disturbances in the function of Pit 1 and Pit 2 are observed. Phosphate transporters from the SLC20 family participate in the calcification of soft tissues, mainly blood vessels, during the course of CKD. The glomerulus and podocytes therein can also be a target of pathological calcification that damages these structures. A few studies have demonstrated the development of Pi-dependent podocyte injury that is mediated by Pit 1 and Pit 2. This paper discusses the role of Pit 1 and Pit 2 proteins in podocyte function, mainly in the context of the development of pathological calcification that disrupts permeability of the renal filtration barrier. We also describe the mechanisms that may contribute to podocyte damage by Pit 1 and Pit 2.

KEYWORDS

diabetic nephropathy, Pit 1, Pit 2, podocytes, sodium-dependent phosphate transporters, vascular calcification

1 | INTRODUCTION

Podocytes are highly specialized, nondividing epithelial cells that are located in the urinary part of the glomerulus (Coward & Fornoni, 2015). They consist of three significant structural elements: a cell body, major processes, and foot processes. Adjacent foot processes of podocytes entwine glomerular capillaries, forming a slit diaphragm (Coward & Fornoni, 2015; Garg, 2018; Pollak et al., 2014; Rachubik & Piwkowska, 2019; Scott & Quaggin, 2015). The slit diaphragm is the most important part of the glomerular filtration barrier. It inhibits the movement of macromolecules, such as proteins, into primary urine (Garg, 2018). Diseases that damage podocytes (e.g., podocytopathies) by

destroying the slit diaphragm and foot process detachment lead to impairments in the filtration and excretion of substances that should be physiologically retained in the blood. These disorders include diabetic nephropathy, nephrotic syndrome, immune complex glomerulonephritis, monoclonal gammopathies, and amyloidosis (Khalighi et al., 2018; Kopp et al., 2020; Tung et al., 2018). These disturbances can lead to the onset of chronic kidney disease (CKD), which in turn causes changes in phosphate homeostasis. Hyperphosphatemia is seen during the course of secondary hyperparathyroidism that is present in the end stages of CKD. These changes can cause the calcification of soft tissues, particularly major blood vessels and heart valves, which also alters renal function by promoting the occurrence of pathological glomerular

calcification (Cozzolino et al., 2017; Tsuchiya et al., 2004; Vervloet et al., 2017). Furthermore, evidence indicates a direct relationship between serum phosphate levels and the progression of CKD (Da et al., 2015; O'Seaghda et al., 2011; Zoccali et al., 2011).

Inorganic phosphate is involved in several biochemical processes in the human body, such as glycolysis, gluconeogenesis, and cellular respiration. It is also the building block of bones and teeth. Phosphate contributes to the maintenance of physiological pH of the blood and is a component of the buffering system (Bergwitz & Jüppner, 2010; Berndt & Kumar, 2009; Blaine et al., 2015; Forster et al., 2013; Hong et al., 2015; Wagner et al., 2014). Phosphate can also manifest toxic actions, such as impairments in bone mineralization, renal dysfunction, pathological calcification, impairments in cell signaling, premature ageing, tumorigenesis, and impairments in fertility (Razzaque, 2011). These findings confirm that phosphate is a key molecule that is required for sustaining life. Given its critical role in cellular biology and wide distribution, phosphate needs to be strongly regulated. In this paper, we discuss the effect of phosphate metabolism on the proper function of podocytes and renal filtration.

2 | PHOSPHATE HOMEOSTASIS

Phosphorus in living organisms occurs in an oxygen-related form, called inorganic phosphate (Pi). Phosphate is the third most common anion in the human body (Wagner et al., 2014). In serum, 72% of Pi appears in the divalent form (HPO_4^{2-}), and 28% appears in the monovalent form (H_2PO_4^-). Intracellular phosphate concentrations range from 0.7 to 2.5 mM (Wagner et al., 2014). The blood concentration of Pi varies between 0.83 and 1.34 mM (Berndt & Kumar, 2009). Increases in serum Pi levels of 0.16 mM above the upper limit significantly increase the risk of end-stage renal disease in the healthy population (Vervloet et al., 2017).

Under physiological conditions, serum phosphate concentrations are mediated by its oral intake, deposition in bones and soft tissues, and excretion in urine and feces. A healthy human consumes from 700 to 2000 mg phosphorus per day in the diet (Blaine et al., 2015). According to the American National Academy of Medicine, the dietary reference intake (DRI) of phosphorus for an adult human is 700 mg/day, which allows maintaining the proper level of phosphatemia (Hong et al., 2015; Institute of Medicine, 1997).

The main organs that control phosphate homeostasis are the kidneys. Pi is practically effortlessly filtered in the renal glomerulus into the primary urine. Between 3700 and 6100 mg Pi is filtered in the kidneys daily, but only 600–1500 mg is excreted in urine (Blaine et al., 2015). These values demonstrate how profoundly renal phosphate reabsorption occurs.

Under physiological conditions, the formation of hydroxyapatite from calcium and phosphate is promoted in bones and teeth but inhibited in soft tissues (Villa-Bellosta & Egido, 2017;

Villa-Bellosta & Sorribas, 2011). This balance is possible because of the existence of substances that act as calcification inhibitors, such as pyrophosphate (PPI), citrate, fetuin A, and osteopontin (Rutsch et al., 2011). PPI is believed to be the main endogenous inhibitor of hydroxyapatite generation in vivo and in vitro (Azpiazu et al., 2018).

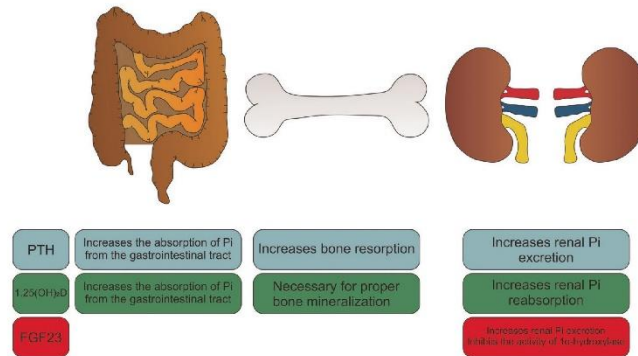
Three major compounds control phosphate equilibrium: parathyroid hormone (PTH), active vitamin D ($1,25[\text{OH}]_2\text{D}$), and fibroblast growth factor 23 (FGF23) and its coreceptor Klotho (Bergwitz & Jüppner, 2010; Lang et al., 2018).

PTH is produced in the parathyroid glands and is known as a "calciostat," but it also mediates Pi levels. High Pi concentrations cause a decrease in serum ionic calcium by forming a Ca–Pi complex, which extends the PTH messenger RNA (mRNA) half-life and enhances PTH release into the bloodstream (Bergwitz & Jüppner, 2010; Razzaque, 2011). PTH reduces serum Pi concentrations by increasing its urinary elimination. PTH acts on target cells mainly via PTH receptor 1 (PTHr1), which is a G protein-linked receptor (GPLR) (Bergwitz & Jüppner, 2010). At the kidney level, the attachment of PTH to PTHr1 in the proximal tubules leads to activation of the $G_{s\alpha}$ /protein kinase A and G_q /phospholipase C/protein kinase C pathways. This leads to the inactivation of specific phosphate transporters and subsequently a reduction of Pi reabsorption and hyperphosphaturia (Bergwitz & Jüppner, 2010).

Active vitamin D (calcitriol; $1,25[\text{OH}]_2\text{D}$) is currently considered a hormone because of its enormous role in maintaining mineral balance and affecting the function of bones, kidneys, and intestines (Gil et al., 2018). Calcitriol synthesis is strictly regulated by PTH and FGF23. PTH increases calcitriol production, whereas FGF23 inhibits it (Jüppner, 2011). Vitamin D performs its functions by connecting to the vitamin D receptor (VDR) (Brown et al., 2015). Calcitriol regulates phosphate homeostasis by enhancing Pi absorption in the intestine, raising serum Pi levels.

FGF23 is a bone-derived hormone that is synthesized by osteoblasts and osteocytes (Bergwitz & Jüppner, 2010; Fukumoto, 2014; Jüppner, 2011). It acts through four main receptors: FGFR1c, FGFR2c, FGFR3c, and FGFR4. To accomplish its role, FGF23 demands Klotho protein as a coreceptor (Bergwitz & Jüppner, 2010; Fukumoto, 2014). The attachment of FGF23 to its receptor leads to activation of the mitogen-activated protein kinase (MAPK)-dependent pathway (Jürg Biber et al., 2013). The main function of FGF23 is to maintain normophosphatemia by decreasing serum Pi levels (Bergwitz & Jüppner, 2010). The mechanism of action of this hormone is based on two main paths. FGF23 downregulates calcitriol synthesis by inhibiting 1α -hydroxylase activity. It promotes the formation of an inactive form of vitamin D ($24,25[\text{OH}]_2\text{D}$) by stimulating 24 -hydroxylase (CYP27A1) activity (Bergwitz & Jüppner, 2010; Fukumoto, 2014; Jüppner, 2011; Lang et al., 2018), which causes a decrease in intestinal Pi absorption. Additionally, FGF23 suppresses renal phosphate reabsorption by internalizing phosphate-specific sodium-dependent transporters in the proximal tubule (Brown et al., 2015; Fukumoto, 2014; Jüppner, 2011; Lang et al., 2018). The mechanism of action of phosphate regulators is summarized in Figure 1.

FIGURE 1 Main components responsible for regulating phosphate homeostasis. PTH and the active form of vitamin D control phosphatemia by regulating Pi absorption from the gastrointestinal tract, Pi mobilization from bones, and urinary phosphate excretion. In contrast, the action of FGF23 is strictly focused on renal Pi excretion. PTH, parathyroid hormone; Pi, inorganic phosphate



3 | NA-DEPENDENT PHOSPHATE COTRANSPORTERS

All major sodium-dependent phosphate transporters belong to the solute carrier (SLC) group of membrane proteins. Type II Pi transporters (SLC34 family) and type III Pi transporters (SLC20 family) are mostly involved in controlling phosphate balance and are sodium-dependent. The SLC34 family consists of three cotransporters, namely NaPi 2a (SLC34A1), NaPi 2b (SLC34A2), and NaPi 2c (SLC34A3). The SLC20 family comprises two proteins: Pit 1 (SLC20A1) and Pit 2 (SLC20A2) (Biber et al., 2004, 2013; Forster et al., 2013; Wagner et al., 2014). Type II cotransporters are involved in the maintenance of physiological serum phosphate levels. Pit 1 and Pit 2 are considered essential for Pi influx in systemic cells.

All SLC34 proteins contain 12 transmembrane domains and transport divalent Pi into cells (Biber et al., 2013). NaPi 2a and NaPi 2c are localized in the brush border of the proximal tubule epithelium where they mediate Pi reabsorption. The NaPi 2c transporter is located in S1 and S2 convoluted fragments of the proximal tubule, whereas the presence of the NaPi 2a transporter was confirmed in S1 and S2 fragments and the straight S3 fragment (Custer et al., 1994) (Figure 2).

NaPi 2b is located in the small intestine and responsible for the absorption of Pi from food (Biber et al., 2013; Forster et al., 2006, 2013; Wagner et al., 2014). NaPi 2a and NaPi 2b display electrogenic transport. For each HPO_4^{2-} ion, they transfer three Na^+ ions. This is different for NaPi 2c, which carries two sodium ions per divalent phosphate ion (electroneutral transport) (Forster et al., 1999, 2006). The aforementioned proteins depend on the strict control of PTH, FGF23, and calcitriol. Thirty percent of intestinal phosphate absorption, which is mainly attributable to NaPi 2b activity, is coordinated by $1,25(\text{OH})_2\text{D}$ (Wilz et al., 1979). Renal Pi handling is mostly regulated by PTH and FGF23. The activation of PTHR1 in the proximal tubule leads to the down-regulation of NaPi 2a (within minutes) and NaPi 2c (within hours) (Biber et al., 2013). NaPi 2a oversees 70% of the renal management of phosphate (Blaine et al., 2015), so its reaction time to any alterations must be fast. In the presence of PTH, NaPi 2a is endocytosed and transferred to lysosomes. NaPi 2c is controlled similarly, but it is not

destroyed in lysosomes (Bacic et al., 2006; Forster et al., 2006; Picard et al., 2010; Segawa et al., 2007). FGF23 acts similarly to PTH, but the precise time at which NaPi 2a/2c is internalized has not been established (Biber et al., 2013).

SLC20 proteins are widely distributed in the human body, but no organ specificity has yet been confirmed (Forster et al., 2013). Similar to type II transporters, they also comprise 12 transmembrane domains (Biber et al., 2013). Viral receptor domains can be distinguished in their structure. Pit 1 was previously known as the gibbon ape leukemia virus receptor (Glv-1), and Pit 2 was called the rat amphotropic leukemia virus receptor (Ram-1) (Forster et al., 2013). Pit 1 and Pit 2 transfer monovalent phosphate into the cell. For each H_2PO_4^- ion, they carry two sodium ions (electrogenic transport). Type III transporters are much more resistant to pH fluctuations than SLC34 proteins and can still maintain their function. Under low pH conditions (e.g., during tubular acidosis), Pit 1 and Pit 2 can provide renal Pi reabsorption without disturbances, even

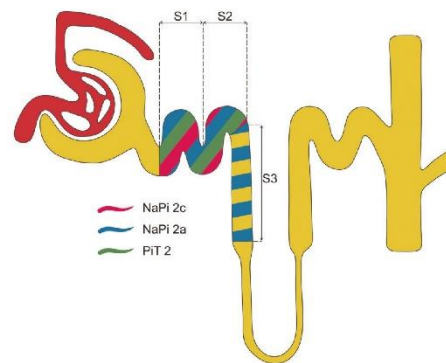


FIGURE 2 Localization of sodium-dependent phosphate transporters in the nephron. Both NaPi2c and Pit 2 proteins are distributed in S1 and S2 convoluted fragments of the proximal tubule. NaPi2a protein is present in the convoluted part and straight part of the proximal tubule

if the function of SLC34 proteins is impaired (Biber et al., 2013). Moreover, the distribution of Pit 2 protein in the kidney is analogous to NaPi 2c (Biber et al., 2009; Villa-Bellosta et al., 2009). Type III Pi transporters are responsible for phosphate reabsorption in the kidneys and necessary to maintain proper cellular function. In bone-forming cells, Pit 1 is necessary to induce extracellular mineralization (Suzuki et al., 2006). Numerous studies have reported significant roles for Pit 1 and Pit 2 in vascular calcification (Crouthamel et al., 2013; Li et al., 2006; Masumoto et al., 2017; Yamada et al., 2018).

4 | PIT 1 AND PIT 2 ARE INVOLVED IN VASCULAR CALCIFICATION

Vascular calcification (VC) is a common complication in patients with CKD and diabetes (Lau et al., 2010). Under these pathophysiological conditions, calcium phosphate is deposited in the walls of the arteries or heart valves. This increases the risk of fatal cardiovascular complications (Li & Giachelli, 2007; Schlieper, 2018). High serum phosphate levels and elevations of the $\text{Ca} \times \text{Pi}$ product contribute to the onset of VC in CKD patients and even in the healthy population (Dhingra et al., 2007; Kestenbaum et al., 2009). The main target of calcification processes are vascular smooth muscle cells (VSMCs).

Over the past two decades, extensive evidence has been reported of the involvement of type III phosphate transporters in the development of VC (Li & Giachelli, 2007; Li et al., 2006; Masumoto et al., 2017; Suzuki et al., 2006; Yamada et al., 2018). The phosphate cotransporter inhibitor phosphonoformic acid (PFA) reduced the influx of Pi into VSMCs and inhibited their calcification (Chen et al., 2002; Jono et al., 2000). This indicates that high phosphate concentrations cause a procalcifying response in VSMCs through a phosphate cotransporter-dependent mechanism (Chen et al., 2002; Jono et al., 2000). Li et al. (2006) generated Pit 1-deficient VSMCs using small-interfering RNA (siRNA). siRNA-treated cells were characterized by a lower amount of Pit 1 at both the mRNA and protein levels compared with control cells. Sodium-dependent phosphate influx also decreased in Pit 1-deficient VSMCs. To evaluate the intensity of calcification, a culture medium with high Pi levels was used. Cells were grown under these conditions and evaluated at three different time points. Pit 1-deficient VSMCs exhibited a decrease in calcification at all time points compared with control cells (Li et al., 2006). The overexpression of Pit 1 in Pit 1-downregulated cells led to the resumption of calcification (Li et al., 2006). These findings indicated that Pi uptake via Pit 1 is a key factor that mediates VSMC calcification and osteochondrogenic differentiation. Masumoto et al. (2017) came to similar conclusions. These authors found that calcification in tissue cultures of rat aortic rings was most marked in both hypercalcemic and hyperphosphatemic environments. Additionally, increasing calcium concentrations during hyperphosphatemic conditions increased Pit 1 expression and VC. This phenomenon was inhibited by PFA, thus demonstrating the relationship between calcium-induced VC and the amount of Pit 1 in aortic tissue (Masumoto et al., 2017).

In vivo studies have shown that Pit 1 mRNA levels increased in the aorta in rats with induced renal failure compared with control

rats (Mizobuchi et al., 2006). Crouthamel et al. (2013) developed mice with targeted Pit 1 deletion in VSMCs. In these animals and in the control group, VC was induced by nephrectomy and a phosphate-rich diet. The authors showed that Pit 1 deletion in mice that were fed a high-phosphate diet did not affect calcification. Additionally, sodium-dependent phosphate transport was comparable for both tested genotypes. This may indicate the existence of compensatory mechanisms because a twofold increase in Pit 2 mRNA expression was observed in VSMCs with Pit 1 deletion. This was confirmed by the fact that Pit 2 overexpression in human VSMCs with Pit 1 deficiency restored VC, and Pit 2 downregulation in these cells inhibited calcification. With the lack of Pit 1 protein, Pit 2 can participate in the development of VC (Crouthamel et al., 2013).

The action of indoxyl sulfate, which is a uremic toxin that causes nephrotoxic and vasotoxic effects, has been studied in cultured VSMCs (Wu et al., 2016). Indoxyl sulfate concentrations increase during the course of CKD. It causes the mineralization of VSMCs and their osteochondrogenic differentiation. This process occurs via Pit 1 upregulation and activation of the c-Jun N-terminal kinase pathway (Wu et al., 2016). The inhibition of this pathway led to the elimination of Pit 1 overexpression and reduced VC. Recent evidence indicates an interaction between Pit 1 and receptor for advanced glycation end products (RAGE) (Belmokhtar et al., 2019). Pit 1 upregulation that is caused by oxidative stress leads to Pi- and RAGE-ligand/RAGE signaling and ultimately the osteoblastic transformation of VSMCs. These data confirm that Pit 1 protein can act as a promoter of VC.

Recent studies highlighted a novel role for Pit 2 protein in VC. Yamada et al. (2018) generated uremic mice with global Pit 2 haploinsufficiency. These authors found that Pit 2 deficiency in animals that were fed a high-phosphate diet increased calcium accumulation in the aorta. Renal function was unaffected in these mice, demonstrated by normal serum biochemistry. In vitro studies of cultured VSMCs showed that Pit 2 haploinsufficiency increased the degree of Pi-induced calcification. The amount of osteoprotegerin protein (OPG), a well-known calcification inhibitor, also decreased in these cells. Furthermore, the addition of OPG to Pit 2-deficient VSMCs reduced the level of calcification. These results suggest that Pit 2 protein may play a protective role in preventing VC and may be a therapeutic target to mitigate vascular complications in CKD patients (Yamada et al., 2018).

Overall, these data indicate that hyperphosphatemia that occurs during the course of CKD is a major factor that leads to the development of VC, and it is mediated by type III sodium-dependent phosphate transporters.

5 | THE ROLE OF PIT 1 AND PIT 2 PROTEINS IN THE KIDNEY AND PODOCYTES

Substantial evidence of the role of SLC34 transporters in the kidney has been reported. NaPi 2a/2c proteins participate in phosphate reabsorption in the proximal tubule and are subjected to strict hormonal control. Unfortunately, data on the function of SLC20

proteins in the kidneys and podocytes are scarce. To date, only a few papers have described the function of Pit 1 and Pit 2, especially in podocytes.

Villa-Bellosta et al. (2009) reported the presence of Pit 2 protein in the proximal tubule of the kidney. This transporter is located in the brush-border membrane of the epithelium that lines the proximal tubule. Rats that were fed a high-Pi diet had a much lower amount of Pit 2 than rats that were fed a low-Pi diet (Villa-Bellosta et al., 2009). This indicates that the presence of Pit 2 in the brush border membrane is regulated by dietary phosphate intake. Interestingly, the time required for Pit 2 to adapt to changes in phosphate concentrations was much longer than for NaPi 2a, which is the main factor that determines Pi reabsorption. The difference in adaptation time suggests the occurrence of various mechanisms that regulate the expression of SLC34 and SLC20 proteins in the proximal tubule.

The effect of chronic hyperphosphatemia on the glomerulus was explained well by Tsuchiya et al. In this study, rats were intravenously administered Na_2HPO_4 solutions in an increasing concentration range (Tsuchiya et al., 2004). Glomerular calcification was observed in the high-dose group, and no calcification of other organs was noted. Electron microscopy revealed pathological changes in the glomerulus, such as basophilic granules and lamellar structures in the glomerular basement membrane (GBM), podocytes, and the mesangial matrix. These lamellar structures were composed of cellular debris and high-density granules that contained calcium and phosphate. The increase in proteinuria that was observed in the high-dose group of rats was generated by glomerular epithelial cell damage and filtration barrier disruption. Based on these observations, the pathogenesis of glomerular injury by high Pi levels was determined. Intravenous Pi administration increases its filtration in the glomerulus. Consequently, local Pi concentrations increase in glomerular cells, including podocytes, likely with the participation of sodium-dependent Pi co-transporters. Phosphate combines with extracellular or intracellular calcium to form $\text{Ca} \times \text{Pi}$ in Bowman's space or inside the cell, respectively. The emerging lamellar structures damage the glomerulus and impair its function (Figure 3).

The first evidence of the involvement of SLC20 proteins in phosphate-dependent podocyte damage was provided by Sekiguchi et al. The aim of their study was to determine changes in renal function in transgenic (TG) rats that overexpressed Pit 1 protein compared with wildtype (WT) rats (Sekiguchi et al., 2011). The overexpression of Pit 1 in podocytes was confirmed by real-time polymerase chain reaction. Hypoalbuminemia and proteinuria were observed in TG rats, which increased with age (Sekiguchi et al., 2011). Most glomeruli in TG rats exhibited sclerotic changes, such as collapse of the GBM, hyperplasia of the mesangial matrix, and capillary adhesion to the walls of Bowman's capsule. Additionally, in rats with Pit 1 overexpression, podocytes lost foot processes and detached from the GBM. Furthermore, an increase in the expression of markers of podocyte damage, such as desmin and connexin 43, was noted. The GBM was significantly thickened in TG rats by the accumulation of proteins that were produced by injured podocytes. Phosphate uptake in podocytes was higher in TG rats than in WT rats, particularly at low Pi

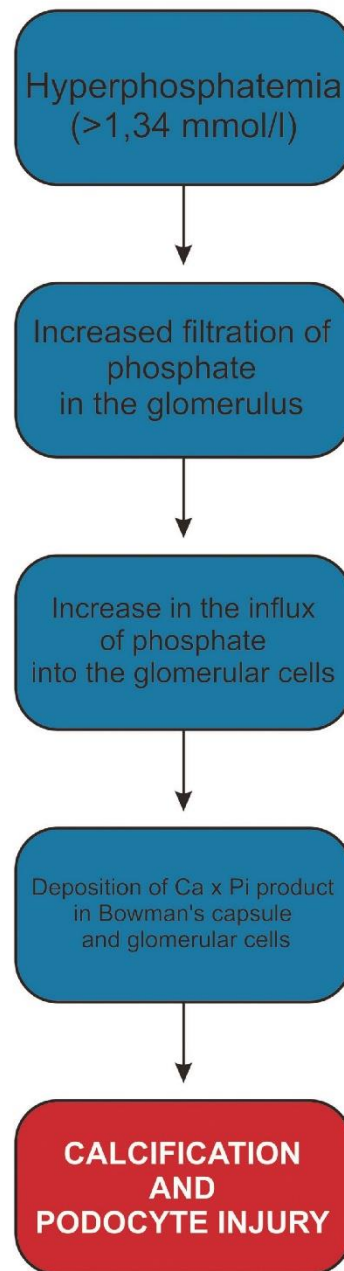


FIGURE 3 Mechanism of injury to the glomerulus caused by hyperphosphatemia (Tsuchiya et al., 2004)

concentrations. To establish the effect of Pi on the glomerular filtration barrier, the rats were fed a normo-phosphate or high-phosphate diet (NP and HP, respectively). The decrease in serum albumin was more pronounced in TG-HP rats than in TG-NP rats. Moreover, proteinuria occurred earlier in TG-HP rats. These authors showed that Pit 1 overexpression caused Pi-dependent podocyte damage, which led to sclerotic changes in the glomerulus and impairments in the renal filtration barrier. However, the mechanism by which Pit 1 protein disrupts podocyte function is currently unknown.

Asada et al. used a similar model of rats that overexpressed Pit 1 protein (TG rats) (Asada et al., 2019). This study assessed the actions of risedronate, a bisphosphonate drug, on rat kidney function and the glomerular filtration barrier. Bisphosphonates are used for the treatment of osteoporosis and related diseases. They restrict the loss of bone density by inhibiting osteoclast activity. These authors found that the supply of risedronate did not affect serum creatinine or phosphate levels in TG and WT rats. In contrast, hyaline and vacuolar degeneration was noted in kidney sections in TG rats. Thickening of the GBM and podocyte detachment were also present. The GBM lost its three-layer structure. These alterations were much less severe in TG rats that were treated with risedronate. Furthermore, TG rats exhibited a higher expression of markers of podocyte injury (i.e., desmin and connexin-43) compared with TG rats, which were administered with risedronate. In summary, risedronate protects the glomerular filtration barrier, particularly podocytes from phosphate-induced injury. The exact mechanism by which bisphosphonates exert their protective actions is not yet known and requires further research. Bisphosphonates, because of their similar structure to Pi, likely compete with phosphate for entry into the cell via SLC20 transporters.

6 | THE FUNCTION OF SLC20 PROTEINS IN THE PODOCYTE: FUTURE PERSPECTIVE

Until now, it was believed that proteins from the SLC20 family perform a housekeeping role, considering their ubiquitous expression in the body (Berndt et al., 2005; Kavanaugh & Kabat, 1996; Nishimura & Naito, 2008). In addition to participating in VC, recent studies suggest novel roles for Pit 1 and Pit 2, in addition to their well-known involvement in phosphate transport (Bon et al., 2018; Forand et al., 2016). These proteins may affect the physiology of podocytes in a different way from causing Pi-induced cellular stress.

Many studies show similarities between podocytes and smooth muscle cells (SMCs). Saleem et al. (2008) reported that podocytes, in addition to their epithelial cell phenotype, have characteristics of SMCs. The epithelial cell features include basement membrane production and cytokeratin expression. Insulin-dependent glucose transport and the presence of TRPC6 calcium channels demonstrate similarity to SMCs. In their structure, podocytes contain a highly specialized actin cytoskeleton that is able to contract (Faul, 2014; Faul et al., 2007). Proteins that mediate contractility, such as smoothelin, calponin, and myocardin, have been found in differentiated podocytes (Saleem et al., 2008). TRPC6

channels play a significant role in maintaining the physiology of podocytes, particularly the proper function of slit diaphragms that are formed by foot processes. We found that insulin-dependent actin cytoskeleton reorganization in podocytes and hence the increase in albumin permeability revolve around TRPC6 channel activity (Rogacka et al., 2017). Furthermore, activation of the adenosine monophosphate-activated protein kinase (AMPK) pathway in a TRPC6-dependent manner regulates glucose transport and actin cytoskeleton rearrangement (Rachubik et al., 2018). Given the similarity between podocytes to SMCs, calcification processes that occur in VSMCs may also occur in podocytes. The glomerulus and podocytes themselves are sensitive to changes in phosphate metabolism. Hyperphosphatemia that is present during the course of CKD, end-stage renal disease and diabetes directly damages podocytes. This action can be mediated by Pit 1 protein that is present on their surface, which actively participates in calcification processes. In the course of our research, we established the expression of the SLC20A1 and SLC20A2 genes in immortalized human podocytes using real-time PCR. These genes code for the Pit 1 and Pit 2 proteins, respectively. Using confocal microscopy, we visualized the cellular localization of these transporters. The cells were counter-stained with synaptopodin as a specific podocyte marker (Figure 4). However, the exact mechanism by which Pit 1 or Pit 2 promotes calcification in podocytes has not yet been discovered.

Insulin signaling and insulin-dependent glucose transport have an enormous impact on the function of podocytes, as demonstrated by our previous studies (Piwkowska et al., 2014, 2015; Rogacka et al., 2014). Recently, Forand et al. (2016) discovered an interaction between the Pit 1 transporter and insulin signaling in hepatocytes. In this study, hepatocyte-specific Pit 1 knockout mice were generated. These mice exhibited prolonged insulin signaling, an increase in insulin sensitivity, and improvements in glucose metabolism. The authors found that Pit 1 protein interacted with ubiquitin-specific peptidase 7 (USP7), which is a deubiquitinating enzyme. USP7 detaches ubiquitin from its substrates, thereby protecting them from proteasomal degradation. Upon Pit 1 deletion, USP7 can interact with insulin receptor substrate 1 (IRS1), which protects it from removal. This results in prolonged insulin signaling, which prevents the development of obesity or diabetes. Importantly, the metabolic actions of Pit 1 occur independently of its function as a phosphate transporter. The overexpression of Pit 1 in podocytes leads to impairments in their physiology. Thus, one of the mechanisms of podocyte injury may involve excessive interactions between Pit 1 and USP7 and weakened insulin signaling.

The functions of Pit 1 and Pit 2 proteins are believed to go beyond intracellular phosphate transport from the extracellular milieu. Recent studies indicate that both Pit transporters are involved in Pi signaling that is associated with extracellular signal-regulated kinase 1/2 (ERK1/2) phosphorylation (Bon et al., 2018). ERK1 and ERK2 are proteins that are part of the MAPK/ERK pathway. This cascade is involved in regulating crucial cellular processes, such as cell division, cell differentiation, and apoptosis (Yao et al., 2003). Chavkin et al. (2015) determined that Pit 1 serves as a Pi sensor, which controls ERK signaling under high-Pi conditions. This leads to osteochondrogenic differentiation of VSMCs and consequently to vascular calcification. Bearing in mind the previously

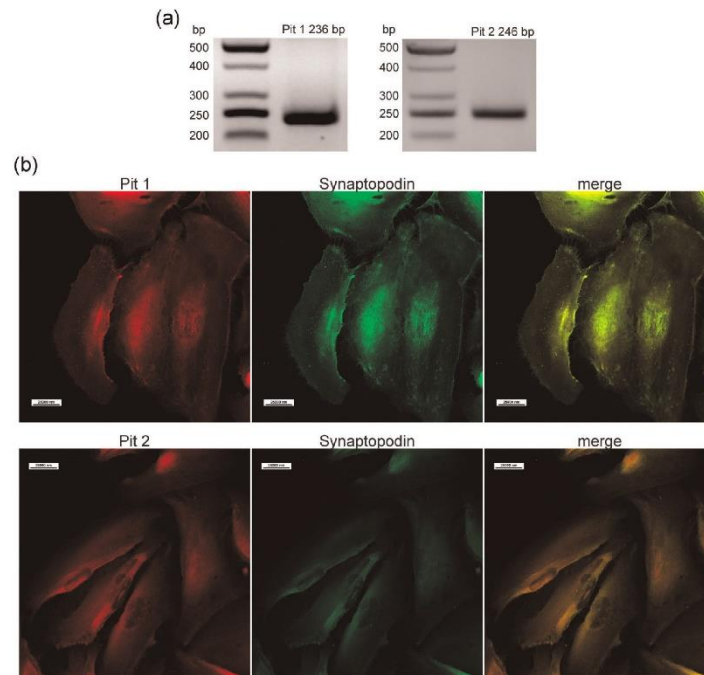


FIGURE 4 Expression of Pit 1 and Pit 2 in immortalized human podocytes. (a) Real-time polymerase chain reaction products imaged on a 2.5% agarose gel, which reflect the amplified Pit 1 and Pit 2 fragments of mRNA isolated from podocytes. (b) Confocal images of Pit 1 and Pit 2 with podocyte marker synaptopodin in human podocytes. Primary antibodies for Pit 1 (Biorbyt, orb 412245) and Pit 2 (Biorbyt, orb 247601) were diluted 1:25, whereas primary antibodies for synaptopodin (Santa Cruz, sc-21537) were diluted 1:15. Secondary antibodies (Invitrogen, Alexa Fluor 488 A32814, and Alexa Fluor 546 A11035) were diluted 1:200 (scale bar = 25 μ m)

described similarity of SMCs to podocytes, an analogous mechanism may contribute to renal calcification. Using osteoblastic and chondrocyte cell lines, Bon et al. (2018) also found that both Pit 1 and Pit 2 serve as extracellular phosphate sensors that can mediate downstream Pi-induced signaling. These authors observed abolition of the Pi-induced upregulation of matrix gla protein and osteopontin (a known inhibitor of mineralization) in Pit 1- or Pit 2-depleted cells. ERK1/2 phosphorylation levels also decreased in these cells. Interestingly, the overexpression of Pit 1 and Pit 2 with impairments in transport function restored ERK signaling. This suggests that the mediation of Pi signaling by Pit 1 and Pit 2 occurs independently of their Pi transport function. Additionally, Pit 1 and Pit 2 can form homo- and hetero-dimers and these heterodimers are sensitive to alterations of extracellular phosphate concentrations (Bon et al., 2018). Furthermore, with the inhibition of Pit 1 or Pit 2 transport function, heterodimers continued to respond to changes in extracellular Pi levels. Therefore, the binding of Pi but not its transport is crucial for the creation of Pit 1/Pit 2 heterodimers. Phosphate-sensitive Pit 1/Pit 2 heterodimers could be a delicate Pi sensor and possibly an on/off switch in ERK signaling. In podocytes, TRPC6 channels directly interact with ERK1/2 and mediate its phosphorylation (Farmer et al., 2019).

Furthermore, gain-of-function mutations of TRPC6 protein increase ERK1/2 phosphorylation (Chiluza et al., 2013). The upregulation of ERK1/2 leads to higher TRPC6 expression, which in turn induces podocyte injury (Yu et al., 2018). Pit 1/Pit 2 heterodimers can mediate ERK signaling, and ERK1/2 affects TRPC6 channel activity. Thus, Pit 1 and Pit 2 transporters may indirectly alter actin cytoskeleton rearrangements, thereby impairing podocyte function.

7 | CONCLUSIONS

The present review describes the participation of SLC20 family phosphate transporters in the development of VC that is caused by hyperphosphatemia during the course of CKD. The glomerulus is sensitive to elevations of phosphate levels. It can be damaged when phosphate homeostasis is disturbed. Glomerular calcification, similar to VC, can be induced by high phosphate levels, and these disorders are likely mediated by Pit 1 and Pit 2 proteins. These sodium-dependent Pi transporters cause podocyte injury, but the precise mechanism by which this occurs has not yet been discovered.

Recent studies indicate much broader functions of Pit 1 and Pit 2 proteins, in addition to their role as Pi transporters. They participate in regulating insulin signaling. These Pi transporters are also phosphate sensors that are able to form heterodimers that regulate signaling pathways that are important for proper cellular function. Perhaps one of these mechanisms is present in podocytes, but this possibility requires further research.

ACKNOWLEDGMENT

This study was supported by the National Science Centre, Poland (grant number 2018/29/B/NZ4/02074).

CONFLICT OF INTERESTS

The authors declare that there are no conflict of interests.

DATA AVAILABILITY STATEMENT

The data that support the findings of this study are available from the corresponding author upon reasonable request.

ORCID

Tomasz Kulesza  <http://orcid.org/0000-0001-5166-7444>

Agnieszka Piwkowska  <http://orcid.org/0000-0002-0086-7777>

REFERENCES

- Asada, Y., Takayanagi, T., Kawakami, T., Tomatsu, E., Masuda, A., Yoshino, Y., Sekiguchi-Ueda, S., Shibata, M., Ide, T., Niimi, H., Yaoita, E., Seino, Y., Sugimura, Y., & Suzuki, A. (2019). Risedronate attenuates podocyte injury in phosphate transporter-overexpressing rats. *International Journal of Endocrinology*, 2019, 1–10. <https://doi.org/10.1155/2019/4194853>
- Azpiazu, D., Gonzalo, S., González-Parra, E., Egido, J., & Villa-Belostta, R. (2018). Role of pyrophosphate in vascular calcification in chronic kidney disease. *Nephrology*, 38(3), 250–257. <https://doi.org/10.1016/j.nefro.2018.03.003>
- Bacic, D., LeHir, M., Biber, J., Kaissling, B., Murer, H., & Wagner, C. A. (2006). The renal Na⁺/phosphate cotransporter NaPi-IIa is internalized via the receptor-mediated endocytic route in response to parathyroid hormone. *Kidney International*, 69(3), 495–503. <https://doi.org/10.1038/sj.ki.5000148>
- Belmokhtar, K., Ortilon, J., Jaisson, S., Massy, Z. A., Boulagnon Rombi, C., Doué, M., Maurice, P., Fritz, G., Gillery, P., Schmidt, A. M., Rieu, P., & Touré, F. (2019). Receptor for advanced glycation end products: a key molecule in the genesis of chronic kidney disease vascular calcification and a potential modulator of sodium phosphate co-transporter PIT-1 expression. *Nephrology, Dialysis, Transplantation: Official Publication of the European Dialysis and Transplant Association - European Renal Association*, 34(12), 2018–2030. <https://doi.org/10.1093/ndt/gfz012>
- Bergwitz, C., & Jüppner, H. (2010). Regulation of phosphate homeostasis by PTH, vitamin D, and FGF23. *Annual Review of Medicine*, 61(1), 91–104. <https://doi.org/10.1146/annurev.med.051308.111339>
- Berndt, T. J., Schiavi, S., & Kumar, R. (2005). "Phosphatonins" and the regulation of phosphorus homeostasis. *American Journal of Physiology—Renal Physiology*, 289(6), F1170–F1182. <https://doi.org/10.1152/ajprenal.00072.2005>
- Berndt, T., & Kumar, R. (2009). Novel mechanisms in the regulation of phosphorus homeostasis. *Physiology*, 24(1), 17–25. <https://doi.org/10.1152/physiol.00034.2008>
- Biber, J., Hernando, N., Forster, I., & Murer, H. (2009). Regulation of phosphate transport in proximal tubules. *Pflügers Archiv. European Journal of Physiology*, 458(1), 39–52. <https://doi.org/10.1007/s00424-008-0580-8>
- Biber, J., Gisler, S. M., Hernando, N., Wagner, C. A., & Murer, H. (2004). PDZ interactions and proximal tubular phosphate reabsorption. *American Journal of Physiology—Renal Physiology*, 287(5), F871–F875. <https://doi.org/10.1152/ajprenal.00244.2004>
- Biber, J., Hernando, N., & Forster, I. (2013). Phosphate transporters and their function. *Annual Review of Physiology*, 75(1), 535–550. <https://doi.org/10.1146/annurev-physiol-030212-183748>
- Blaine, J., Chonchol, M., & Levi, M. (2015). Renal control of calcium, phosphate, and magnesium homeostasis. *Clinical Journal of the American Society of Nephrology*, 10(7), 1257–1272. <https://doi.org/10.2215/CJN.09750913>
- Bon, N., Couasny, G., Bourguin, A., Sourice, S., Beck-Cormier, S., Guicheux, J., & Beck, L. (2018). Phosphate (Pi)-regulated heterodimerization of the high-affinity sodium-dependent Pi transporters Pit1/SLC20A1 and Pit2/SLC20A2 underlies extracellular Pi sensing independently of Pi uptake. *Journal of Biological Chemistry*, 293(6), 2102–2114. <https://doi.org/10.1074/jbc.M117.807339>
- Brown, R. B., Haq, A., Stanford, C. F., & Razzaque, M. S. (2015). Vitamin D, phosphate, and vasculotoxicity. *Canadian Journal of Physiology and Pharmacology*, 93(12), 1077–1082. <https://doi.org/10.1139/cjpp-2015-0083>
- Chavkin, N. W., Chia, J. J., Crouthamel, M. H., & Giachelli, C. M. (2015). Phosphate uptake-independent signaling functions of the type III sodium-dependent phosphate transporter, PIT-1, in vascular smooth muscle cells. *Experimental Cell Research*, 333(1), 39–48. <https://doi.org/10.1016/j.yexcr.2015.02.002>
- Chen, N. X., O'Neill, K. D., Duan, D., & Moe, S. M. (2002). Phosphorus and uremic serum up-regulate osteopontin expression in vascular smooth muscle cells. *Kidney International*, 62(5), 1724–1731. <https://doi.org/10.1046/j.1523-1755.2002.00625.x>
- Chiluiza, D., Krishna, S., Schumacher, V. A., & Schliöndorff, J. (2013). Gain-of-function mutations in transient receptor potential C6 (TRPC6) activate extracellular signal-regulated kinases 1/2 (ERK1/2). *Journal of Biological Chemistry*, 288(25), 18407–18420. <https://doi.org/10.1074/jbc.M113.463059>
- Coward, R., & Fornoni, A. (2015). Insulin signaling: Implications for podocyte biology in diabetic kidney disease. *Current Opinion in Nephrology and Hypertension*, 24(1), 104–110. <https://doi.org/10.1097/MNH.0000000000000078>
- Cozzolino, M., Foque, D., Ciceri, P., & Galassi, A. (2017). Phosphate in chronic kidney disease progression. *Contributions to Nephrology*, 190, 71–82. <https://doi.org/10.1159/000468915>
- Crouthamel, M. H., Lau, W. L., Leaf, E. M., Chavkin, N. W., Wallingford, M. C., Peterson, D. F., Li, X., Liu, Y., Chin, M. T., Levi, M., & Giachelli, C. M. (2013). Sodium-dependent phosphate cotransporters and phosphate-induced calcification of vascular smooth muscle cells: Redundant roles for PIT-1 and PIT-2. *Arteriosclerosis, Thrombosis, and Vascular Biology*, 33(11), 2625–2632. <https://doi.org/10.1161/ATVBAHA.113.302249>
- Custer, M., Lotscher, M., Biber, J., Murer, H., & Kaissling, B. (1994). Expression of Na-P(i) cotransport in rat kidney: Localization by RT-PCR and immunohistochemistry. *American Journal of Physiology—Renal Physiology*, 266(5), F767–F774. <https://doi.org/10.1152/ajprenal.1994.266.5.f767>
- Da, J., Xie, X., Wolf, M., Disthabanchong, S., Wang, J., Zha, Y., Lv, J., Zhang, L., & Wang, H. (2015). Serum phosphorus and progression of CKD and mortality: A meta-analysis of cohort studies. *American Journal of Kidney Diseases*, 66(2), 258–265. <https://doi.org/10.1053/j.ajkd.2015.01.009>
- Dhingra, R., Sullivan, L. M., Fox, C. S., Wang, T. J., D'Agostino, R. B., Gaziano, J. M., & Vasan, R. S. (2007). Relations of serum phosphorus and calcium levels to the incidence of cardiovascular disease in the community. *Archives of Internal Medicine*, 167(9), 879–885. <https://doi.org/10.1001/archinte.167.9.879>
- Farmer, L. K., Rollason, R., Whitcomb, D. J., Ni, L., Goodliff, A., Lay, A. C., Birnbaumer, L., Heesom, K. J., Xu, S. Z., Saleem, M. A., & Welsh, G. I.

- (2019). TRPC6 binds to and activates calpain, independent of its channel activity, and regulates podocyte cytoskeleton, cell adhesion, and motility. *Journal of the American Society of Nephrology*, 30(10), 1910–1924. <https://doi.org/10.1681/ASN.2018070729>
- Faul, C. (2014). The podocyte cytoskeleton: key to a functioning glomerulus in health and disease. *Podocytopathy*, Basel, Karger, 183, 22–53. <https://doi.org/10.1159/000359923>
- Faul, C., Asanuma, K., Yanagida-Asanuma, E., Kim, K., & Mundel, P. (2007). Actin up: regulation of podocyte structure and function by components of the actin cytoskeleton. *Trends in Cell Biology*, 17(9), 428–437. <https://doi.org/10.1016/j.tcb.2007.06.00>
- Forand, A., Koumakis, E., Rousseau, A., Sassier, Y., Journe, C., Merlin, J. F., Leroy, C., Boitez, V., Codogno, P., Friedlander, G., & Cohen, I. (2016). Disruption of the phosphate transporter Pit1 in hepatocytes improves glucose metabolism and insulin signaling by modulating the USP7/IRS1 interaction. *Cell Reports*, 16(10), 2736–2748. <https://doi.org/10.1016/j.celrep.2016.08.012>
- Forster, I. C., Hernando, N., Biber, J., & Murer, H. (2006). Proximal tubular handling of phosphate: A molecular perspective. *Kidney International*, 70(9), 1548–1559. <https://doi.org/10.1038/sj.ki.5001813>
- Forster, I. C., Hernando, N., Biber, J., & Murer, H. (2013). Phosphate transporters of the SLC20 and SLC34 families. *Molecular Aspects of Medicine*, 34(2–3), 386–395. <https://doi.org/10.1016/j.mam.2012.07.007>
- Forster, I. C., Loo, D. D. R., & Eskandari, S. (1999). Stoichiometry and Na⁺ binding cooperativity of rat and flounder renal type II Na⁺-Pi cotransporters. *American Journal of Physiology*, 276(4), F644–F649. <https://doi.org/10.1152/ajprenal.1999.276.4.f644>
- Fukumoto, S. (2014). Phosphate metabolism and vitamin D. *BoneKey Reports*, 3, 1–5. <https://doi.org/10.1038/bonekey.2013.231>
- Garg, P. (2018). A review of podocyte biology. *American Journal of Nephrology*, 47(suppl. 1), 3–13. <https://doi.org/10.1159/000481633>
- Gil, Á., Plaza-Díaz, J., & Mesa, M. D. (2018). Vitamin D: Classic and novel actions. *Annals of Nutrition and Metabolism*, 72(2), 87–95. <https://doi.org/10.1159/000486536>
- Hong, S. H., Park, S. J., Lee, S., Kim, S., & Cho, M. H. (2015). Biological effects of inorganic phosphate: Potential signal of toxicity. *Journal of Toxicological Sciences*, 40(1), 55–69. <https://doi.org/10.2131/jts.40.55>
- Institute of Medicine. (1997). *Dietary reference intakes for calcium, phosphorus, magnesium, vitamin D, and fluoride*. The National Academies Press. <https://doi.org/10.17226/5776>
- Jono, S., McKee, M. D., Murry, C. E., Shioi, A., Nishizawa, Y., Mori, K., Morii, H., & Giachelli, C. M. (2000). Phosphate regulation of vascular smooth muscle cell calcification. *Circulation Research*, 87(7), 10–17. <https://doi.org/10.1161/01.res.87.7.e10>
- Jüppner, H. (2011). Phosphate and FGF-23. *Kidney International*, 79(suppl. 121), 25–28. <https://doi.org/10.1038/ki.2011.27>
- Kavanaugh, M. P., & Kabat, D. (1996). Identification and characterization of a widely expressed phosphate transporter/retrovirus receptor family. *Kidney International*, 49(4), 959–963. <https://doi.org/10.1038/ki.1996.135>
- Kestenbaum, B. R., Adeney, K. L., Boer, I. H. D., Ix, J. H., Shlipak, M. G., & Siscovick, D. S. (2009). Incidence and progression of coronary calcification in chronic kidney disease: The multi-ethnic study of atherosclerosis. *Kidney International*, 76(9), 991–998. <https://doi.org/10.1038/ki.2009.298>
- Khalighi, M. A., Gallan, A. J., Chang, A., & Meehan, S. M. (2018). Collapsing glomerulopathy in lambda light chain amyloidosis: A report of 2 cases. *American Journal of Kidney Diseases*, 72(4), 612–616. <https://doi.org/10.1053/j.ajkd.2018.04.009>
- Kopp, J. B., Anders, H. J., Susztak, K., Podestà, M. A., Remuzzi, G., Hildebrandt, F., & Romagnani, P. (2020). Podocytopathies. *Nature Reviews Disease Primers*, 6(1), 68. <https://doi.org/10.1038/s41572-020-0196-7>
- Lang, F., Leibrock, C., Pandyrá, A. A., Stournaras, C., Wagner, C. A., & Föller, M. (2018). Phosphate homeostasis, inflammation and the regulation of FGF-23. *Kidney and Blood Pressure Research*, 43(6), 1742–1748. <https://doi.org/10.1159/000495393>
- Lau, W. L., Festing, M. H., & Giachelli, C. M. (2010). Phosphate and vascular calcification: Emerging role of the sodium-dependent phosphate co-transporter PIT-1. *Thrombosis and Haemostasis*, 104(3), 464–470. <https://doi.org/10.1160/TH09-12-0814>
- Li, X., & Giachelli, C. M. (2007). Sodium-dependent phosphate cotransporters and vascular calcification. *Current Opinion in Nephrology and Hypertension*, 16, 325–328. <https://doi.org/10.1097/MNH.0b013e3281c55ef1>
- Li, X., Yang, H. Y., & Giachelli, C. M. (2006). Role of the sodium-dependent phosphate cotransporter, Pit-1, in vascular smooth muscle cell calcification. *Circulation Research*, 98, 905–912. <https://doi.org/10.1161/01.RES.0000216409.20863.e7>
- Masumoto, A., Sonou, T., Ohya, M., Yashiro, M., Nakashima, Y., Okuda, K., Iwashita, Y., Mima, T., Negi, S., & Shigematsu, T. (2017). Calcium overload accelerates phosphate-induced vascular calcification via pit-1, but not the calcium-sensing receptor. *Journal of Atherosclerosis and Thrombosis*, 24, 716–724. <https://doi.org/10.5551/jat.36574>
- Mizobuchi, M., Ogata, H., Hatamura, I., Koïwa, F., Saji, F., Shizaki, K., Negi, S., Kinugasa, E., Ooshima, A., Koshikawa, S., & Akizawa, T. (2006). Up-regulation of Cbfa1 and Pit-1 in calcified artery of uraemic rats with severe hyperphosphataemia and secondary hyperparathyroidism. *Nephrology Dialysis Transplantation*, 21(4), 911–916. <https://doi.org/10.1093/ndt/gfk008>
- Nishimura, M., & Naito, S. (2008). Tissue-specific mRNA expression profiles of human solute carrier transporter superfamilies. *Drug Metabolism and Pharmacokinetics*, 23(1), 22–44. <https://doi.org/10.2133/dmpk.23.22>
- O'Seaghdha, C. M., Hwang, S. J., Muntner, P., Melamed, M. L., & Fox, C. S. (2011). Serum phosphorus predicts incident chronic kidney disease and end-stage renal disease. *Nephrology Dialysis Transplantation*, 26(9), 288–2890. <https://doi.org/10.1093/ndt/gfq808>
- Picard, N., Capuano, P., Stange, G., Mihailova, M., Kaissling, B., Murer, H., Biber, J., & Wagner, C. A. (2010). Acute parathyroid hormone differentially regulates renal brush border membrane phosphate cotransporters. *Pflügers Archiv. European Journal of Physiology*, 460, 677–687. <https://doi.org/10.1007/s00424-010-0841-1>
- Piwkowska, A., Rogacka, D., Angielski, S., & Jankowski, M. (2014). Insulin stimulates glucose transport via protein kinase G type I alpha-dependent pathway in podocytes. *Biochemical and Biophysical Research Communications*, 446(1), 328–334. <https://doi.org/10.1016/j.bbrc.2014.02.108>
- Piwkowska, A., Rogacka, D., Audzeyenka, I., Angielski, S., & Jankowski, M. (2015). Combined effect of insulin and high glucose concentration on albumin permeability in cultured rat podocytes. *Biochemical and Biophysical Research Communications*, 461(2), 383–389. <https://doi.org/10.1016/j.bbrc.2015.04.043>
- Piwkowska, A., Rogacka, D., Audzeyenka, I., Kasztan, M., Angielski, S., & Jankowski, M. (2015). Insulin increases glomerular filtration barrier permeability through PKG α -dependent mobilization of BKCa channels in cultured rat podocytes. *Biochimica et Biophysica Acta—Molecular Basis of Disease*, 1852(8), 1599–1609. <https://doi.org/10.1016/j.bbdis.2015.04.024>
- Pollak, M. R., Quaggin, S. E., Hoenig, M. P., & Dworkin, L. D. (2014). The glomerulus: The sphere of influence. *Clinical Journal of the American Society of Nephrology*, 9(8), 1461–1469. <https://doi.org/10.2215/CJN.09400913>
- Rachubik, P., & Piwkowska, A. (2019). The role of vasodilator-stimulated phosphoprotein in podocyte functioning. *Cell Biology International*, 43(10), 1092–1101. <https://doi.org/10.1002/cbin.11149>
- Rachubik, P., Szejder, M., Rogacka, D., Audzeyenka, I., Rychlowski, M., Angielski, S., & Piwkowska, A. (2018). The TRPC6-AMPK pathway is involved in insulin-dependent cytoskeleton reorganization and glucose uptake in cultured rat podocytes. *Cellular Physiology and Biochemistry*, 51(1), 393–410. <https://doi.org/10.1159/000495236>

- Razzaque, M. S. (2011). Phosphate toxicity: New insights into an old problem. *Critical Science*, 120(3), 91–97. <https://doi.org/10.1042/CS20100377>
- Rogacka, D., Audzeyenka, I., Rachubik, P., Rychtowski, M., Kasztan, M., Jankowski, M., Angielski, S., & Piwkowska, A. (2017). Insulin increases filtration barrier permeability via TRPC6-dependent activation of PKG α signaling pathways. *Biochimica et Biophysica Acta—Molecular Basis of Disease*, 1863(6), 1312–1325. <https://doi.org/10.1016/j.bbdis.2017.03.002>
- Rogacka, D., Piwkowska, A., Audzeyenka, I., Angielski, S., & Jankowski, M. (2014). Involvement of the AMPK-PTEN pathway in insulin resistance induced by high glucose in cultured rat podocytes. *International Journal of Biochemistry and Cell Biology*, 51, 120–130. <https://doi.org/10.1016/j.ijocel.2014.04.008>
- Rutsch, F., Nitschke, Y., & Terkeltaub, R. (2011). Genetics in arterial calcification: Pieces of a puzzle and cogs in a wheel. *Circulation Research*, 109(5), 578–592. <https://doi.org/10.1161/CIRCRESAHA.111.247965>
- Saleem, M. A., Zavadil, J., Bailly, M., McGee, K., Witherden, I. R., Pavenstadt, H., Hsu, H., Sanday, J., Satchell, S. C., Lennon, R., Ni, L., Bottinger, E. P., Mundel, P., & Mathieson, P. W. (2008). The molecular and functional phenotype of glomerular podocytes reveals key features of contractile smooth muscle cells. *American Journal of Physiology—Renal Physiology*, 295(4), F959–F970. <https://doi.org/10.1152/ajprenal.00559.2007>
- Schlieper, G. (2018). Impact of cellular phosphate handling on vascular calcification. *Kidney International*, 94(4), 655–656. <https://doi.org/10.1016/j.kint.2018.06.027>
- Scott, R. P., & Quaggin, S. E. (2015). The cell biology of renal filtration. *Journal of Cell Biology*, 209(2), 199–210. <https://doi.org/10.1083/jcb.201410017>
- Segawa, H., Yamanaka, S., Onitsuka, A., Tomoe, Y., Kuwahata, M., Ito, M., Taketani, Y., & Miyamoto, K. I. (2007). Parathyroid hormone-dependent endocytosis of renal type IIc Na-Pi cotransporter. *American Journal of Physiology - Renal Physiology*, 292(1), F395–F403. <https://doi.org/10.1152/ajprenal.00100.2006>
- Sekiguchi, S., Suzuki, A., Asano, S., Nishiwaki-Yasuda, K., Shibata, M., Nagao, S., Yamamoto, N., Matsuyama, M., Sato, Y., Yan, K., Yaoita, E., & Itoh, M. (2011). Phosphate overload induces podocyte injury via type III Na-dependent phosphate transporter. *American Journal of Physiology—Renal Physiology*, 300(4), 848–856. <https://doi.org/10.1152/ajprenal.00334.2010>
- Suzuki, A., Ghayor, C., Guicheux, J., Magne, D., Quillard, S., Kakita, A., Ono, Y., Miura, Y., Oiso, Y., Itoh, M., & Caverzasio, J. (2006). Enhanced expression of the inorganic phosphate transporter Pit-1 is involved in BMP-2-induced matrix mineralization in osteoblast-like cells. *Journal of Bone and Mineral Research*, 21(5), 674–683. <https://doi.org/10.1359/jbmr.020603>
- Tsuchiya, N., Matsushima, S., Takasu, N., Kyokawa, Y., & Torii, M. (2004). Glomerular calcification induced by bolus injection with dibasic sodium phosphate solution in Sprague-Dawley Rats. *Toxicologic Pathology*, 32(4), 408–412. <https://doi.org/10.1080/01926230490452490>
- Tung, C. W., Hsu, Y. C., Shih, Y. H., Chang, P. J., & Lin, C. L. (2018). Glomerular mesangial cell and podocyte injuries in diabetic nephropathy. *Nephrology*, 23(54), 32–37. <https://doi.org/10.1111/nep.13451>
- Vervloet, M. G., Sezer, S., Massy, Z. A., Johansson, L., Cozzolino, M., & Fouque, D. (2017). The role of phosphate in kidney disease. *Nature Reviews Nephrology*, 13(1), 27–38. <https://doi.org/10.1038/nrneph.2016.164>
- Villa-Bellocosta, R., & Egado, J. (2017). Phosphate, pyrophosphate, and vascular calcification: a question of balance. *European Heart Journal*, 38(23), 1801–1804. <https://doi.org/10.1093/eurheartj/ehv605>
- Villa-Bellocosta, R., Ravera, S., Sorribas, V., Stange, G., Levi, M., Murer, H., Biber, J., & Forster, I. C. (2009). The Na⁺-Pi cotransporter Pit-2 (SLC20A2) is expressed in the apical membrane of rat renal proximal tubules and regulated by dietary Pi. *American Journal of Physiology—Renal Physiology*, 296(4), 691–699. <https://doi.org/10.1152/ajprenal.90623.2008>
- Villa-Bellocosta, R., & Sorribas, V. (2011). Calcium phosphate deposition with normal phosphate concentration: Role of pyrophosphate. *Circulation Journal*, 75(11), 2705–2710. <https://doi.org/10.1253/circj.CJ-11-0477>
- Wagner, C. A., Hernando, N., Forster, I. C., & Biber, J. (2014). The SLC34 family of sodium-dependent phosphate transporters. *Pflügers Archiv. European Journal of Physiology*, 466(1), 139–153. <https://doi.org/10.1007/s00424-013-1418-6>
- Wilz, D. R., Gray, R. W., Dominguez, J. H., & Lemann, J. (1979). Plasma 1,25-(OH)₂-vitamin D concentrations and net intestinal calcium, phosphate, and magnesium absorption in humans. *American Journal of Clinical Nutrition*, 32(10), 2052–2060. <https://doi.org/10.1093/ajcn/32.10.2052>
- Wu, Y., Han, X., Wang, L., Diao, Z., & Liu, W. (2016). Indoxyl sulfate promotes vascular smooth muscle cell calcification via the JNK/Pit-1 pathway. *Renal Failure*, 38(10), 1702–1710. <https://doi.org/10.3109/0886022X.2016.1155397>
- Yamada, S., Leaf, E. M., Chia, J. J., Cox, T. C., Speer, M. Y., & Giachelli, C. M. (2018). Pit-2, a type III sodium-dependent phosphate transporter, protects against vascular calcification in mice with chronic kidney disease fed a high-phosphate diet. *Kidney International*, 94(4), 716–727. <https://doi.org/10.1016/j.kint.2018.05.015>
- Yao, Y., Li, W., Wu, J., Germann, U. A., Su, M. S. S., Kuida, K., & Boucher, D. M. (2003). Extracellular signal-regulated kinase 2 is necessary for mesoderm differentiation. *Proceedings of the National Academy of Sciences of the United States of America*, 100(22), 12759–12764. <https://doi.org/10.1073/pnas.2134254100>
- Yu, Y., Zhang, L., Xu, G., Wu, Z., Li, Q., Gu, Y., & Niu, J. (2018). Angiotensin II type I receptor agonistic autoantibody induces podocyte injury via activation of the TRPC6-calcium/calciueurin pathway in pre-eclampsia. *Kidney and Blood Pressure Research*, 43, 1666–1676. <https://doi.org/10.1159/000494744>
- Zoccali, C., Ruggenenti, P., Perna, A., Leonardis, D., Tripepi, R., Tripepi, G., Mallamaci, F., & Remuzzi, G. (2011). Phosphate may promote CKD progression and attenuate renoprotective effect of ACE inhibition. *Journal of the American Society of Nephrology*, 22(10), 1923–1930. <https://doi.org/10.1681/ASN.2011020175>

How to cite this article: Kulesza, T., & Piwkowska, A. (2021). The impact of type III sodium-dependent phosphate transporters (Pit 1 and Pit 2) on podocyte and kidney function. *Journal of Cellular Physiology*, 1–10. <https://doi.org/10.1002/jcp.30368>

10. Pisemne oświadczenia autorów prac tworzących zbiór

10.1. Oświadczenie kandydata określające jego indywidualny wkład w powstanie każdej z prac tworzących niniejszy zbiór

Gdańsk, 29 maja 2023

mgr Tomasz Kulesza
Pracownia Molekularnej i Komórkowej Nefrologii
Instytut Medycyny Doświadczalnej i Klinicznej
im. M. Mossakowskiego PAN
ul. A. Pawińskiego 5
02-106 Warszawa

OŚWIADCZENIE

Oświadczam, że w pracy „Kulesza T, Typiak M, Rachubik P, Audzeyenka I, Rogacka D, Angielski S, Saleem MA, Piwkowska A. Hyperglycemic environment disrupts phosphate transporter function and promotes calcification processes in podocytes and isolated glomeruli. *J Cell Physiol*, 2022, 237(5): 2478-2491” mój udział polegał na uczestnictwie w formułowaniu hipotezy badawczej, prowadzeniu hodowli ludzkich komórek podocytarnych, zaplanowaniu i przeprowadzeniu doświadczeń, wykonaniu obliczeń statystycznych i analizie otrzymanych wyników, a także na przygotowaniu rycin i pierwotnej wersji manuskryptu oraz na dyskusji z recenzentami i finalnego redagowania manuskryptu.

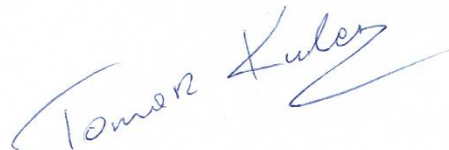


Gdańsk, 29 maja 2023

mgr Tomasz Kulesza
Pracownia Molekularnej i Komórkowej Nefrologii
Instytut Medycyny Doświadczalnej i Klinicznej
im. M. Mossakowskiego PAN
ul. A. Pawińskiego 5
02-106 Warszawa

OŚWIADCZENIE

Oświadczam, że w pracy „Kulesza T, Typiak M, Rachubik P, Rogacka D, Audzeyenka I, Saleem MA, Piwkowska A. Pit 1 transporter (SLC20A1) as a key factor in the NPP1-mediated inhibition of insulin signaling in human podocytes. *J Cell Physiol*, 2023, doi: 10.1002/jcp.31051” mój wkład polegał na uczestnictwie w tworzeniu hipotezy badawczej, prowadzeniu hodowli ludzkich podocytów, wyciszaniu genu *SLC20A1* poprzez transdukcję lentiwirusową, planowaniu i przeprowadzeniu eksperymentów, analizie statystycznej otrzymanych wyników, przygotowaniu pierwotnej wersji manuskryptu wraz z rycinami oraz na dyskusji z recenzentami pracy przed jej publikacją.

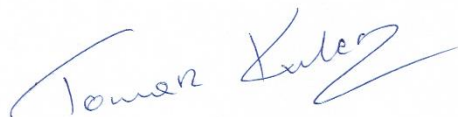


Gdańsk, 29 maja 2023

mgr Tomasz Kulesza
Pracownia Molekularnej i Komórkowej Nefrologii
Instytut Medycyny Doświadczalnej i Klinicznej
im. M. Mossakowskiego PAN
ul. A. Pawińskiego 5
02-106 Warszawa

OŚWIADCZENIE

Oświadczam, że w pracy „Kulesza T, Piwkowska A. The impact of type III sodium-dependent phosphate transporters (Pit 1 and Pit 2) on podocyte and kidney function. *J Cell Physiol*, 2021, 236(10): 7176-7185” mój udział polegał na przygotowaniu pierwotnej wersji rycin i manuskryptu, wykonaniu zdjęć komórkom barwionym immunofluorescencyjnie za pomocą mikroskopu konfokalnego oraz na wprowadzeniu zmian w artykule sugerowanych przez recenzentów.



10.2. Oświadczenia wszystkich pozostałych współautorów, w których określają swój indywidualny wkład w powstanie każdej z prac tworzących niniejszy zbiór

Gdańsk, 29 maja 2023

dr hab. Agnieszka Piwkowska, prof. IMDiK
Pracownia Molekularnej i Komórkowej Nefrologii
Instytut Medycyny Doświadczalnej i Klinicznej
im. M. Mossakowskiego PAN
ul. A. Pawińskiego 5
02-106 Warszawa

OŚWIADCZENIE

Oświadczam, że w pracy „Kulesza T, Typiak M, Rachubik P, Audzeyenka I, Rogacka D, Angielski S, Saleem MA, Piwkowska A. Hyperglycemic environment disrupts phosphate transporter function and promotes calcification processes in podocytes and isolated glomeruli. *J Cell Physiol*, 2022, 237(5): 2478-2491” mój udział polegał na sformułowaniu hipotezy badawczej, sprawowaniu nadzoru merytorycznego nad wykonaniem projektu, interpretacji otrzymanych wyników, a także na przygotowaniu pierwotnej wersji manuskryptu i jego końcowej akceptacji.

Wyrażam zgodę na wykorzystanie publikacji w postępowaniu doktorskim mgr Tomasza Kuleszy.

Piwkowska

Gdańsk, 29 maja 2023

dr hab. Agnieszka Piwkowska, prof. IMDiK
Pracownia Molekularnej i Komórkowej Nefrologii
Instytut Medycyny Doświadczalnej i Klinicznej
im. M. Mossakowskiego PAN
ul. A. Pawińskiego 5
02-106 Warszawa

OŚWIADCZENIE

Oświadczam, że w pracy „Kulesza T, Typiak M, Rachubik P, Rogacka D, Audzeyenka I, Saleem MA, Piwkowska A. Pit 1 transporter (SLC20A1) as a key factor in the NPP1-mediated inhibition of insulin signaling in human podocytes. *J Cell Physiol*, 2023, doi: 10.1002/jcp.31051” mój udział polegał na sporządzeniu harmonogramu prac doświadczalnych, sprawowaniu nadzoru merytorycznego nad wykonaniem projektu, przeprowadzeniu doświadczeń oceniających stres oksydacyjny w podocytach oraz na końcowej akceptacji manuskryptu.

Wyrażam zgodę na wykorzystanie publikacji w postępowaniu doktorskim mgr Tomasza Kuleszy.

Piwkowska

Gdańsk, 29 maja 2023

dr hab. Agnieszka Piwkowska, prof. IMDiK
Pracownia Molekularnej i Komórkowej Nefrologii
Instytut Medycyny Doświadczalnej i Klinicznej
im. M. Mossakowskiego PAN
ul. A. Pawińskiego 5
02-106 Warszawa

OŚWIADCZENIE

Oświadczam, że w pracy „Kulesza T, Piwkowska A. The impact of type III sodium-dependent phosphate transporters (Pit 1 and Pit 2) on podocyte and kidney function. *J Cell Physiol*, 2021, 236(10): 7176-7185” mój udział polegał na sprawowaniu nadzoru merytorycznego nad tworzeniem manuskryptu oraz jego ostatecznej akceptacji.

Wyrażam zgodę na wykorzystanie publikacji w postępowaniu doktorskim mgr Tomasza Kuleszy.

Piwkowska

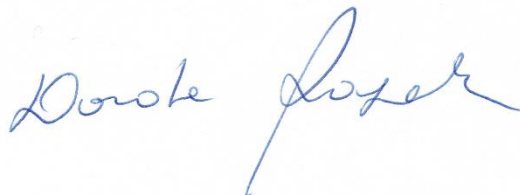
Gdańsk, 29 maja 2023

dr hab. Dorota Rogacka, prof. IMDiK
Pracownia Molekularnej i Komórkowej Nefrologii
Instytut Medycyny Doświadczalnej i Klinicznej
im. M. Mossakowskiego PAN
ul. A. Pawińskiego 5
02-106 Warszawa

OŚWIADCZENIE

Oświadczam, że w pracy „Kulesza T, Typiak M, Rachubik P, Audzeyenka I, Rogacka D, Angielski S, Saleem MA, Piwkowska A. Hyperglycemic environment disrupts phosphate transporter function and promotes calcification processes in podocytes and isolated glomeruli. *J Cell Physiol*, 2022, 237(5): 2478-2491” mój udział polegał na uczestnictwie w stworzeniu harmonogramu badawczego, przygotowaniu pierwotnej wersji manuskryptu, jego redagowaniu i akceptacji finalnej wersji dokumentu.

Wyrażam zgodę na wykorzystanie publikacji w postępowaniu doktorskim mgr Tomasza Kuleszy.



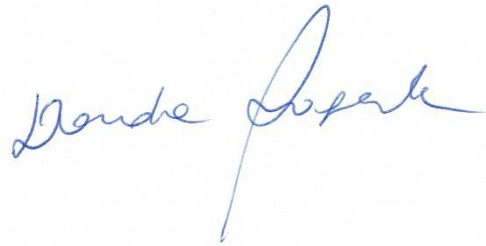
Gdańsk, 29 maja 2023

dr hab. Dorota Rogacka, prof. IMDiK
Pracownia Molekularnej i Komórkowej Nefrologii
Instytut Medycyny Doświadczalnej i Klinicznej
im. M. Mossakowskiego PAN
ul. A. Pawińskiego 5
02-106 Warszawa

OŚWIADCZENIE

Oświadczam, że w pracy „Kulesza T, Typiak M, Rachubik P, Rogacka D, Audzeyenka I, Saleem MA, Piwkowska A. Pit 1 transporter (SLC20A1) as a key factor in the NPP1-mediated inhibition of insulin signaling in human podocytes. *J Cell Physiol*, 2023, doi: 10.1002/jcp.31051” mój udział polegał na wykonaniu doświadczeń opierających się na pomiarze insulinozależnego dokomórkowego transportu glukozy w komórkach podocytarnych oraz na redagowaniu i akceptacji ostatecznej wersji manuskryptu.

Wyrażam zgodę na wykorzystanie publikacji w postępowaniu doktorskim mgr Tomasza Kuleszy.



Gdańsk, 29 maja 2023

dr Irena Audzeyenka
Pracownia Molekularnej i Komórkowej Nefrologii
Instytut Medycyny Doświadczalnej i Klinicznej
im. M. Mossakowskiego PAN
ul. A. Pawińskiego 5
02-106 Warszawa

OŚWIADCZENIE

Oświadczam, że w pracy „Kulesza T, Typiak M, Rachubik P, Audzeyenka I, Rogacka D, Angielski S, Saleem MA, Piwkowska A. Hyperglycemic environment disrupts phosphate transporter function and promotes calcification processes in podocytes and isolated glomeruli. *J Cell Physiol*, 2022, 237(5): 2478-2491” mój udział polegał na wykonaniu doświadczeń genetycznych oraz wykonaniu barwień immunohistochemicznych, a także na redagowaniu manuskryptu i jego ostatecznej akceptacji.

Wyrażam zgodę na wykorzystanie publikacji w postępowaniu doktorskim mgr Tomasza Kuleszy.



Gdańsk, 29 maja 2023

dr Irena Audzeyenka
Pracownia Molekularnej i Komórkowej Nefrologii
Instytut Medycyny Doświadczalnej i Klinicznej
im. M. Mossakowskiego PAN
ul. A. Pawińskiego 5
02-106 Warszawa

OŚWIADCZENIE

Oświadczam, że w pracy „Kulesza T, Typiak M, Rachubik P, Rogacka D, Audzeyenka I, Saleem MA, Piwkowska A. Pit 1 transporter (SLC20A1) as a key factor in the NPP1-mediated inhibition of insulin signaling in human podocytes. *J Cell Physiol*, 2023, doi: 10.1002/jcp.31051” mój udział polegał na wykonaniu doświadczeń genetycznych oraz na analizie danych kolokalizacji badanych białek uzyskanych dzięki obrazowaniu wykorzystującego mikroskopię konfokalną, a także na końcowej redakcji manuskryptu.

Wyrażam zgodę na wykorzystanie publikacji w postępowaniu doktorskim mgr Tomasza Kuleszy.



Gdańsk, 29 maja 2023

dr Marlena Typiak
Katedra Biochemii Ogólnej i Medycznej
Wydział Biologii Uniwersytetu Gdańskiego
ul. Wita Stwosza 59
80-308 Gdańsk

OŚWIADCZENIE

Oświadczam, że w pracy „Kulesza T, Typiak M, Rachubik P, Audzeyenka I, Rogacka D, Angielski S, Saleem MA, Piwkowska A. Hyperglycemic environment disrupts phosphate transporter function and promotes calcification processes in podocytes and isolated glomeruli. *J Cell Physiol*, 2022, 237(5): 2478-2491” mój udział polegał na przeprowadzeniu doświadczeń genetycznych, tj. izolacji mRNA, wykonaniu PCR z odwrotną transkrypcją oraz PCR w czasie rzeczywistym, a także wykonaniu obliczeń i interpretacji wyników powyższych eksperymentów oraz na opisie wykorzystanych metod w manuskrypcie publikacji i ostatecznej akceptacji dokumentu.

Wyrażam zgodę na wykorzystanie publikacji w postępowaniu doktorskim mgr Tomasza Kuleszy.

Marlena Typiak

Gdańsk, 29 maja 2023

dr Marlena Typiak
Katedra Biochemii Ogólnej i Medycznej
Wydział Biologii Uniwersytetu Gdańskiego
ul. Wita Stwosza 59
80-308 Gdańsk

OŚWIADCZENIE

Oświadczam, że w pracy „Kulesza T, Typiak M, Rachubik P, Rogacka D, Audzeyenka I, Saleem MA, Piwkowska A. Pit 1 transporter (SLC20A1) as a key factor in the NPP1-mediated inhibition of insulin signaling in human podocytes. *J Cell Physiol*, 2023, doi: 10.1002/jcp.31051” mój udział polegał na analizie badanych genów za pomocą PCR w czasie rzeczywistym, z wcześniejszą izolacją materiału genetycznego, przeprowadzeniu obliczeń statystycznych i interpretacji otrzymanych wyników, a także na uczestniczeniu w przygotowywaniu końcowej wersji manuskryptu.

Wyrażam zgodę na wykorzystanie publikacji w postępowaniu doktorskim mgr Tomasza Kuleszy.

Marlena Typiak

Gdańsk, 29 maja 2023

dr Patrycja Rachubik
Pracownia Molekularnej i Komórkowej Nefrologii
Instytut Medycyny Doświadczalnej i Klinicznej
im. M. Mossakowskiego PAN
ul. A. Pawińskiego 5
02-106 Warszawa

OŚWIADCZENIE

Oświadczam, że w pracy „Kulesza T, Typiak M, Rachubik P, Audzeyenka I, Rogacka D, Angielski S, Saleem MA, Piwkowska A. Hyperglycemic environment disrupts phosphate transporter function and promotes calcification processes in podocytes and isolated glomeruli. *J Cell Physiol*, 2022, 237(5): 2478-2491” mój udział polegał na przeprowadzeniu eksperymentów *in vivo* na szczurach rasy Wistar z wykorzystaniem klatek metabolicznych, indukcji cukrzycy u badanych zwierząt za pomocą streptozotocyny, pomiarze stężenia glukozy we krwi i prowadzenia dobowej zbiórki moczu, a także przygotowaniu opisu prowadzonych doświadczeń i wykorzystanych procedur w manuskrypcie publikacji.

Wyrażam zgodę na wykorzystanie publikacji w postępowaniu doktorskim mgr Tomasza Kuleszy.

Patrycja Rachubik

Gdańsk, 29 maja 2023

dr Patrycja Rachubik
Pracownia Molekularnej i Komórkowej Nefrologii
Instytut Medycyny Doświadczalnej i Klinicznej
im. M. Mossakowskiego PAN
ul. A. Pawińskiego 5
02-106 Warszawa

OŚWIADCZENIE

Oświadczam, że w pracy „Kulesza T, Typiak M, Rachubik P, Rogacka D, Audzeyenka I, Saleem MA, Piwkowska A. Pit 1 transporter (SLC20A1) as a key factor in the NPP1-mediated inhibition of insulin signaling in human podocytes. *J Cell Physiol*, 2023, doi: 10.1002/jcp.31051” mój udział polegał na wykonywaniu zdjęć z wykorzystaniem mikroskopu konfokalnego komórek barwionych immunofluorescencyjnie oraz przyżyciowo w celu obrazowania rozmieszczenia wczesnych endosomów, a także na uczestnictwie w opracowywaniu ostatecznej wersji manuskryptu.

Wyrażam zgodę na wykorzystanie publikacji w postępowaniu doktorskim mgr Tomasza Kuleszy.

Patrycja Rachubik

Gdańsk, 29 maja 2023

mgr Tomasz Kulesza
Pracownia Molekularnej i Komórkowej Nefrologii
Instytut Medycyny Doświadczalnej i Klinicznej
im. M. Mossakowskiego PAN
ul. A. Pawińskiego 5
02-106 Warszawa

OŚWIADCZENIE

Oświadczam, że udział prof. Moin A. Saleema w pracy „Kulesza T, Typiak M, Rachubik P, Audzeyenka I, Rogacka D, Angielski S, Saleem MA, Piwkowska A. Hyperglycemic environment disrupts phosphate transporter function and promotes calcification processes in podocytes and isolated glomeruli. *J Cell Physiol*, 2022, 237(5): 2478-2491” oraz w pracy „Kulesza T, Typiak M, Rachubik P, Rogacka D, Audzeyenka I, Saleem MA, Piwkowska A. Pit 1 transporter (SLC20A1) as a key factor in the NPP1-mediated inhibition of insulin signaling in human podocytes. *J Cell Physiol*, 2023, doi: 10.1002/jcp.31051” polegał na zapewnieniu materiału badawczego, jakim była linia komórkowa ludzkich podocytów oraz na końcowej akceptacji manuskryptów.

